

STABILITY ASSESSMENT OF THE LANDSLIDE IN BARTIN KİRAZLI
BRIDGE DAM DIVERSION KM: 18 + 325 – 18 + 421 SEGMENT

A THESIS SUBMITTED TO
THE GRADUATE SCHOOL OF NATURAL AND APPLIED SCIENCES
OF
MIDDLE EAST TECHNICAL UNIVERSITY

BY

BARIŞ GÖRBİL

IN PARTIAL FULFILLMENT OF THE REQUIREMENTS
FOR
THE DEGREE OF MASTER OF SCIENCE
IN
GEOLOGICAL ENGINEERING

FEBRUARY 2019

Approval of the thesis:

**STABILITY ASSESSMENT OF THE LANDSLIDE IN BARTIN KIRAZLI
BRIDGE DAM DIVERSION KM: 18 + 325 – 18 + 421 SEGMENT**

submitted by **BARIŞ GÖRBİL** in partial fulfillment of the requirements for the degree of **Master of Science in Geological Engineering Department, Middle East Technical University** by,

Prof. Dr. Halil Kalıpçılar
Dean, Graduate School of **Natural and Applied Sciences**

Prof. Dr. Erdin Bozkurt
Head of Department, **Geological Engineering**

Prof. Dr. Haluk Akgün
Supervisor, **Geological Engineering, METU**

Assoc. Prof. Dr. Mustafa Kerem Koçkar
Co-Supervisor, **Civil Engineering Dept., Hacettepe Uni.**

Examining Committee Members:

Prof. Dr. Erdal Çokça
Civil Engineering Dept., METU

Prof. Dr. Haluk Akgün
Geological Engineering, METU

Prof. Dr. Murat Ercanoğlu
Geological Engineering Dept., Hacettepe University

Assoc. Prof. Dr. Hakan Ahmet Nefeslioğlu
Geological Engineering Dept., Hacettepe University

Assist. Prof. Dr. M. Abdullah Sandıkkaya
Civil Engineering Dept., Hacettepe University

Date: 01.02.2019

I hereby declare that all information in this document has been obtained and presented in accordance with academic rules and ethical conduct. I also declare that, as required by these rules and conduct, I have fully cited and referenced all material and results that are not original to this work.

Name, Surname: Barış Görbil

Signature:

ABSTRACT

STABILITY ASSESSMENT OF THE LANDSLIDE IN BARTIN KIRAZLI BRIDGE DAM DIVERSION KM: 18 + 325 – 18 + 421 SEGMENT

Görbil, Barış
Master of Science, Geological Engineering
Supervisor: Prof. Dr. Haluk Akgün
Co-Supervisor: Assoc. Prof. Dr. Mustafa Kerem Koçkar

February 2019, 124 pages

Bartın Kirazlı Bridge Dam construction has started on Gökırmak stream in 1999 for the purposes of irrigation and power generation and is continuing at present. By the end of construction, Gökırmak stream level will reach +105 meters, and the existing Bartın – Safranbolu (D755) Highway will be submerged under water. A new alignment is determined for the relocation of the submerged road and named as the “Kirazlı Bridge Dam Diversion”. With the start of the new highway construction, the paleo – landslide regions over the new alignment area were triggered and a mass movement occurred at the Km: 18 + 325 – 18 + 421 section.

The purpose of this thesis is to define the characteristics of this landslide, to determine the sliding surface location, to reveal the mobilized mass amount and to specify the appropriate remediation and measurements for long term stability. For this purpose, in – situ site investigations and laboratory tests were conducted. With the data obtained from the investigation works, the landslide model was formed, and the shear strength parameters of the landslide mass were determined by back analysis performed on three critical sections of the model.

In addition, slope stability analysis was performed by limit equilibrium method for both static and dynamic (seismic) conditions. As a result of these studies, ground water

level reduction by pumping in short term, rock buttress application after temporary toe excavation and dewatering of the area by surface and subsurface drainage remediation phases were found suitable for the long term stability of the landslide.

Keywords: Bartın – Safranbolu (D755) Highway, Kirazlı Bridge Dam, Landslide, Slope stability, Inclinator, Back analysis, Remediation, Limit equilibrium analysis.

ÖZ

BARTIN KİRAZLI KÖPRÜ BARAJI VARYANT YOLU KM: 18 + 325 – 18 + 421 KESİMİNDEKİ HEYELANIN STABİLİTE AÇISINDAN DEĞERLENDİRİLMESİ

Görbil, Barış
Yüksek Lisans, Jeoloji Mühendisliği
Tez Danışmanı: Prof. Dr. Haluk Akgün
Ortak Tez Danışmanı: Doç. Dr. Mustafa Kerem Koçkar

Şubat 2019, 124 sayfa

Bartın ili sınırlarından geçmekte olan Gökırmak Çayı üzerinde, 1999 yılında sulama ve enerji üretimi amacıyla projelendirilen Kirazlı Köprü Barajı'nın yapımı günümüzde halen devam etmektedir. Baraj inşaatının tamamlanmasının ardından, su kotunun +105 metreye ulaşmasıyla birlikte mevcut Bartın – Safranbolu (D755) Devlet Karayolu su altında kalacaktır. Su altında kalacak olan mevcut yolun yerine “Kirazlı Köprü Varyant Yolu” olarak isimlendirilen yeni bir güzergah belirlenmiş ve bu yol güzergahının geçtiği kesimlerde paleo heyelanların varlığı gözlenmiştir. Yeni yolun imalat çalışmalarının başlamasıyla birlikte, paleo heyelanlı bölgeler tetiklenmiş olup, Km: 18 + 325 – 18 + 421 kesiminde büyük bir kütle hareketi meydana gelmiştir.

Bu tez çalışmasının amacı; incelenen alanda gelişen hareketli kütlelerin tanımlanması, harekete geçen bu kütlelerin miktarı ve kayma dairesinin belirlenmesi çalışmaları sonrasında, bu kütleleri durdurmaya yönelik uygun iyileştirme tekniklerini belirleyerek önlem ölçümleri almaktır. Bu amaçla, yerinde arazi çalışmaları (jeoteknik sondajlarla birlikte SPT ve presiyometre deneyleri, inklinometre ile izleme, vb.) ile laboratuvar çalışmalarından oluşan jeolojik – jeoteknik araştırmalar yapılmıştır. Elde edilen veriler ile heyelan modeli oluşturularak, üç farklı kesit üzerinde gerçekleştirilen geriye

dönük analizler ile heyelan kütesine ait kayma mukavemeti parametreleri belirlenmiştir.

Limit denge yöntemiyle heyelanın statik ve dinamik (deprem) durumu analizleri yapılmıştır. Bu çalışmanın sonucunda uygun iyileştirme yöntemlerinin, sırasıyla; pompaj ile yeraltı su seviyesinin düşürülmesi, topuk bölgesinde yerdeğiştirme kazısı ile kaya dolgu yapılması ve son aşamada uygun yeraltı ve yüzey drenajları ile suyun heyelanlı kütleden uzaklaştırılması yöntemleri uygun görülmüştür.

Anahtar Kelimeler: Bartın – Safranbolu (D755) Devlet Karayolu, Kirazlı Köprü Barajı, Heyelan, Şev stabilitesi, İnklinometre, Geriye dönük analiz, İyileştirme, Limit denge analizi.

For the memory of my grandmother...

ACKNOWLEDGEMENTS

I would like to express my sincere thanks to my supervisor Prof. Dr. HALUK AKGÜN for his patience and motivation at every phase of this study.

I would like to express my special thanks to my co-supervisor Assoc. Prof. Dr. MUSTAFA KEREM KOÇKAR for his endless support, guidance and belief in me.

It was a long, tiring road for us. But the greatest family in the world was always right behind me: My dad MUAMMER GÖRBİL, my mom VİLDAN GÖRBİL and my sister ALEV GÖRBİL, I love you all.

I owe my one and only aunt GÜLDEN ÇETİN and my uncle METİN ÇETİN for their invaluable presence in my life.

I appreciate EMRE YILDIZ, who suffered all my trouble.

I feel gratitude to MEHMET ALİ TEMUR for his support and embracement.

My best friend OYA BAL, be in my life forever.

I am grateful to my big man SERTAN ÇAYCI for his priceless encouragements.

I am so glad to have you in my life again MERVE BOZDEMİR.

Since the first day at the campus, I am indebted to my man HASAN YARADILMIŞ.

You were always there when I needed, my newest friend BURCU TURAN.

Also, my appreciations to my friendship crew; AYBERK ÇAL, CEREN SARIBIYIK, FATİH ULUSOY, GÖKÇE YAVUZ, ÖMER CEM KAYA, TAYLAN ÖZGÜR ULUDAĞ.

Sincere thanks to SEDA BİRSOY, the only one who could understand me completely.

Many thanks to ARZU ARSLAN KELAM for worthy help.

Heartfelt thanks to my former manager and last climbing partner ALPER ŐENGÜL, who gave me the key to start this study.

I appreciate my manager ALI BAYRAM, HASAN ÖZASLAN, MUSTAFA KEMAL AKMAN, ERKİL ONUR TARI, KÜRŐAT TOKGÖZÖĐLU and the entire YÜKSEL PROJE family for their valuable support.

Lastly, acknowledgements to GENERAL DIRECTORATE OF HIGHWAYS 15TH REGIONAL DIRECTORATE for permission to perform this study.

TABLE OF CONTENTS

ABSTRACT	v
ÖZ	vii
ACKNOWLEDGEMENTS.....	x
TABLE OF CONTENTS	xii
LIST OF TABLES.....	xv
LIST OF FIGURES	xvii
CHAPTERS	
1. INTRODUCTION.....	1
1.1. Purpose and Scope	1
2. GEOLOGY.....	3
2.1. Local Geology / Stratigraphy.....	3
2.1.1. Geology of the Study Area.....	5
2.1.1.1. Ulus Formation (Ku).....	5
2.1.1.2. Alluvium (Qal).....	6
2.2. Structural Geology and Tectonism	7
2.3. Hydrogeology.....	7
2.4. Seismicity and Seismotectonics	8
2.4.1. A Deterministic Approach to Estimate PGA Value.....	13
3. PHYSIOGRAPHY AND CLIMATE.....	17
3.1. Geographical Location of the Study Area.....	17
3.2. Climate	18
4. SITE INVESTIGATION.....	21

4.1. Engineering Geological Mapping	21
4.2. Drilling Study	26
4.3. In – Situ Tests	27
4.3.1. Standard Penetration Test (SPT).....	27
4.3.2. Pressuremeter Test	30
4.3.3. Inclinometers	33
4.4. Laboratory Tests	33
5. ENGR. GEOLOGICAL CHARACTERIZATION OF THE LANDSLIDE	35
5.1. Landslide Phenomenon and Types	35
5.2. Mechanism of Mass Movement	39
5.2.1. Depth of Sliding Mass	41
5.3. Geomechanical Properties of Units	42
5.3.1. Landslide Material (Hm)	42
5.3.2. Artificial Fill (Yd).....	43
5.3.3. Highly to completely weathered Ulus Formation (Ku – W5)	44
5.3.4. Ulus Formation (Ku).....	45
6. DETERMINATION OF GEOTECHNICAL PARAMETERS	47
6.1. Empirical Approach (Effective Parameters)	47
6.2. Rock Mass Rating (RMR)	49
6.3. Geological Strength Index (GSI).....	52
6.4. Analysis of Rock Strength Using RocData	55
7. GEOTECHNICAL ASSESMENT OF SLOPE	59
7.1. Slope Stability Analysis Methods	59
7.1.1. Limit Equilibrium Methods	59

7.1.1.1. The Method of Slices.....	61
7.1.1.2. Selection of the Appropriate Slice Method	66
7.1.2. Seismic Slope Stability Method	67
7.2. Geotechnical Parameters of the Sliding Surface.....	70
7.2.1. Empirical Approach (Residual Parameters)	70
7.2.2. RocData Analysis	72
7.2.3. Back Analysis.....	74
7.3. Slope Stability Assessment	83
7.3.1. Subsurface Drainage by Pumping	87
7.3.2. Toe Excavation.....	89
7.3.3. Rock Buttress	91
7.3.4. Increase of Water Level after Dam Construction.....	93
7.3.5. Surface and Subsurface Drainage.....	95
7.3.6. Seismic Load	99
7.3.7. Assessment of the Stability Analysis	100
8. DISCUSSION, CONCLUSIONS AND RECOMMENDATIONS	101
REFERENCES	103
APPENDICES	
A. Borehole Logs	111
B. Core Box Photographs.....	115
C. Pressuremeter Test Results.....	119
D. Inclinator Readings.....	121
E. Laboratory Test Results.....	123

LIST OF TABLES

TABLES

Table 2.1. The list of earthquakes with a magnitude greater than 3.5 that have occurred in the study area and its close vicinity	12
Table 2.2. Summary of the estimated PGA values	14
Table 4.1. Summary of borehole study	27
Table 4.2. A summary of the Standard Penetration Test results	28
Table 4.3. A summary of the pressuremeter test results	30
Table 5.1. Classification of Landslides (Varnes, 1978)	36
Table 5.2. A summary of inclinometer readings	41
Table 6.1. Typical values of natural density (Carter & Bentley, 1991)	47
Table 6.2. α coefficient values for different soil types (Lunne et al., 1997)	48
Table 6.3. Rock Mass Rating (Bieniawski, 1989) for highly to completely weathered Ulus formation (Ku – W5)	50
Table 6.4. Rock Mass Rating (Bieniawski, 1989) for Ulus formation (Ku)	51
Table 6.5. Summary of RMR values of the rock units	52
Table 6.6. Geological Strength Index (Sonmez and Ulusay, 2002) for the highly to completely weathered Ulus formation (Ku – W5)	53
Table 6.7. Geological Strength Index (Sonmez and Ulusay, 2002) for the Ulus formation (Ku)	54
Table 6.8. Calculation of Geological Strength Index (GSI) ratings with Sonmez and Ulusay's (2002) Chart	55
Table 6.9. Input rock mass parameters	56
Table 7.1. Limit equilibrium methods	66
Table 7.2. Suggested Methods for Performing Pseudostatic Screening Analysis (Duncan, 2014)	69
Table 7.3. Typical values of natural density (Carter & Bentley, 1991)	70

Table 7.4. α coefficient values for different soil types (Lunne et al., 1997)	71
Table 7.5. Geological Strength Index (Sonmez and Ulusay, 2002) for the landslide material (Hm).....	72
Table 7.6. Calculation of Geological Strength Index (GSI) rating with Sonmez and Ulusay's (2002) Chart.....	73
Table 7.7. Rock mass parameters (For slope, height = 15.00 m)	73
Table 7.8. $c - \phi$ pair values satisfying F.S. = 1.0 condition for each section	76
Table 7.9. A summary of the estimated geotechnical parameters of the landslide material	83
Table 7.10. Summary of material parameters used in stability analysis	84
Table 7.11. Summary of factor of safety values	100

LIST OF FIGURES

FIGURES

Figure 1.1. Location map of the study area (Esri, 2018).....	2
Figure 2.1. Regional geological map of the study area (MTA, 2002)	4
Figure 2.2. The sandstone and claystone units of the Ulus formation (Ku)	6
Figure 2.3. View to the Gökırmak stream and Kirazlı Bridge Dam construction area	6
Figure 2.4. Seismicity of the study area and its vicinity (AFAD, 2018).....	8
Figure 2.5. Active fault map of Bartın region (Modified from Esri (2018), Şengör et al. (1985), Barka (1997), Bozkurt (2001))	10
Figure 2.6. Earthquakes with a magnitude greater than 3.5 that have occurred in the study area and its close vicinity (The earthquake data is obtained from KOERI (2018) and modified on the Esri (2018) map)	11
Figure 3.1. Avg. temperature values of the Derbent Village (Climate Data, 2018) ..	19
Figure 3.2. Avg. precipitation values of the Derbent Village (Climate Data, 2018...)	19
Figure 4.1. A view from field studies	21
Figure 4.2. Engineering geological map of the study area.....	22
Figure 4.3. Geological – geotechnical cross section 1-1' (Km: 18 + 353)	23
Figure 4.4. Geological – geotechnical cross section 2-2' (Km: 18 + 368)	24
Figure 4.5. Geological – geotechnical cross section 3-3' (Km: 18 + 407)	25
Figure 4.6. Location of boreholes at the study area	26
Figure 5.1. Landslide classification by Varnes (1978) and Cruden and Varnes (1996) based on the type of movement and material.....	38
Figure 5.2. A side view of the morphology of the landslide area	40
Figure 5.3. A view of the morphology of the landslide area.....	40
Figure 6.1. Range of shearing resistance angle and PI in clays (Gibson, 1953).....	48
Figure 6.2. Normal vs Shear Stress graph for weathered Ulus frm. (Ku – W5).....	56
Figure 6.3. Normal vs Shear Stress graph for the Ulus formation (Ku)	57

Figure 7.1. Division of a potential sliding mass into slices (Abramson, 2002).....	61
Figure 7.2. Forces acting on a typical slice (Abramson, 2002)	62
Figure 7.3. Slice with forces for the Simplified Bishop	63
Figure 7.4. Slice with forces for the Simplified Janbu	64
Figure 7.5. Slice with forces for the Morgensten – Price	65
Figure 7.6. Slice with forces for the Spencer’s Method	65
Figure 7.7. Range of shearing resistance angle and PI in clays (Gibson, 1953)	71
Figure 7.8. Normal vs shear stress graph for the landslide material (Hm)	74
Figure 7.9. Best fit lines of $c - \phi$ pairs obtained from back analysis.....	76
Figure 7.10. Back Analysis of Sec. 1-1’ (Km: 18 + 353) (Exported form Slide 6.0)77	
Figure 7.11. Back Analysis of Section 1-1’ (Km: 18 + 353) (Detailed view).....	78
Figure 7.12. Back Analysis of Sec. 2-2’ (Km: 18 + 368) (Exported from Slide 6.0)79	
Figure 7.13. Back Analysis of Section 2-2’ (Km: 18 + 368) (Detailed view).....	80
Figure 7.14. Back Analysis of Sec. 3-3’ (Km: 18 + 407) (Exported from Slide 6.0)81	
Figure 7.15. Back Analysis of Section 3-3’ (Km: 18 + 407) (Detailed view).....	82
Figure 7.16. Initial Phase of Section 2-2’ (Exported from Slide 6.0).....	85
Figure 7.17. Initial Phase of Section 2-2’ (Detailed view)	86
Figure 7.18. Pumping Drainage Dewatering Phase for Section 2-2’ (Exported from Slide 6.0).....	87
Figure 7.19. Pumping Drainage Dewatering Phase for Sec. 2-2’ (Detailed view)....	88
Figure 7.20. Toe Excavation Phase of Section 2-2’ (Exported from Slide 6.0)	89
Figure 7.21. Toe Excavation Phase of Section 2-2’ (Detailed view)	90
Figure 7.22. Rock Buttress App. Phase of Section 2-2’ (Exported from Slide 6.0)..	91
Figure 7.23. Rock Buttress Application Phase of Section 2-2’ (Detailed view)	92
Figure 7.24. Increase of Water Level after Dam Construction for Section 2-2’ (Exported from Slide 6.0)	93
Figure 7.25. Increase of Water Level after Dam Construction for Section 2-2’ (Detailed view)	94
Figure 7.26. Details of the surface and subsurface drainage	96

Figure 7.27. Surface and Subsurface Dewatering Phase of Section 2-2' (Static Condition) (Exported from Slide 6.0)97

Figure 7.28. Surface – Subsurface Dewatering Phase of Sec. 2-2' (Detailed view)..98

Figure 7.29. Surface and Subsurface Dewatering Phase of Section 2-2' (Seismic Condition) (Exported from Slide 6.0)99

CHAPTER 1

INTRODUCTION

1.1. Purpose and Scope

The Bartın Kirazlı Bridge Dam construction project that is located on the Gökırmak stream has started in 1999 for irrigation and power generation. By the help of the Dam, which will have over 66 million cubic meters of water storage capacity, 31000 decares of cultivated area will be irrigated and the flood hazard and risk over the city of Bartın will be prevented. After the Dam construction project is finished, the elevation of the Gökırmak stream level will increase to + 105 meters and the current Bartın – Safranbolu Highway (D755) will be submerged. Thus, a new highway alignment project has started by Yüksel Proje International Inc., and a number of geological instability zones have been occurred on that new highway alignment during the site investigations.

This thesis covers the investigation and assessment works for the landslide that is located in between the Km: 18 + 325 – 18 + 421 segment of the new highway alignment, which is referred to as the Bartın Kirazlı Bridge Dam Diversion. The investigation and assessment works include; site observation and surveys, in – situ boring tests and monitoring measurements, laboratory tests, geotechnical parameter estimations, landslide characterization and analysis.

As a consequence of the investigation works, landslide modelling and prevention and remediation measures were purposed for the landslide that is located at the Km: 18 + 325 – 18 + 421 segment of the Bartın Kirazlı Bridge Dam Diversion.

The location map of the study area and its vicinity is given in Figure 1.1.

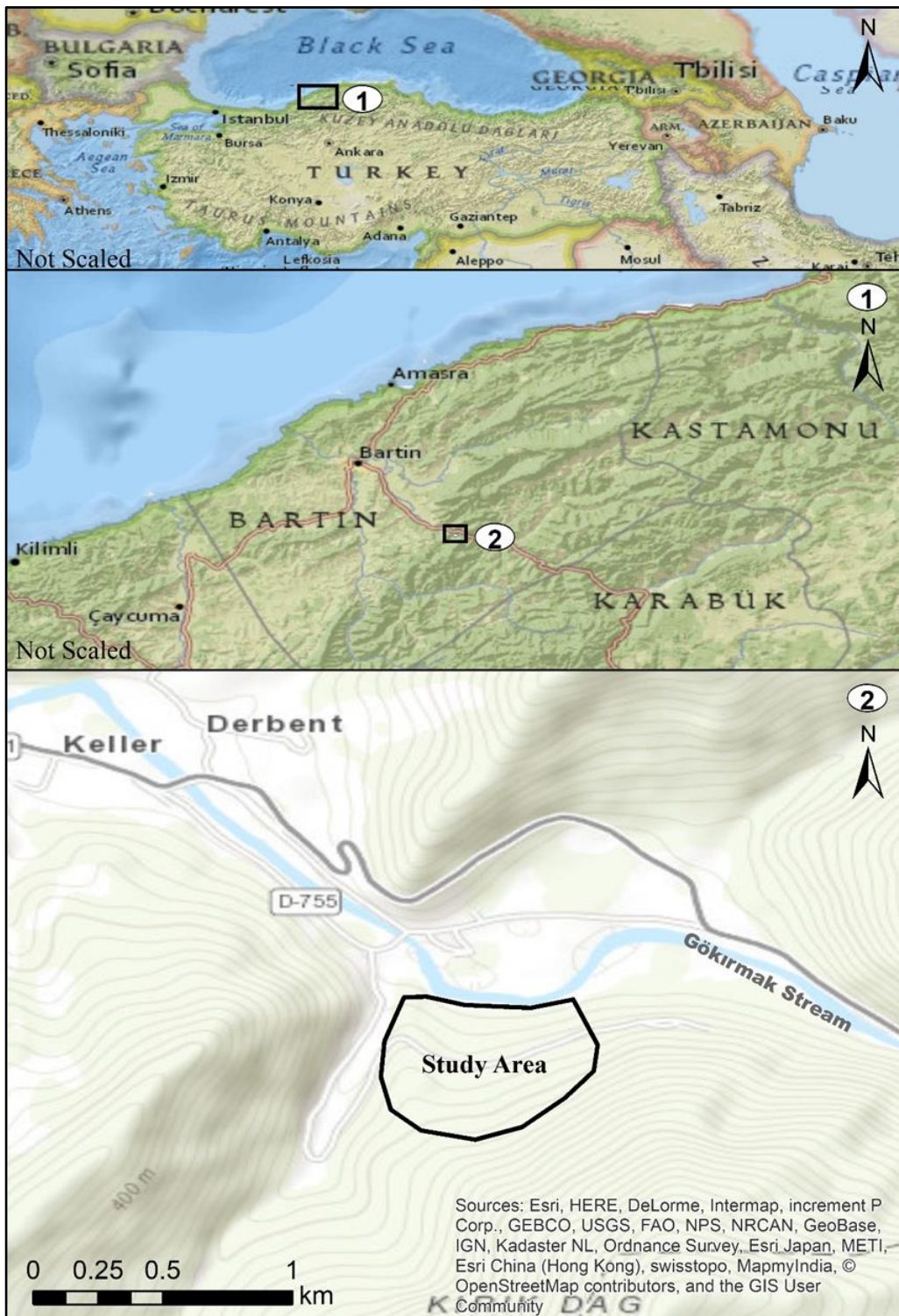


Figure 1.1. Location map of the study area (Esri, 2018)

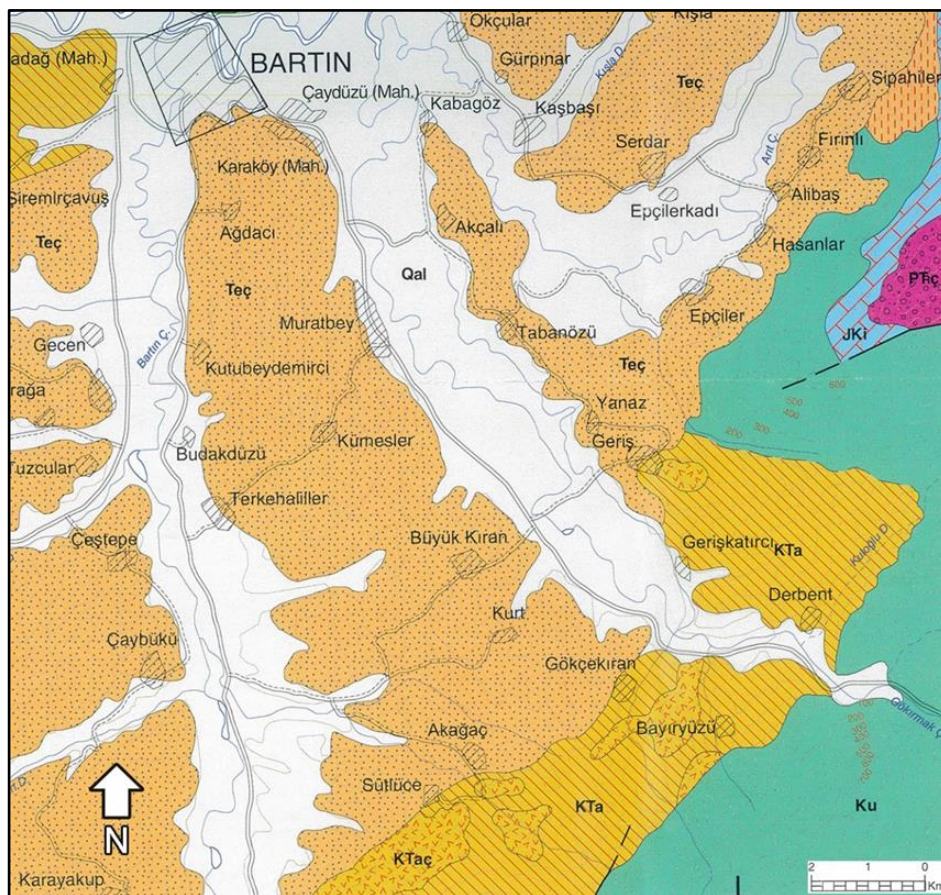
CHAPTER 2

GEOLOGY

2.1. Local Geology / Stratigraphy

The Middle Ordovician – Lower Devonian Ereğli formation consisting of shale, sandstone and limestone units forms the lower base area of Bartın City and its close vicinity (Serdar and Demir, 1983). The Middle Devonian – Lower Carboniferous aged limestones and dolomites forming the Yılanlı formation conformably overly the Ereğli formation (Saner, 1979). Lower – Middle Carboniferous Alacağzı formation consisting of coal bearing shale, mudstone and sandstone has conformity with the Yılanlı formation at the bottom and the Karadon formation at the top (Ralli, 1933). The Karadon formation is Upper Carboniferous aged and contains conglomerate, sandstone, claystone and diatomite. Permian – Triassic mudstones and conglomerates forming the Çakraz formation has a lateral conformity with Triassic aged Çakrazboz formation which contains shale, claystone, marl, sandstone and limestone (Akman, 1993). Both the Çakraz and Çakrazboz formations have an unconformity with the underlying units. Transgressively sedimented neritic limestones of Middle Cretaceous aged İnaltı formation, flysh sediments of the Lower Cretaceous Ulus formation and sandstones, shales of the Lower Cretaceous Kilimli formation both have conformity with each other from the bottom to the top (Saner et al., 1981). These formations both unconformably overly the older units and are conformably overlain by the Upper Cretaceous – Lower Eocene aged Akveren formation (Ketin and Gümüş, 1963) consisting of semi pelagic limestone, shale, calcarenite, sandstone, conglomerate and basaltic / andesitic lavas of the Çangaza volcanic member (Aksay et al., 2001). Lower – Middle Eocene Yığılca formation (Kaya et al., 1986) containing agglomerate, tuff, volcanogenic sandstone, andesite and basalt has conformity with the Akveren formation. Lower – Middle Eocene aged sandstone, shale, conglomerate units of the

Çaycuma formation (Tokay, 1954) and the limestone, shale units of the Kaynarca member conformably overly the Yığılca formation. The regional geological map of study area is given in Figure 2.1.



DESCRIPTION OF MAP UNITS

QUATERNARY		Alluvium
	UNCONFORMITY	
LOWER - MIDDLE EOCENE		Kaynarca member (Teç): Limestone, marl
		Çaycuma formation (Teç): Sandstone, shale, conglomerate
	TRANSITIONAL	
UPPER CAMPANIAN - LOWER EOCENE		Çangaza volcanic member (KTaç): Basalt, andesite
		Akveren formation (KTa): Hemipelagic limestone, shale, calcarenite, sandstone, conglomerate
	TRANSITIONAL	
LOWER CRETACEOUS		Ulus formation: Sandstone, shale, conglomerate, limestone
	TRANSITIONAL	
MALM - APTIAN		İnalı formation: Neritic limestone
	UNCONFORMITY	
PERMIAN - TRIASSIC		Çakraz formation: Mudstone, sandstone, conglomerate (continental)

Figure 2.1. Regional geological map of the study area (MTA, 2002)

2.1.1. Geology of the Study Area

The Ulus formation (Ku) forms the general geological unit observed in the study area. Alluvium deposits (Qal) also outcrop at the lower elevations. The lithological and stratigraphic properties of these formations are specified below.

2.1.1.1. Ulus Formation (Ku)

Akyol et al. (1974) named the alternation of turbiditic sandstones, claystones and shales as the Ulus Formation. The name of the formation comes from the Ulus district of Bartın City. The units are widely observed at the east of Bartın.

Green – grey, partly black colored, thin to middle-thick layered, turbiditic sandstone, claystone, shale and the alternation of these units form the Ulus formation (Figure 2.2). The sandstone layers have graded, parallel and convolute lamination. Partly polygenic conglomerates were observed through the contact of the Ulus and İnaltı formations. Lenticular limestones (Clastic limestones and megabreccias), which were formed by transportation of the sedimented mud, carbonate, angular limestone gravels and blocks from the İnaltı formation to the Ulus formation regarding mass flows and gravity effects, forms the characteristic rock units of the Ulus formation. Partly volcanic blocks were observed in the unit. The Ulus formation has lateral and vertical conformity with the İnaltı formation. The Akveren formation unconformably overlies the Ulus formation (MTA, 2002).

The thickness of the Ulus formation is estimated to be about 2000 meters. The fossil content of the unit is not known clearly. However, there is much more clear data about the sedimentation age of the İnaltı formation which occurred in the same period with the İnaltı formation. According to these data and considering the stratigraphical position of the unit, the geological age of the Ulus formation is attributed as Lower Cretaceous (MTA, 2002).

The unit is represented by hill, hillside and basin deposits.



Figure 2.2. The sandstone and claystone units of the Ulus formation (Ku)

2.1.1.2. Alluvium (Qal)

Alluvium units are current deposits of gravel, sand and mud which sedimented over stream beds, valley bottoms and flat areas that have formed over earlier trenches. The closest and biggest water source passing through the study area is the Gökırmak Stream (Figure 2.3).



Figure 2.3. View to the Gökırmak stream and Kirazlı Bridge Dam construction area

2.2. Structural Geology and Tectonism

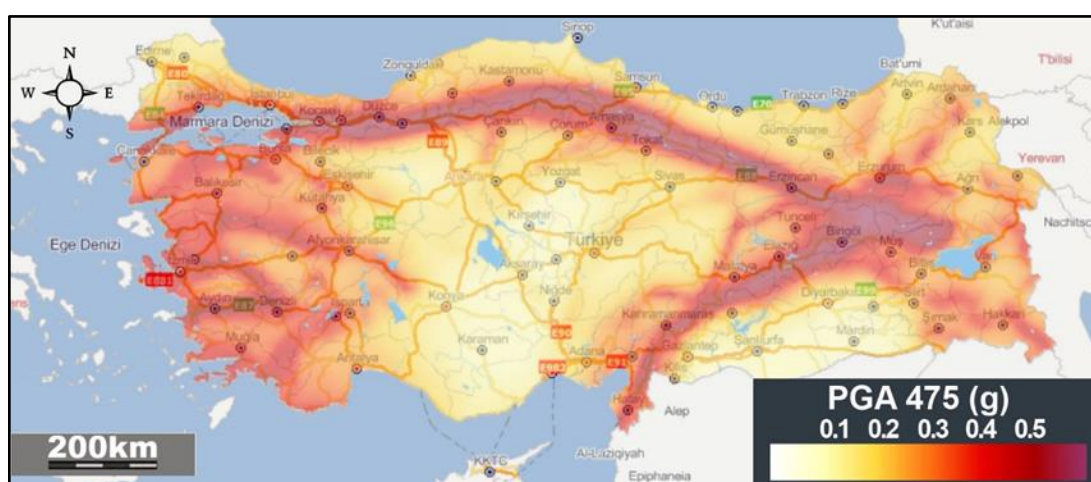
With the increase of tectonic activity in the Late Jurassic period, the Ereğli, Yılanlı, Alacağızı, Karadon, Çakraz and Çakrazboz formations were uplifted and created a weathering zone. With downward eustatic movements at this period, the upland areas reached the level of shelves / platforms (İnaltı Subsidence) and later at Middle Cretaceous, reached the level of hillsides / deep sea (From Late Jurassic to Middle Cretaceous periods, basin conditions became suitable for the sedimentation of the Ulus formation to occur). Tectonic activities increased during Turonian and Santonian ages. The İnaltı formation deposits were transferred to the Yemişliçay formation following the basinal uplifting. The following tectonic activity increment that occurred in the Campanian and Maastrichtian ages caused the submerged movements of the Çakraz, İnaltı, Kilimli and Ulus formations in terms of compressional and horizontal movements. In addition, the pelagic limestones conformably overlaid the volcanics during that period (MTA, 2002).

2.3. Hydrogeology

The formations observed in the study area and its vicinity may transport groundwater depending on their lithological character. These formations may allow groundwater circulation through the joint sets and faults. The Ulus formation observed in the study area mainly consists of claystone, siltstone and sandstone units (MTA, 2002). These units are highly to completely weathered at the upper levels and partly contain clay, sand and gravel units. The clay units are impermeable to groundwater but clay levels which contain sand and gravel may allow water transport depending on the coarse grain proportions. Moreover, claystone and siltstone units are also impermeable, but the rock units may transport groundwater through their discontinuity systems. On the other hand, alluvium units, which are observed at lower levels of study area are permeable to groundwater. The primary watercourse at the study area is the Gökırmak Stream.

2.4. Seismicity and Seismotectonics

The Earthquake Hazard Map of Turkey which was lastly enacted in 1996 has been revised by AFAD Earthquake Research Department and issued on 18th March 2018. The revised and issued Map became effective on 1st January 2019. According to the mentioned map, the peak ground acceleration (PGA 475) value in the study area is expected to be 0.220 g (Figure 2.4).



Earthquake hazard map of Turkey



Earthquake hazard map of Bartın region

Figure 2.4. Seismicity of the study area and its vicinity (AFAD, 2018)

In this study, the map of 475 years return period is considered instead of 43, 72 and 2475 years, because the peak ground acceleration expected to be exceeded with a 10% probability in 50 years is the standard design earthquake of ground motion level. Hence, it is considered as a more predictable hazard assessment for a 50 years of structural design life.

Karabük Fault, which is the closest active fault to the study area lies approximately 36 km to the south – southwest of the study area. The Karabük fault which has a total length about 35 km, is a thrust fault that has a general trend of NNE – SSW with SE to NE dipping fault planes (Bengü, 2017). The Devrek Fault, which is an active fault lies approximately 70 km to the southwest of the study area. It is a strike slip fault that has a total length about 40 km and a general trend of NE – SW (MTA, 2012). In addition, The North Anatolian Fault (NAF) is also a strike slip fault with a total length of 1100 kilometers (Şengör, 1979) and it is situated about 70 km to the south – southwest of the study area. Since the most recent intense tectonic activities that have occurred in Anatolia have been triggered by the North Anatolian Fault, the source of a potential seismic activity that is expected to occur in the study area is expected to be triggered by the North Anatolian Fault. The Active Fault Map of the study area and its close vicinity is shown in Figure – 2.5.

Earthquakes that have occurred within a radius of 100 kilometers of the study area in the last 50 years, with a magnitude of 3.5 and over are obtained from the Boğaziçi University, Kandilli Observatory and Earthquake Research Institute (KOERI), Regional Earthquake – Tsunami Monitoring and Evaluation Centre, Earthquake Query System. The distribution and range thematic map of these earthquakes are shown in Figure – 2.6 and the list of those earthquakes is given in Table – 2.1. Accordingly, the major earthquake in this region is the Amasra Earthquake that occurred on the 3rd of September 1968 with a magnitude of 6.5.

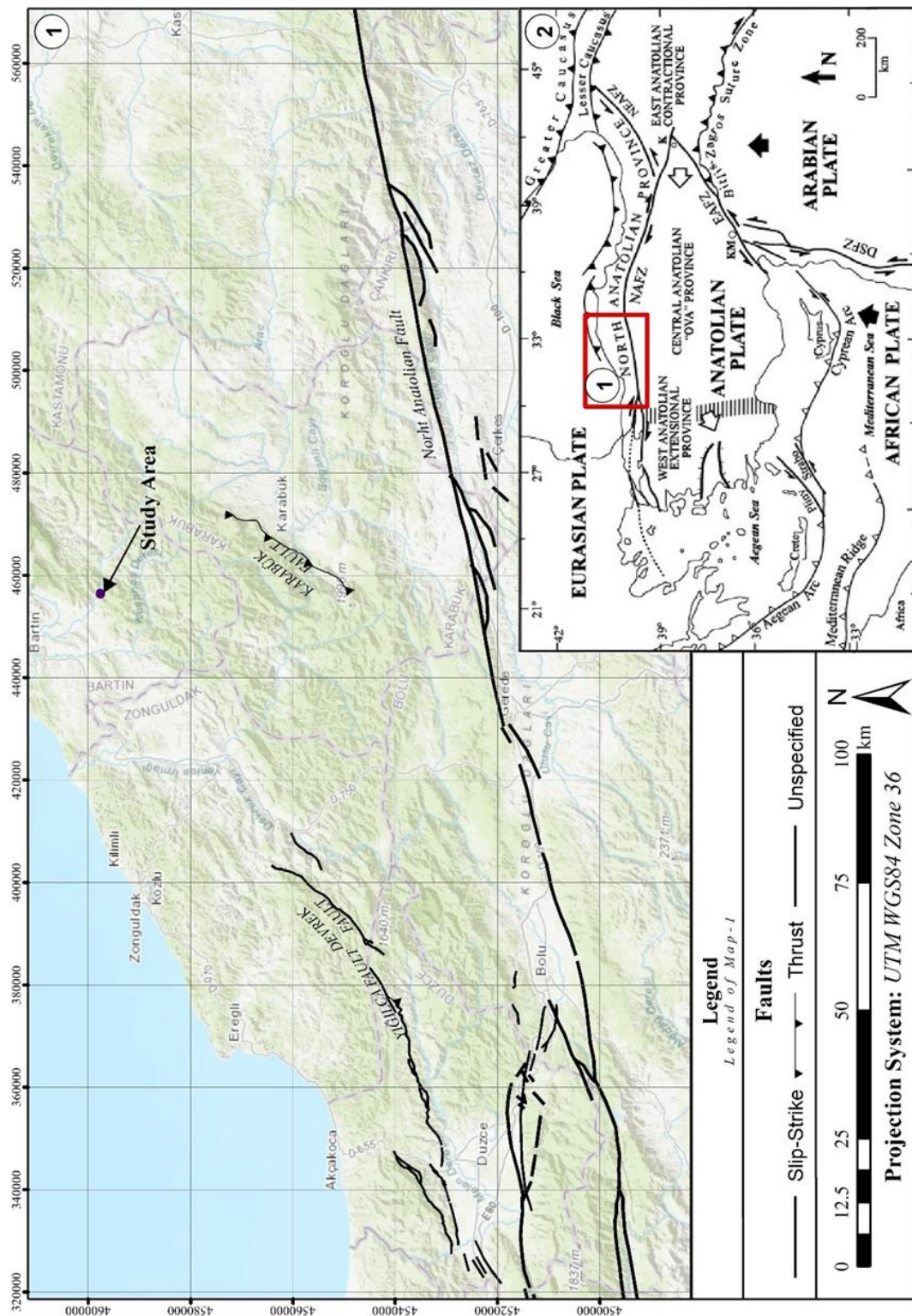


Figure 2.5. Active fault map of Bartın region (Modified from Esri (2018), Şengör et al. (1985), Barka (1997), Bozkurt (2001))

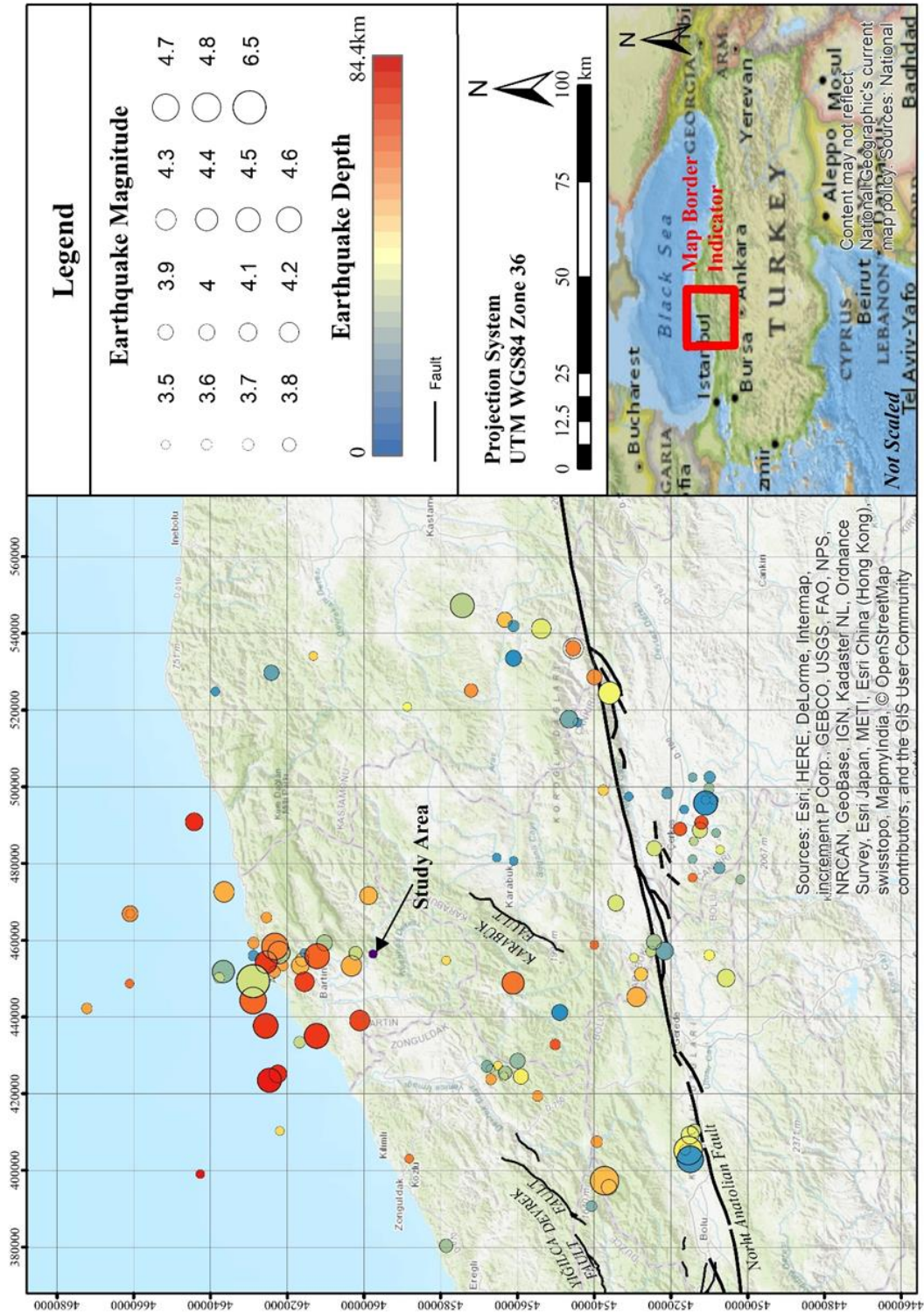


Figure 2.6. Earthquakes with a magnitude greater than 3.5 that have occurred in the study area and its close vicinity (The earthquake data is obtained from KOERI (2018) and modified on the Esri (2018) map)

Table 2.1. *The list of earthquakes with a magnitude greater than 3.5 that have occurred in the study area and its close vicinity*

No	Date	Depth (km)	Magnitude
1	28.12.2017	5.00	3.60
2	26.07.2017	5.00	3.90
3	15.12.2016	84.40	3.50
4	01.12.2016	2.40	3.50
5	18.01.2016	1.70	3.70
6	08.11.2015	8.00	3.50
7	01.11.2015	2.40	3.50
8	08.05.2015	1.30	3.90
9	02.05.2015	1.80	4.10
10	28.01.2015	7.80	3.50
11	04.09.2014	4.50	4.00
12	24.11.2013	6.50	3.60
13	24.11.2013	7.60	4.80
14	24.07.2013	5.00	3.80
15	21.07.2013	5.30	4.20
16	25.02.2011	5.40	3.50
17	20.12.2009	5.40	3.50
18	22.11.2009	5.00	4.50
19	03.06.2009	4.00	3.50
20	12.11.2008	5.00	3.50
21	12.11.2008	5.00	3.80
22	12.11.2008	6.20	4.10
23	15.10.2007	5.00	3.50
24	07.07.2006	4.00	3.60
25	28.12.2005	6.40	4.40
26	04.10.2005	7.60	3.50
27	04.10.2005	5.00	3.50
28	04.10.2005	4.40	3.80
29	08.02.2005	3.70	3.90
30	18.07.2004	11.00	4.30
31	02.07.2004	2.00	3.70
32	17.04.2004	9.00	3.50
33	28.01.2004	10.00	3.60
34	07.09.2003	5.00	3.50
35	01.09.2003	9.00	3.80
36	17.08.2003	10.00	3.60
37	12.08.2003	7.00	3.90
38	23.07.2002	5.00	4.00
39	19.12.2000	0.00	3.50
40	13.08.2000	0.00	3.50
41	17.07.2000	9.00	3.50
42	09.06.2000	0.00	3.50
43	09.06.2000	0.00	3.50
44	09.06.2000	1.00	3.70
45	09.06.2000	0.00	4.50
46	08.06.2000	0.00	3.50
47	27.05.2000	9.00	3.90
48	14.02.2000	2.00	3.60
49	14.02.2000	9.00	4.80
50	16.07.1999	23.00	3.80
51	05.07.1999	0.00	3.50
52	04.07.1999	22.00	3.80
53	27.04.1999	0.00	3.70
54	12.03.1999	2.00	3.50
55	17.02.1999	9.00	3.60
56	05.11.1998	4.00	3.90
57	22.10.1998	9.00	3.90
58	28.07.1998	1.00	3.50
59	24.04.1998	13.00	3.50
60	02.04.1998	11.00	3.50
61	06.01.1998	12.00	3.50
62	11.08.1997	7.00	3.50
63	09.06.1997	4.00	3.80
64	01.11.1994	13.00	3.50
65	18.05.1994	10.00	3.70
66	20.02.1993	10.00	3.90
67	03.02.1993	5.00	3.90
68	19.05.1992	7.00	3.60
69	14.04.1991	10.00	3.60
70	06.03.1991	10.00	3.50
71	11.12.1990	10.00	3.60
72	26.05.1990	10.00	4.00
73	09.02.1990	10.00	3.70
74	01.12.1989	10.00	3.60
75	02.10.1989	10.00	3.70
76	17.10.1986	12.00	4.40
77	15.05.1983	10.00	3.60
78	14.02.1983	33.00	4.10
79	28.06.1979	0.00	4.70
80	27.03.1979	10.00	3.80

Table 2.1. (Continued) *The list of earthquakes with a magnitude greater than 3.5 that have occurred in the study area and its close vicinity*

No	Date	Depth (km)	Magnitude
81	03.11.1978	10.00	4.20
82	12.10.1978	2.00	4.10
83	26.08.1978	0.00	4.00
84	15.11.1977	23.00	3.60
85	25.08.1977	0.00	3.50
86	20.09.1976	0.00	3.70
87	18.02.1976	3.00	4.40
88	04.06.1975	0.00	4.00
89	28.02.1975	0.00	3.60
90	27.08.1974	5.00	3.60
91	21.10.1973	5.00	4.10
92	04.07.1972	10.00	4.10
93	11.10.1971	5.00	3.70
94	20.09.1971	10.00	4.30
95	20.09.1971	10.00	4.10

No	Date	Depth (km)	Magnitude
96	20.09.1971	5.00	3.80
97	05.07.1971	5.00	4.40
98	04.05.1970	10.00	4.30
99	25.02.1969	31.00	4.30
100	10.01.1969	18.00	4.60
101	28.09.1968	38.00	4.10
102	10.09.1968	33.00	4.20
103	09.09.1968	33.00	4.60
104	03.09.1968	55.00	4.50
105	03.09.1968	14.00	4.70
106	03.09.1968	33.00	4.40
107	03.09.1968	11.00	4.70
108	03.09.1968	33.00	4.60
109	03.09.1968	5.00	6.50

2.4.1. A Deterministic Approach to Estimate PGA Value

Methods for the Next Generation Attenuation of Ground Motions (NGA) were released by the Pacific Earthquake Research Center (PEER) in 2008 to implement the earthquake ground – motion prediction equations. These methods were developed to estimate ground – motion parameters for shallow crustal earthquakes in active tectonic regions. During the NGA project, five different ground – motion prediction equations (GMPE) developed were the Abrahamson and Silva (2008), Boore and Atkinson (2008), Campbell and Bozorgnia (2008), Chiou and Youngs (2008) and Idriss (2008) equations. Site response is recognized as one of the most important factors for influence of ground motions. Accordingly, these ground motion influences are required to be modeled in engineering applications. In this study, all of the GMPE were implemented except Idriss (2008), because it does not clearly include site response. The other four models include site response more explicitly and use the same variable to describe the site condition (V_{s30}). These models also provide predictive relationships for the average horizontal component of ground motions (i.e., PGA) (USCS, 2010).

In this thesis, the weighted average value of the 2008 NGA models were determined by the procedure proposed by Al Atik (2009). In this procedure, the parameters; moment magnitude (M), surface and subsurface rupture lengths (R_{RUP} , R_{JB} , R_X) from source to site, rupture width (W), local average shear – wave velocity (V_{s30}) and fault type were evaluated. Moment magnitude was estimated by the $M = a + b \log(\text{SRL})$ relation (Wells and Coppersmith, 1994). In this relation; SRL is the Surface Rupture Length and a and b are the coefficients according to the fault type. V_{s30} was estimated by Standard Penetration Test (SPT) Correlations of Hasancebi and Ulusay (2007). Thereafter by this calculation, peak ground acceleration (PGA), peak ground velocity (PGV) and 5% – damped pseudo – absolute acceleration spectrum were estimated.

This method was performed for three different fault lines passing close to the study area, which are; the Karabük Fault, the Devrek Fault and the North Anatolian Fault. The Karabük Fault is a reverse fault with a total length of 35 kilometers and its distance to the study area is about 36 kilometers. The Devrek Fault is a strike slip fault with a total length of 40 kilometers and its distance to the study area is about 70 kilometers. Lastly, the North Anatolian Fault is also a strike slip fault with a total length of 1100 kilometers and its distance to the study area is about 70 kilometers.

The estimated PGA values with median plus one standard error predictions ($\text{PGA} + \sigma$) for three different fault lines are summarized in Table 2.2.

Table 2.2. Summary of the estimated PGA values

Fault Line	M (assigned)	PGA ($\text{PGA} + \sigma$) (g)
Karabük Fault	6.40	0.140 (0.244)
Devrek Fault	6.50	0.043 (0.075)
North Anatolian Fault	7.40	0.079 (0.135)

Regarding the calculated results, median plus one standard deviation ($\text{PGA} + \sigma$) values are accepted to give a more critical and predictable estimation. In other words, $\text{PGA} + \sigma$ values indicate the maximum horizontal accelerations. In addition, Karabuk Fault generates the most critical PGA value (0.244 g) for the study area that is relatively consistent with the PGA value proposed by the recently revised 2018 AFAD Earthquake Hazard Map of Turkey for the study area.

CHAPTER 3

PHYSIOGRAPHY AND CLIMATE

3.1. Geographical Location of the Study Area

Bartın is located at the western part of the Black Sea region in Northern Anatolia. The Province is surrounded by the Black Sea at the north and has 59 km of shoreline. Neighbouring provinces are Kastamonu at the east, Karabük at the southeast and Zonguldak at the west. The Bartın Province has a total area of 2330 km². Bartın is surrounded by steep mountains and cliffs at the east, west and north, which are not higher than 2000 m. The highest point is Keçikıran Hill (1619 m). The major watercourse of the Province is the Bartın stream. The other main streamline of the Bartın stream is the Gökırmak stream, which passes through the study area. The Gökırmak stream merges the Bartın stream at Cape Gazhane and eventually reaches the Black Sea. Bartın has a rugged terrain. The reason for the rugged terrain is the high energy flow of the Bartın stream and its intense erosion. However, flatter areas spread around the city center of Bartın (Bartın Provincial Planning and Coordination Directorate, 2015).

The study area is located approximately 1.5 km southeast of the Derbent Village. The Gökırmak stream and the D755 highway is close to the examination area to the north. Additionally, the study area and its vicinity are examined geomorphologically throughout a circular area with a radius of 2.5 km. Accordingly, the highest point is 892 m and the lowest point is 41 m above the sea level in this area. The average altitude is around 321 m above the sea level. The maximum slope throughout the area is measured to be 52 % in the north – northwestward direction and the minimum slope is measured as 0 %. The average slopes are in between 19 – 27 % and classified as “Dip steep slope” (Erol, 1993). The basin properties were also examined. The nearest

valley is the Gökırmak stream valley, which is 50 m to the north and has a base elevation of + 52 m. The study area has approximately + 170 m altitude where the basin relief of the area is calculated as $170 - 52 = 118$ m.

3.2. Climate

Bartın which is located in the Black Sea region has a typical marine climate. The summers are cool and the winters are warm and rainy. Bartın, which is a high precipitation area in almost all seasons, gets more precipitation especially in autumns and winters. Precipitation is as rain in the summers and as rain and snow in the winters.

The average temperature is 21° C in the summer and 6° C in the winter. Bartın has a humid climate and the relative humidity varies between 75 – 85 %. Bartın receives most of its precipitation in October, November and December. The average precipitation varies between 50 – 60 mm in the summer and 100 – 120 mm in the winter. The average annual precipitation is in between 1000 – 1200 mm (Karabük Provincial Directorate of Environment and Urbanization, 2012).

The climatic data of the Derbent Village, which is the nearest location to the study area, was obtained from Climate Data (2018). According to the data of years between 1982 and 2012, the annual average temperature of the Derbent Village is 13.5 °C. July has the highest average temperature with 22.1 °C and January has the lowest with 4.7 °C. The annual average precipitation of Derbent is 861 mm. The most arid month is July with an average precipitation of 51 mm and the most fluvial month December has 116 mm. The most fluvial period is between October and January. The annual temperature data graph is shown in Figure 3.1, and the annual precipitation data graph is shown in Figure 3.2.

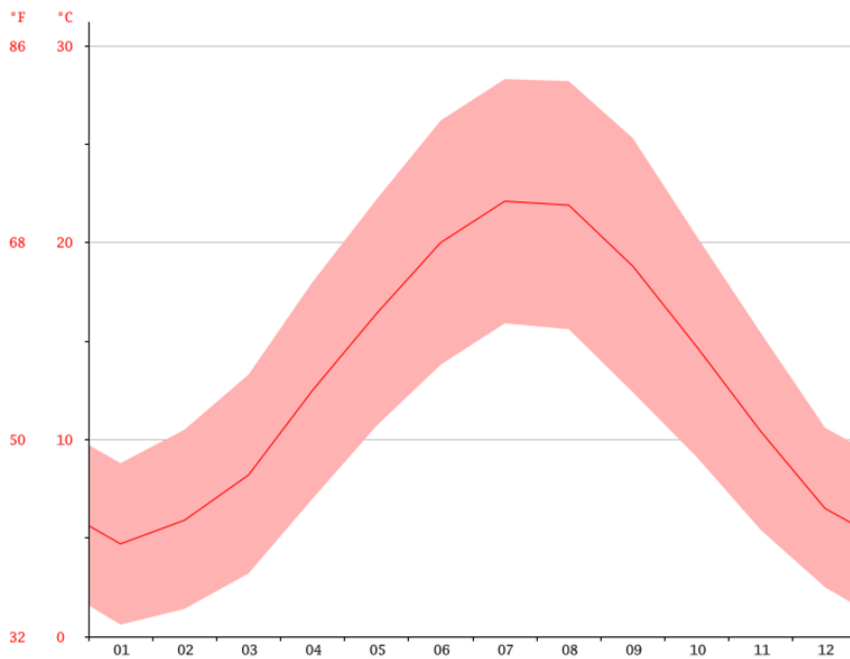


Figure 3.1. Average temperature values of the Derbent Village (Climate Data, 2018)

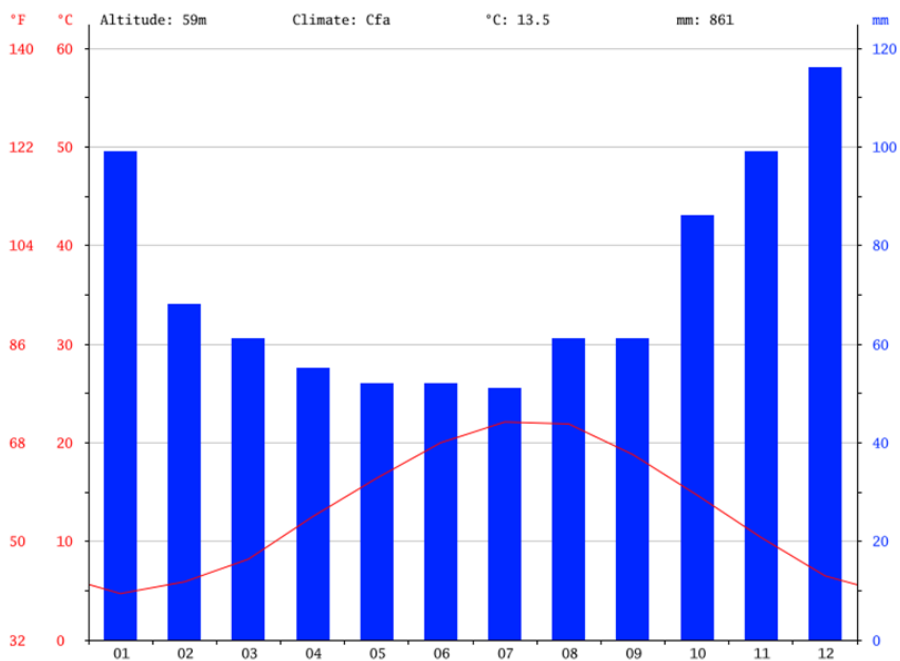


Figure 3.2. Average precipitation values of the Derbent Village (Climate Data, 2018)

CHAPTER 4

SITE INVESTIGATION

The site investigation consisting of site observation and surveys, in – situ tests, monitoring and laboratory tests are explained in this section.

4.1. Engineering Geological Mapping

Engineering geological map and cross sections of the study area were prepared based on site observations and previous geological mapping studies (Figures 4.1, 4.2, 4.3, 4.4 and 4.5). According to borehole and inclinometer data, the geological model of the area was created. The locations of the boreholes, cross sections, landslide and formation boundaries, groundwater level and the alignment of the new highway are shown in the engineering geological map and in the geological – geotechnical cross sections of the study area. The depth and the landslide boundary of the sliding mass were determined according to inclinometer readings. The area is represented by Landslide Material (Hm), Ulus Formation (Ku) and its weathered levels (Ku – W5).



Figure 4.1. A view from field studies

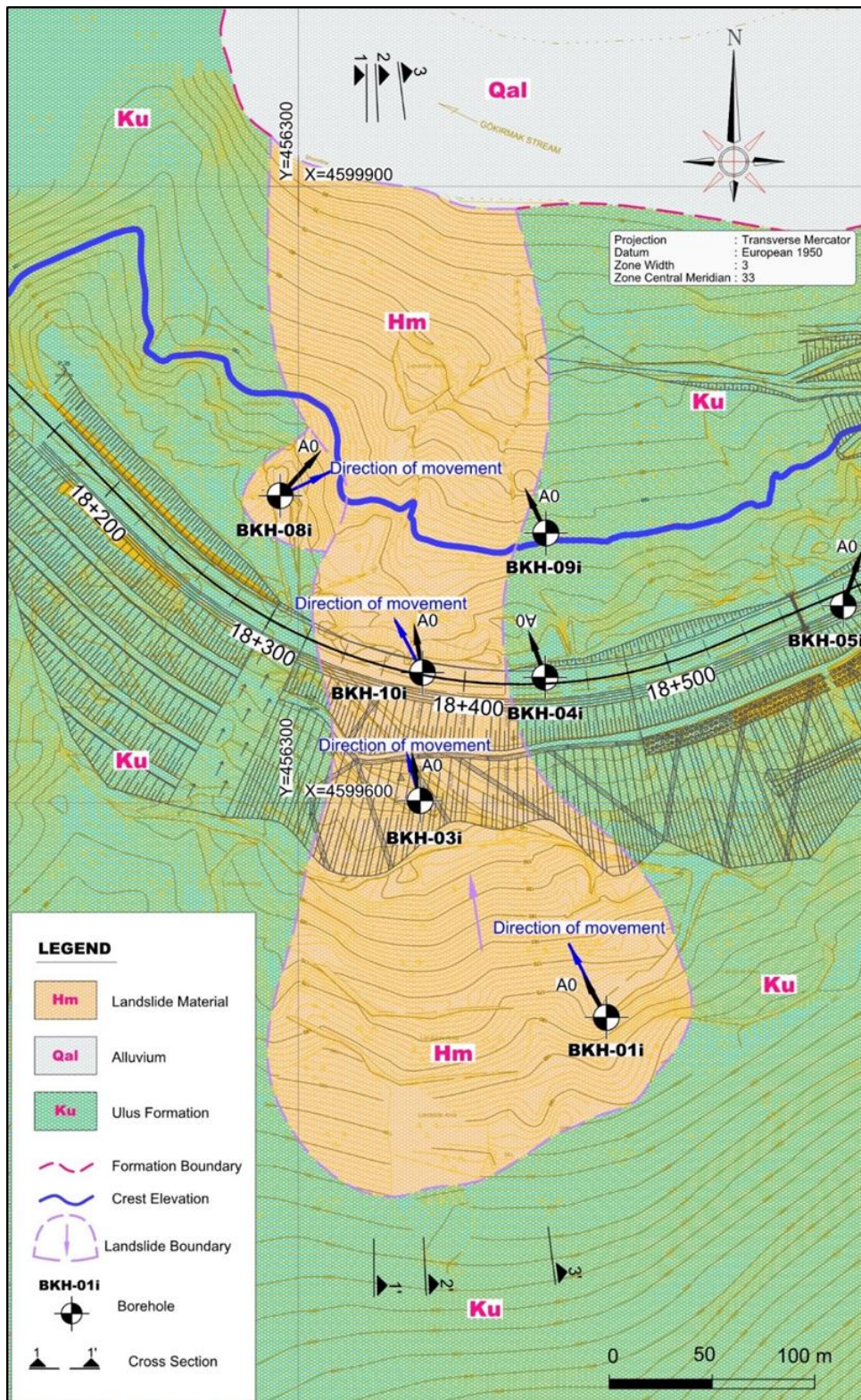


Figure 4.2. Engineering geological map of the study area

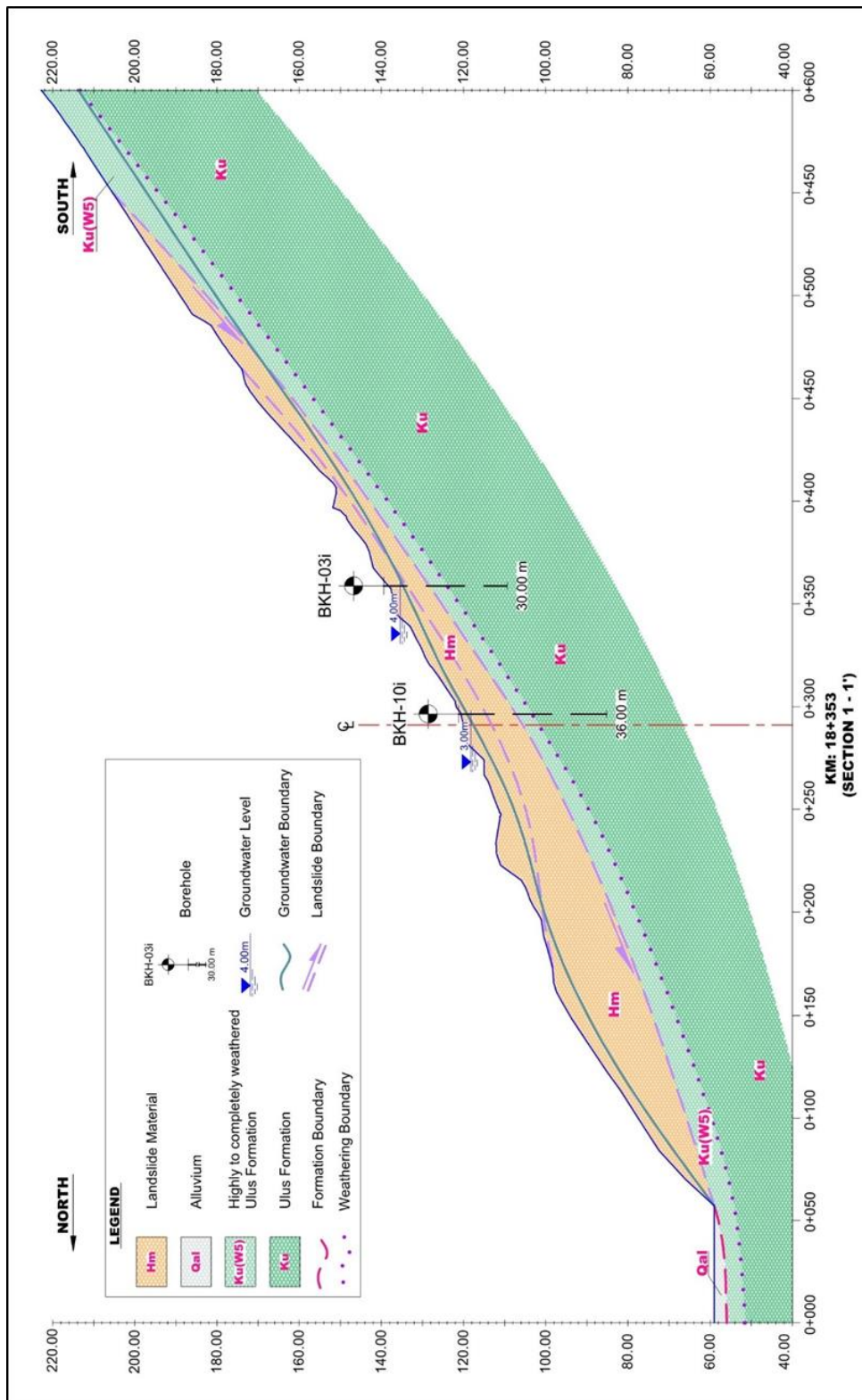


Figure 4.3. Geological – geotechnical cross section 1-1' (Km: 18 + 353)

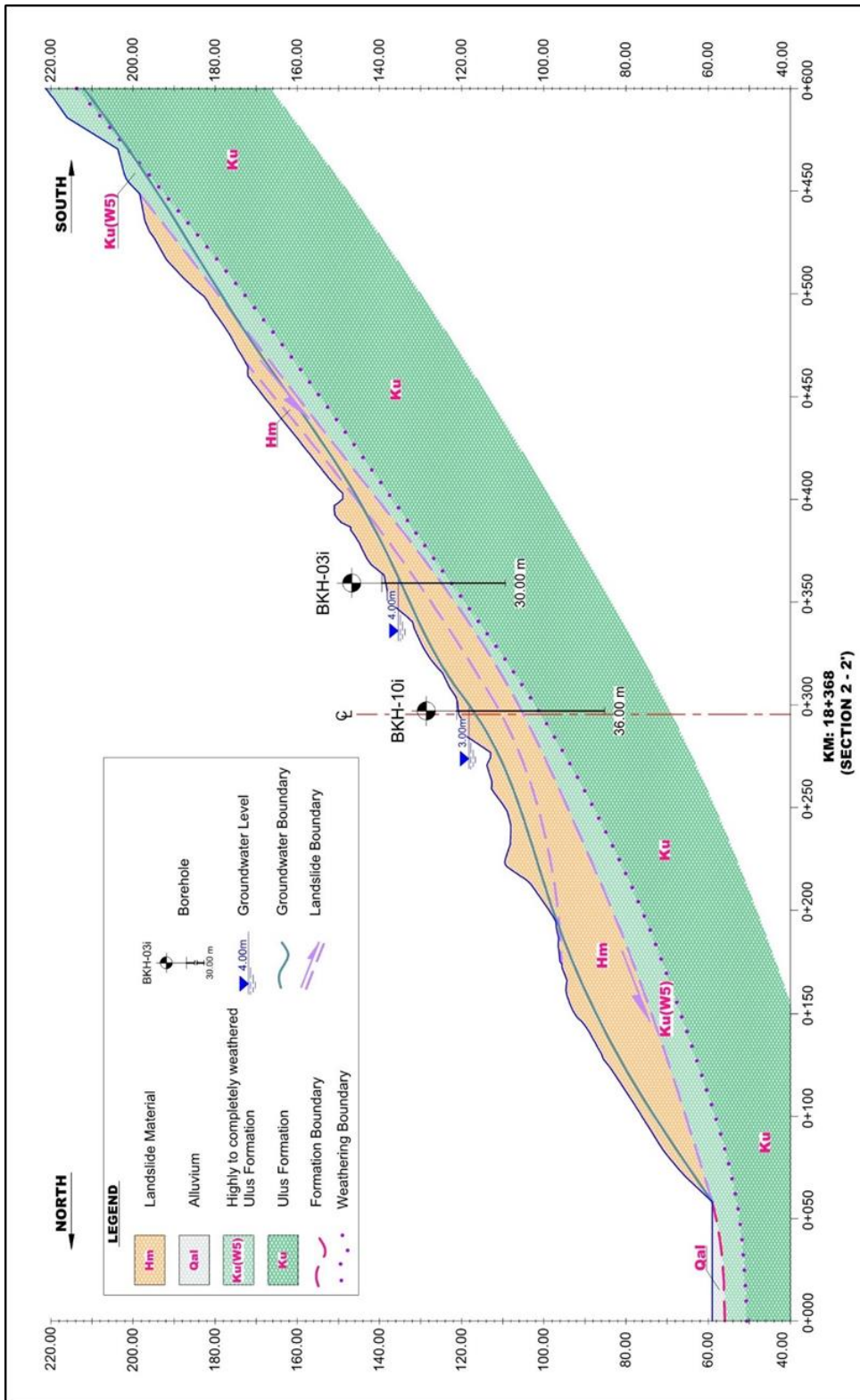


Figure 4.4. Geological – geotechnical cross section 2-2' (Km: 18 + 368)

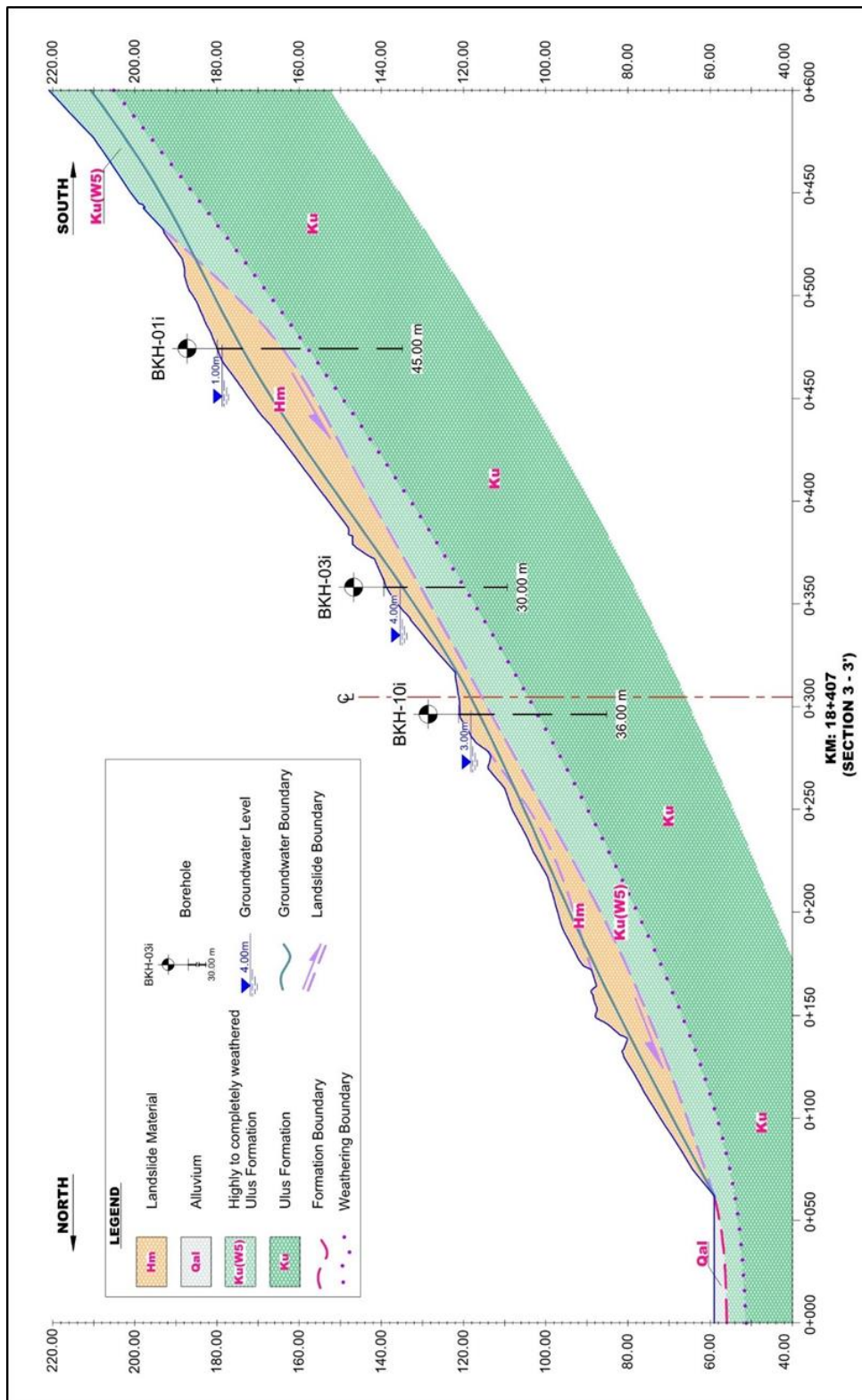


Figure 4.5. Geological – geotechnical cross section 3-3' (Km: 18 + 407)

4.2. Drilling Study

Borings with a total depth of 451.00 meters at 11 locations were executed in the project area for identifying the soil / rock types and structural features along the landslide area, determining the engineering geological properties of the formations, observing the groundwater level (GWL), selection of disturbed (SPT) soil samples and rock core samples representing the ground profile for laboratory testing. Boreholes and in – situ tests were conducted in accordance with the Research Engineering Services Technical Specification (2005); prepared by Republic of Turkey General Directorate of Highways, Department of Research and Development. Soil and rock (core) samples obtained by boreholes were placed and kept in core boxes. To measure GWL; circulation water in the boreholes was emptied by using the “bailer” bucket at the end of each work day and GWL measurements were recorded for each borehole next morning. In addition, perforated PVC pipes were installed in the completed boreholes for periodic observation of GWL. The results were recorded on the borehole logs.

Borehole locations are given in Figure 4.6, a summary of borehole data is given in Table 4.1, and a representative example of the borehole logs and core box photographs are submitted in App. – A and App. – B respectively.



Figure 4.6. Location of boreholes at the study area

Table 4.1. Summary of borehole study

Borehole ID	Coordinates (TM33 – ED50)			Depth (m)	Inclinometer Depth (m)	GWL (m)
	N (X)	E (Y)	Elevation (m)			
BKH – 01i (*)	4 599 495.579	456 450.029	173.406	45.00	45.00	1.00
BKH – 02i	4 599 636.964	456 590.094	151.344	45.00	45.00	5.00
BKH – 03i	4 599 601.066	456 359.258	139.428	30.00	30.00	4.00
BKH – 04i	4 599 661.164	456 420.183	122.17	50.00	50.00	3.00
BKH – 05i	4 599 695.943	456 565.305	122.056	60.00	60.00	2.50
BKH – 06i	4 599 699.783	456 694.801	141.500	45.00	45.00	6.00
BKH – 07i	4 599 751.403	456 665.867	122.973	45.00	43.50	2.50
BKH – 08i	4 599 749.419	456 291.134	120.083	30.00	30.00	2.30
BKH – 09i	4 599 731.255	456 420.500	104.500	35.00	35.00	7.50
BKH – 10i	4 599 663.391	456 360.472	121.250	36.00	36.00	3.00
BKH – 11	4 599 768.087	456 663.142	118.250	30.00	–	1.50

(*) “i” represents the boreholes with inclinometer measurements.

4.3. In – Situ Tests

Tests consisting of Standard Penetration Tests (SPT), pressuremeters and inclinometers were performed in boreholes. A summary of the in – situ tests are presented below.

4.3.1. Standard Penetration Test (SPT)

Standard Penetration Tests (SPT) were performed at regular depth intervals of 1.50 meters. Representative disturbed samples were taken in accordance with the standards of Republic of Turkey General Directorate of Highways, Research Engineering Services Technical Specification (2005) and ASTM D1586 – 11 standards, in order to determine the consistency of the soil and of the completely weathered upper sections of the rock units. SPT (N) values are presented numerically and graphically in borehole logs and a representative example is given in App. – A. It should be noted that the soil / rock samples were transferred to Yüksel Proje International Inc. Soil and Rock Mechanics Laboratory for laboratory geotechnical testing and geotechnical characterization. Table 4.2 gives a summary of the Standard Penetration Test results.

Table 4.2. A summary of the Standard Penetration Test results

Borehole ID	Depth (m)		SPT Blow Numbers			SPT N Value	Formation
			0 – 15 (cm)	15 – 30 (cm)	30 – 45 (cm)		
BKH – 01i	1.50	1.95	3	5	5	10	Landslide material (Hm)
	3.00	3.45	1	2	3	5	Landslide material (Hm)
	4.50	4.95	3	3	4	7	Landslide material (Hm)
	6.00	6.45	3	3	3	6	Landslide material (Hm)
	7.50	7.95	5	6	8	14	Landslide material (Hm)
	9.00	9.45	7	11	12	23	Landslide material (Hm)
	10.50	10.95	18	20	22	42	Ulus formation (Ku – W5)
	12.00	12.18	14	R	–	R	Ulus formation (Ku – W5)
BKH – 02i	1.50	1.95	2	4	6	10	Landslide material (Hm)
	3.00	3.45	6	6	5	11	Landslide material (Hm)
	4.50	4.95	13	40	19	59	Ulus formation (Ku – W5)
	6.00	6.45	18	23	38	61	Ulus formation (Ku – W5)
	7.50	7.63	R	–	–	R	Ulus formation (Ku – W5)
BKH – 03i	1.50	1.95	2	3	6	9	Landslide material (Hm)
	3.00	3.45	3	5	6	11	Landslide material (Hm)
	4.50	4.95	2	5	8	13	Landslide material (Hm)
	6.00	6.45	6	10	25	35	Landslide material (Hm)
	7.50	7.80	6	13	R	R	Landslide material (Hm)
	9.00	9.45	4	11	15	26	Landslide material (Hm)
	10.50	10.95	10	18	27	45	Landslide material (Hm)
	12.00	12.45	8	19	23	42	Landslide material (Hm)
	13.50	13.95	9	14	17	31	Landslide material (Hm)
	14.00	14.45	6	11	13	24	Landslide material (Hm)
	15.00	15.45	7	15	13	28	Ulus formation (Ku – W5)
	16.50	16.91	26	36	R	R	Ulus formation (Ku)
BKH – 04i	1.50	1.95	4	5	12	17	Ulus formation (Ku – W5)
	3.00	3.45	5	7	8	15	Ulus formation (Ku – W5)
	4.50	4.95	8	10	10	20	Ulus formation (Ku – W5)
	7.50	7.95	11	15	20	35	Ulus formation (Ku – W5)
	9.00	9.45	9	16	22	38	Ulus formation (Ku – W5)
	10.50	10.95	10	28	36	64	Ulus formation (Ku – W5)
	12.00	12.45	25	43	36	79	Ulus formation (Ku – W5)
BKH – 05i	1.50	1.72	13	R	–	R	Ulus formation (Ku – W5)
	3.00	3.45	24	26	38	64	Ulus formation (Ku – W5)
	4.50	4.75	23	R	–	R	Ulus formation (Ku – W5)
	7.50	7.95	10	22	24	46	Ulus formation (Ku – W5)
	9.00	9.20	40	R	–	R	Ulus formation (Ku – W5)
BKH – 06i	1.50	1.62	R	–	–	R	Landslide material (Hm)
	3.00	3.45	5	8	7	15	Landslide material (Hm)
	4.50	4.95	4	7	8	15	Landslide material (Hm)
	6.00	6.45	4	11	15	26	Landslide material (Hm)
	7.50	7.60	R	–	–	R	Landslide material (Hm)
	9.00	9.45	9	11	15	26	Landslide material (Hm)
	10.50	10.95	28	33	45	78	Landslide material (Hm)
	12.00	12.45	14	29	40	69	Ulus formation (Ku – W5)

Table 4.2. (Continued) A summary of the Standard Penetration Test results

Borehole ID	Depth (m)		SPT Blow Numbers			SPT N Value	Formation
			0 – 15 (cm)	15 – 30 (cm)	30 – 45 (cm)		
BKH – 07i	1.50	1.95	8	13	23	36	Ulus formation (Ku – W5)
	3.00	3.45	6	12	19	31	Ulus formation (Ku – W5)
	4.50	4.95	7	10	15	25	Ulus formation (Ku – W5)
	6.00	6.45	16	28	25	53	Ulus formation (Ku – W5)
	7.50	7.95	21	28	30	58	Ulus formation (Ku – W5)
BKH – 08i	1.50	1.95	2	2	3	5	Landslide material (Hm)
	3.00	3.45	0	1	2	3	Landslide material (Hm)
	4.50	4.95	3	3	4	7	Landslide material (Hm)
	6.00	6.45	6	11	16	27	Landslide material (Hm)
	7.50	7.95	20	27	31	58	Ulus formation (Ku – W5)
	9.00	9.45	22	33	47	80	Ulus formation (Ku – W5)
BKH – 09i	1.50	1.95	7	26	10	36	Ulus formation (Ku – W5)
	3.00	3.45	6	8	12	20	Ulus formation (Ku – W5)
	4.50	4.95	6	8	25	33	Ulus formation (Ku – W5)
	6.00	6.45	7	9	15	24	Ulus formation (Ku – W5)
	7.50	7.95	9	10	12	22	Ulus formation (Ku – W5)
	9.00	9.45	7	10	11	21	Ulus formation (Ku – W5)
	10.50	10.95	6	9	12	21	Ulus formation (Ku – W5)
	12.00	12.45	6	11	18	29	Ulus formation (Ku – W5)
	13.50	13.95	11	20	22	42	Ulus formation (Ku – W5)
	15.00	15.45	13	19	28	47	Ulus formation (Ku – W5)
	16.50	16.95	14	20	30	50	Ulus formation (Ku – W5)
BKH – 10i	1.50	1.95	3	4	7	11	Landslide material (Hm)
	3.00	3.45	5	10	12	22	Landslide material (Hm)
	4.50	4.95	6	33	15	48	Landslide material (Hm)
	6.00	6.45	5	7	12	19	Landslide material (Hm)
	7.50	7.95	8	13	19	32	Landslide material (Hm)
	9.00	9.45	5	11	15	26	Landslide material (Hm)
	10.50	10.95	8	33	28	61	Landslide material (Hm)
	12.00	12.45	7	21	20	41	Landslide material (Hm)
	13.50	13.95	12	18	26	44	Landslide material (Hm)
	15.00	15.45	10	12	17	29	Ulus formation (Ku – W5)
	16.50	16.95	14	24	46	70	Ulus formation (Ku – W5)
BKH – 11	1.50	1.95	10	10	12	22	Artificial fill (Yd)
	3.00	3.45	12	17	21	38	Artificial fill (Yd)
	4.50	4.95	12	12	11	23	Artificial fill (Yd)
	6.00	6.45	13	16	10	26	Ulus formation (Ku – W5)
	7.50	7.95	18	32	25	57	Ulus formation (Ku – W5)

4.3.2. Pressuremeter Test

Pressuremeter tests were performed in accordance with ASTM D4719 – 07 standards in order to determine the elastic properties of the geological units in the study area. Louis Menard GA type pressuremeter with a 60 mm N type probe was utilized. For each test location, deformation modulus (E_p), limit (P_l) and net limit (P_{ln}) pressure with respect to variable depth were determined. All of the test results are given in Table 4.3 and a representative example of the test graphs are given in App. – C.

Table 4.3. A summary of the pressuremeter test results

Borehole ID	Depth (m)	Pressuremeter limit pressure (P_{ln}) (kg / cm ²)	Pressuremeter modulus (E_p) (kg / cm ²)	Formation
BKH – 01i	3.90	0.44	64.25	Landslide material (Hm)
	6.90	3.21	25.00	Landslide material (Hm)
	9.90	13.76	249.04	Ulus formation (Ku – W5)
	12.90	21.64	499.25	Ulus formation (Ku – W5)
	16.40	30.58	300.85	Ulus formation (Ku)
	20.40	44.17	401.23	Ulus formation (Ku)
	24.40	59.20	2486.78	Ulus formation (Ku)
	28.40	65.69	914.71	Ulus formation (Ku)
	31.40	49.48	1540.85	Ulus formation (Ku)
	35.40	43.65	70490.07	Ulus formation (Ku)
BKH – 02i	2.40	3.12	67.50	Landslide material (Hm)
	5.40	17.55	199.98	Ulus formation (Ku – W5)
	8.40	15.03	153.96	Ulus formation (Ku – W5)
	11.40	27.78	602.37	Ulus formation (Ku – W5)
	14.40	66.72	1585.46	Ulus formation (Ku)
	17.40	44.83	3303.34	Ulus formation (Ku)
	20.40	43.75	1209.49	Ulus formation (Ku)
	23.40	75.87	9408.80	Ulus formation (Ku)
	26.40	44.63	71799.87	Ulus formation (Ku)
	29.40	44.68	70567.01	Ulus formation (Ku)
	32.40	62.17	913.90	Ulus formation (Ku)
	35.40	69.35	3502.27	Ulus formation (Ku)
	38.40	43.44	848.06	Ulus formation (Ku)
41.40	44.27	5051.70	Ulus formation (Ku)	
BKH – 03i	3.90	3.90	64.83	Landslide material (Hm)
	6.90	9.80	93.94	Landslide material (Hm)
	9.90	7.21	90.65	Landslide material (Hm)
	13.40	18.99	440.94	Landslide material (Hm)
	14.90	3.66	89.61	Ulus formation (Ku – W5)
	17.40	78.51	1331.87	Ulus formation (Ku)
	20.40	43.13	1365.04	Ulus formation (Ku)
	23.40	46.25	5688.28	Ulus formation (Ku)
	26.40	43.48	7078.85	Ulus formation (Ku)
	29.40	45.03	4552.72	Ulus formation (Ku)

Table 4.2. (Continued) *A summary of the pressuremeter test results*

Borehole ID	Depth (m)	Pressuremeter limit pressure (P_{lm}) (kg / cm²)	Pressuremeter modulus (E_p) (kg / cm²)	Formation
BKH – 04i	3.90	7.57	62.84	Ulus formation (Ku – W5)
	6.90	8.97	154.62	Ulus formation (Ku – W5)
	9.90	19.6	292.74	Ulus formation (Ku – W5)
	12.90	43.29	1782.05	Ulus formation (Ku – W5)
	15.90	42.84	1022.93	Ulus formation (Ku)
	18.90	43.31	1652.56	Ulus formation (Ku)
	21.90	49.97	8110.05	Ulus formation (Ku)
	24.90	43.01	2643.88	Ulus formation (Ku)
	27.90	49.64	4655.49	Ulus formation (Ku)
	30.90	43.55	70426.45	Ulus formation (Ku)
	33.90	43.46	70271.73	Ulus formation (Ku)
	36.90	55.31	5888.56	Ulus formation (Ku)
39.90	43.13	71045.23	Ulus formation (Ku)	
BKH – 05i	2.40	12.08	223.14	Ulus formation (Ku – W5)
	5.40	41.01	1205.77	Ulus formation (Ku – W5)
	9.90	38.92	595.16	Ulus formation (Ku – W5)
	12.90	50.53	1064.79	Ulus formation (Ku – W5)
	15.90	44.04	5933.49	Ulus formation (Ku)
	18.90	46.25	7032.67	Ulus formation (Ku)
	21.90	42.40	4871.49	Ulus formation (Ku)
	24.90	43.78	3466.59	Ulus formation (Ku)
	29.40	42.27	728.46	Ulus formation (Ku)
	32.40	63.76	2699.67	Ulus formation (Ku)
	35.40	68.01	6289.03	Ulus formation (Ku)
	38.40	42.52	1980.16	Ulus formation (Ku)
BKH – 06i	2.40	3.35	64.56	Landslide material (Hm)
	5.40	7.90	99.95	Landslide material (Hm)
	8.40	29.13	975.63	Landslide material (Hm)
	11.40	30.28	297.95	Ulus formation (Ku – W5)
	15.90	33.32	413.10	Ulus formation (Ku – W5)
	21.90	42.19	332.24	Ulus formation (Ku)
	26.40	43.25	838.67	Ulus formation (Ku)
	30.90	77.87	1533.13	Ulus formation (Ku)
	35.40	36.05	237.55	Ulus formation (Ku)
	38.40	38.04	1088.23	Ulus formation (Ku)
BKH – 07i	3.90	12.38	135.45	Ulus formation (Ku – W5)
	6.90	23.01	489.36	Ulus formation (Ku – W5)
	11.40	44.00	3947.69	Ulus formation (Ku)
	14.40	45.20	868.02	Ulus formation (Ku)
	17.40	43.79	3684.93	Ulus formation (Ku)
	20.40	43.80	2397.32	Ulus formation (Ku)
	23.40	47.97	6476.09	Ulus formation (Ku)
	26.40	67.99	1643.74	Ulus formation (Ku)
	29.40	61.37	4237.14	Ulus formation (Ku)
	32.40	43.72	5608.53	Ulus formation (Ku)
	35.40	44.18	8612.24	Ulus formation (Ku)
	37.40	65.75	4054.51	Ulus formation (Ku)

Table 4.2. (Continued) *A summary of the pressuremeter test results*

Borehole ID	Depth (m)	Pressuremeter limit pressure (P_{ln}) (kg / cm²)	Pressuremeter modulus (E_p) (kg / cm²)	Formation
BKH – 08i	5.40	2.66	50.66	Landslide material (Hm)
	8.40	19.58	393.15	Ulus formation (Ku – W5)
	11.40	19.75	285.44	Ulus formation (Ku – W5)
	14.40	37.34	938.11	Ulus formation (Ku)
	17.40	42.56	1691.18	Ulus formation (Ku)
	20.40	42.90	1314.63	Ulus formation (Ku)
	23.40	43.74	74029.69	Ulus formation (Ku)
	26.40	80.95	3538.41	Ulus formation (Ku)
	29.40	45.19	5162.32	Ulus formation (Ku)
BKH – 09i	3.90	5.60	94.48	Ulus formation (Ku – W5)
	6.90	7.02	186.17	Ulus formation (Ku – W5)
	9.90	11.52	255.66	Ulus formation (Ku – W5)
	14.40	11.58	366.95	Ulus formation (Ku – W5)
	17.40	11.91	113.26	Ulus formation (Ku – W5)
	20.40	46.08	1010.43	Ulus formation (Ku)
	23.40	34.26	348.56	Ulus formation (Ku)
	26.40	62.57	1388.11	Ulus formation (Ku)
	29.40	43.74	2253.06	Ulus formation (Ku)
	32.40	43.58	3824.89	Ulus formation (Ku)
BKH – 10i	3.90	5.72	95.66	Landslide material (Hm)
	8.40	7.71	215.07	Landslide material (Hm)
	11.40	9.89	166.20	Landslide material (Hm)
	14.40	7.52	101.25	Ulus formation (Ku – W5)
	17.40	10.82	212.22	Ulus formation (Ku – W5)
	20.40	57.90	1110.43	Ulus formation (Ku)
	23.40	51.89	2072.51	Ulus formation (Ku)
	27.40	42.94	1618.55	Ulus formation (Ku)
	31.40	42.93	875.90	Ulus formation (Ku)
	35.40	43.30	2284.14	Ulus formation (Ku)
BKH – 11	2.40	5.10	36.45	Artificial fill (Yd)
	5.40	7.73	157.66	Artificial fill (Yd)
	8.40	35.21	590.15	Ulus formation (Ku – W5)
	11.40	25.08	447.14	Ulus formation (Ku)
	14.40	40.53	749.64	Ulus formation (Ku)
	17.40	28.07	248.91	Ulus formation (Ku)
	20.40	33.37	352.09	Ulus formation (Ku)
	23.40	43.12	981.31	Ulus formation (Ku)
	26.40	52.50	2243.92	Ulus formation (Ku)
	29.40	51.81	1054.34	Ulus formation (Ku)

4.3.3. Inclinometers

In slope stability problems, it is necessary to verify the shape and location of the failure surfaces and the character of the mass movement. As the slope movements can be very slow and insensible to the eye, instrumentation and monitoring is highly important and desirable for the analysis of slope stability. Inclinometers are used to monitor and measure deformation through the profile of borehole in landslide areas. The philosophy of this method is measuring deformation normal to the axis of borehole by passing a probe along the borehole and measuring the inclination of the probe with respect to the line of gravity. Accordingly, inclinometers with a total depth of 419.50 meters have been installed in 10 boreholes at the study area and readings have been taken according to the ASTM 6230 – 13 standard during the period from 07.06.2016 to 13.07.2016 (Table 4.1). All collected data were converted into “Displacement vs. Depth and Time” graphs and a representative example is given in App – D. Also a summary of inclinometer readings are given in Table 5.2.

4.4. Laboratory Tests

In order to determine the relevant physical and index properties of the disturbed (SPT) samples taken from the soil units and completely weathered zones of the rock units in the course of the drilling works, the following laboratory tests were executed on the samples collected from the borings:

- Natural water content
- Atterberg limits
- Sieve analyses
- Unified Soil Classification (USCS)

On the other hand, core samples were tested at Yüksel Proje International Inc. Soil and Rock Mechanics Laboratory for determining the physical and mechanical properties of the rock samples obtained from boreholes. The relevant rock mechanics tests were unit weight, uniaxial compressive strength, modulus of elasticity. A representative example of the laboratory test results were given in App. – E.

CHAPTER 5

ENGINEERING GEOLOGICAL CHARACTERIZATION OF THE LANDSLIDE

5.1. Landslide Phenomenon and Types

Nearly all slopes ultimately degrade by the natural processes of weathering and down-slope transport. On most slopes, this is a continuous and a very slow process. Landslides occur where a slope remains static for a long period and then fails in a single dramatic event (Waltham, 2009). Landslides may occur in various material types such as (Varnes, 1978):

- Rock described as a hard or firm mass that was intact and in its natural place before the initiation of movement.
- Soil described as an aggregate of solid particles, generally of minerals and rocks that either was transported or was formed by the weathering of rock in place. Gases or liquids filling the pores of the soil form part of the soil.
- Earth described as material in which 80 % or more of the particles are smaller than 2 mm, the upper limit of sand sized particles.
- Mud described as material in which 80 % or more of the particles are smaller than 0.06 mm, the upper limit of silt sized particles
- Debris containing a significant ratio of coarse material where 20 % to 80 % of the particles are larger than 2 mm, and the remainder are less than 2 mm.

Slope failures are the result of gravitational forces acting on a mass which can creep slowly, fall freely, slide along some failure surface, or flow as a slurry. Stability can depend on a few complex variables, which can be placed into four general categories (Hunt, 2005);

- Topography — in terms of slope inclination and height
- Geology — in terms of material structure and strength
- Weather — in terms of seepage forces and run-off quantity and velocity
- Seismic activity — as it affects inertial and seepage forces

Varnes (1978) classified the landslides into five kinematically distinct types. These types are; fall, topple, slide, spread and flow (Table 5.1).

Table 5.1. *Classification of Landslides (Varnes, 1978)*

TYPE OF MOVEMENT		TYPE OF MATERIAL		
		BEDROCK	ENGINEERING SOILS	
			Predominantly coarse	Predominantly fine
FALLS		Rock fall	Debris fall	Earth fall
TOPPLES		Rock topple	Debris topple	Earth topple
SLIDES	ROTATIONAL	Rock slide	Debris slide	Earth slide
	TRANSLATIONAL			
LATERAL SPREADS		Rock spread	Debris spread	Earth spread
FLOWS		Rock flow (deep creep)	Debris flow (soil creep)	Earth flow
COMPLEX		Combination of two or more principal types of movement		

- Falls are abrupt movements of geologic material masses, such as rocks and boulders that become detached from steep slopes or cliffs. Separation occurs along discontinuities such as fractures, joints, bedding planes, and movement occurs by free – fall, bouncing, and rolling. Falls are strongly influenced by gravity, mechanical weathering and the presence of interstitial water.
- Toppling failures are distinguished by the forward rotation of a unit or units about some pivotal point, below or low in the unit, under the actions of gravity and forces exerted by adjacent units or by fluids in cracks.

- Slides: Although many types of mass movements are included in the general term “landslide,” the more restrictive use of the term refers only to mass movements, where there is a distinct zone of weakness that separates the slide material from more stable underlying material. The two major types of slides are rotational slides and translational slides.
- Lateral Spreads: Lateral spreads are distinctive because they usually occur on very gentle slopes or flat terrain. The dominant mode of movement is lateral extension accompanied by shear or tensile fractures. The failure is caused by liquefaction, the process whereby saturated, loose, cohesionless sediments (usually sands and silts) are transformed from a solid into a liquefied state.
- Flows are very rapid movements of soil and rock debris which may, or may not, begin with rupture along a failure surface.

In addition to these types, a combination of two or more of the above types is known as a complex landslide.

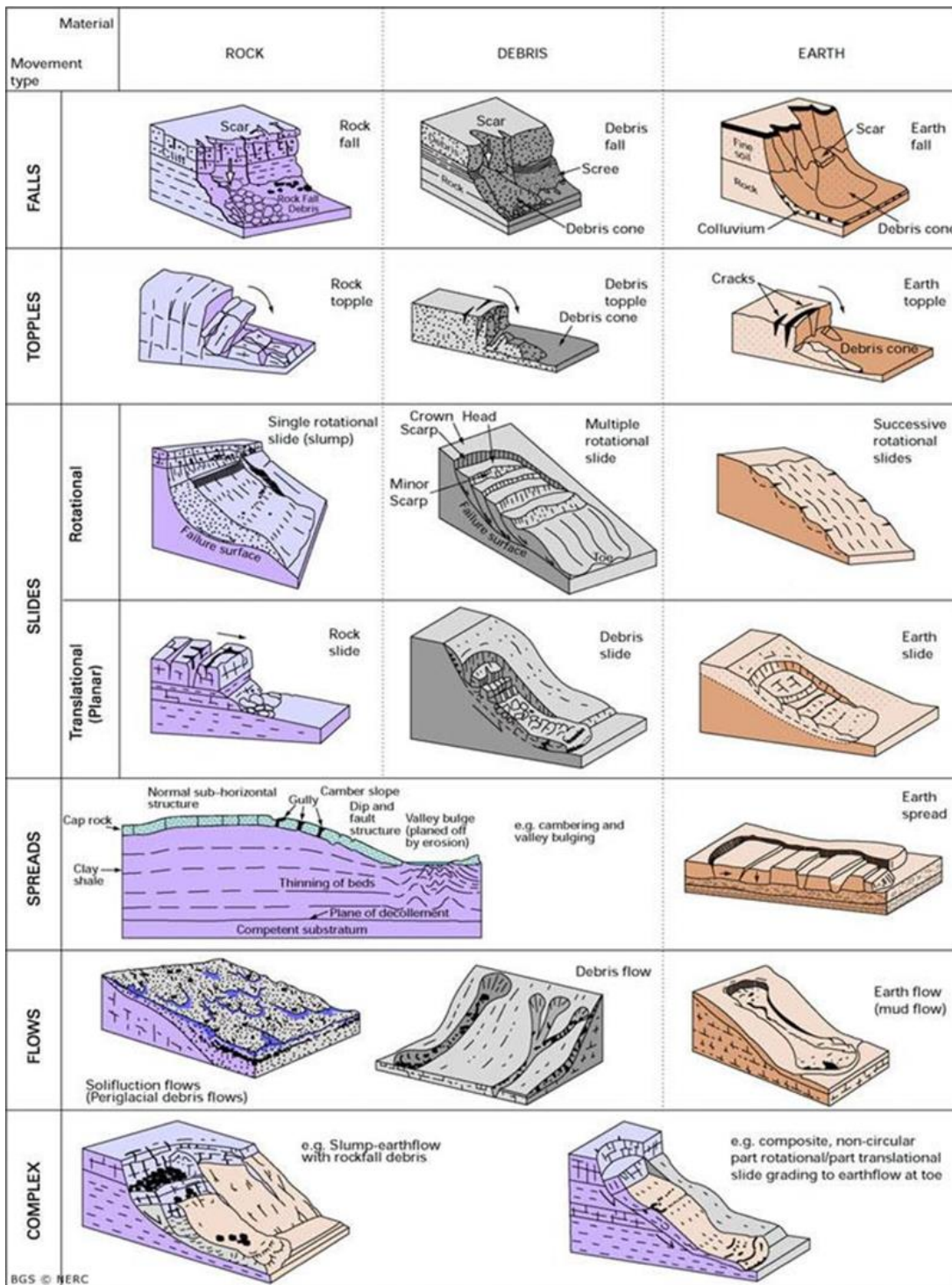


Figure 5.1. Landslide classification by Varnes (1978) and Cruden and Varnes (1996) based on the type of movement and material

5.2. Mechanism of Mass Movement

According to the results of the in – situ tests performed at the study area, a mass movement is determined at Km: 18 + 325 – 18 + 421 segment of the Bartın Kirazlı Bridge Dam Diversion (Figure – 5.2 and 5.3). The crown of the landslide is located at an elevation of + 205 m and has a width of 200 m at the southern slope of the road cut. The landslide narrows down to 95 m towards the middle part of the road. The toe of the landslide descends to elevation + 60 m towards the Gökırmak Stream Valley. The main mass of the landslide has a length of 490 meters and the width varies between 90 to 210 meters. The maximum thickness of the landslide mass is measured to be 30 meters.

The area has the characteristics of a fossil landslide terrain. A new mass movement activation has occurred in the fossil landslide area by the effects of surface and groundwater conditions and disturbance during road construction. However, the most important factor of this landslide hazard should be mentioned as the man – made influence on nature. The toe of the activated mass is observed to extend towards the Gökırmak Stream Valley.

According to drilling and inclinometer data, the mass movement is located at the contact of the Ulus formation (Ku) and its highly to completely weathered (Ku – W5) levels. The landslide material (Hm) observed in the study area is represented by sandy lean clay with gravel (CL), silty gravel with sand (GM) and blocks of the weathered levels of the claystone – siltstone – sandstone units. Hence, the grain size of the landslide material has a very wide range. Accordingly, movement characteristics of the sliding mass differ variously, such as slump – earth flows and debris slides observed together. Within this context, the movement type of the mass is classified as “Complex Movement” according to Varnes 1978.

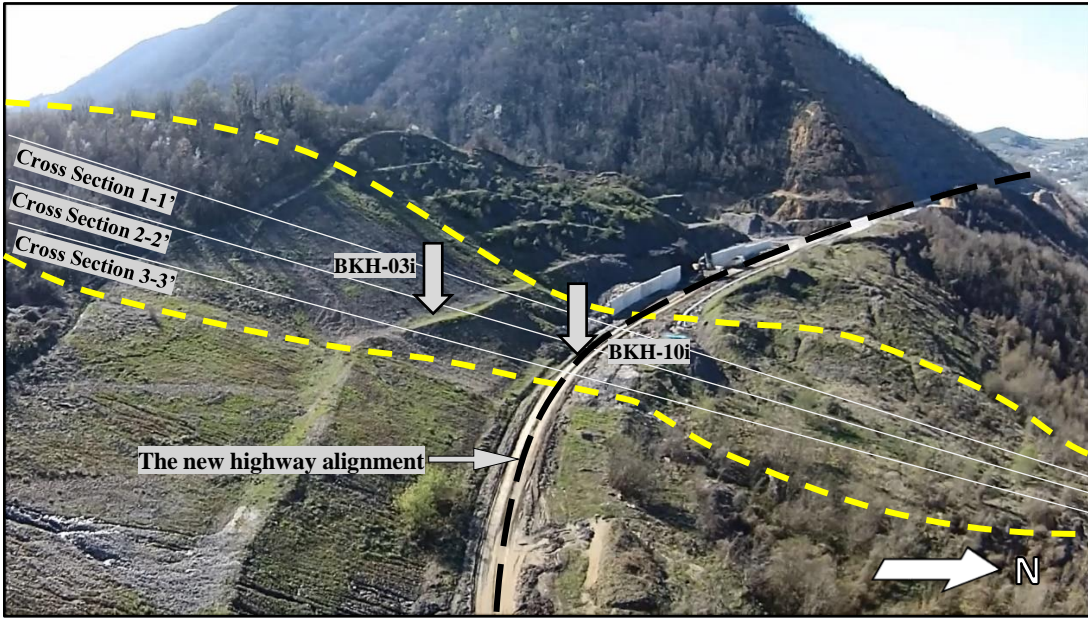


Figure 5.2. A side view of the morphology of the landslide area



Figure 5.3. A view of the morphology of the landslide area

5.2.1. Depth of Sliding Mass

A total number of 10 inclinometers were installed in the boreholes in the study area in order to determine the mass movement and the depth of the sliding surface. Six (6) of these inclinometers (Table – 5.2) were evaluated within the investigation related with the landslide. On the average, readings were taken for a period of 30 days in each location. Three of these inclinometers (BKH – 04i, 08i and 09i) were located outside of the landslide area but the other 3 (BKH – 01i, 03i and 10i) were located inside the landslide area. According to the readings, the depth of sliding mass was measured to lie between 9.20 to 14.20 meters. BKH – 01i is located at upper levels and 30 m north of the landslide crown. The velocity of the sliding mass is measured to vary between 0.43 and 3.91 mm / day. The fastest movement amongst all measurement points was measured at a depth of 14.80 m that possessed a velocity of 11.85 cm / month in BKH – 03i. In addition, no movement was observed in BKH – 04i and 09i. In addition, a small scaled landslide occurred at the artificial fill – rock contact as detected in BKH – 08i.

Table 5.2. A summary of inclinometer readings

Borehole ID	Depth (m)	Inclinometer Depth (m)	Sliding mass				
			Reading Time (days)	Depth (m)	Amount (mm)	Velocity (mm / day)	Velocity (cm / month)
BKH – 01i	45.00	45.00	32	9.80	43.00	1.34	4.06
BKH – 03i	30.00	30.00	32	9.20	85	2.66	8.06
				14.80	125	3.91	11.85
BKH – 04i	50.00	50.00	31	–	–	–	–
BKH – 08i	30.00	30.00	32	6.80	23.00	0.72	2.18
BKH – 09i	35.00	35.00	26	–	–	–	–
BKH – 10i	36.00	36.00	23	12.00	10.00	0.43	1.30
				14.20	23.00	1.00	3.03

5.3. Geomechanical Properties of Units

The borings, in – situ and laboratory tests have been conducted in order to determine the mechanical and physical properties of the soil and rock units prevailing in the project area and for obtaining the relevant parameters for geotechnical design. The lithological and geomechanical properties of these units are explained in this section.

The study area is represented by Landslide Material (Hm), Artificial Fill (Yd), Ulus Formation (Ku) and its highly to completely weathered levels (Ku – W5). The geological and geotechnical properties for these units are summarized below. Note that, degrees of rock mass weathering are classified as; W1 (Unweathered (Fresh)), W2 (Slightly weathered), W3 (Moderately weathered), W4 (Highly weathered) and W5 (Completely weathered) according to ISRM (1981).

5.3.1. Landslide Material (Hm)

Landslide material (Hm) with a varying thickness of 4.10 – 14.80 meters was observed in the investigation area to consist of sandy lean clay with gravel units. Sandy lean clay with gravel (CL) consisted of grey – dark grey – greenish grey – light brown – yellow – yellowish brown, stiff to very stiff, locally moderately stiff, moist, low to medium, locally high plastic; 20 – 30 % sandy, fine to coarse grained, locally friable; 15 – 20 % gravelly, fine to coarse grained, angular fragments of claystone – sandstone origin.

The results of the laboratory tests performed on samples taken from Standard Penetration Tests (SPT) and pressuremeter tests performed on the landslide material are given below.

SPT (N)	$5 \leq \text{SPT (N)} \leq \text{R (Refusal)}$ (Avg. 21)
Water content (W_n)	$8.80 \% \leq W_n \leq 25.00 \%$
Liquid limit (LL)	NP and $30.30 \% \leq \text{LL} \leq 50.70 \%$
Plasticity index (PI)	NP and $13.10 \leq \text{PI} \leq 26.30$
Sieve analysis (+4)	$1.10 \% \leq +4 \leq 38.00 \%$

Sieve analysis (-200)	$34.40 \% \leq -200 \leq 89.90 \%$
Soil classification (USCS)	CH, CL, SC, SM, GM
Pressuremeter limit pressure (P_{ln})	$0.44 \text{ kgf / cm}^2 \leq P_{ln} \leq 18.99 \text{ kgf / cm}^2$
Pressuremeter modulus (E_p)	$25.00 \text{ kgf / cm}^2 \leq E_p \leq 975.63 \text{ kgf / cm}^2$

5.3.2. Artificial Fill (Yd)

The artificial fill (Yd) observed in the study area has a varying thickness of 0.40 – 5.80 meters and is formed of fills of the existing roads in the study area and geomaterial residues of cut slope that were constructed in the past. In addition, artificial fills are represented by sandy lean clay with gravel units. Sandy lean clay with gravel consisted of grey – dark grey – yellowish brown, stiff, moist, low to medium plastic; 20 – 30 % sandy, fine to coarse grained, friable; 15 – 25 % gravelly, fine to coarse grained, angular fragments of sandstone origin.

The results of the laboratory tests performed on samples taken from Standard Penetration Tests (SPT) and pressuremeter tests performed on the artificial fill are given below.

SPT (N)	$22 \leq \text{SPT (N)} \leq 38$
Water content (W_n)	$10.90 \% \leq W_n \leq 12.50 \%$
Liquid limit (LL)	$29.60 \% \leq \text{LL} \leq 30.50 \%$
Plasticity index (PI)	$13.00 \leq \text{PI} \leq 13.20$
Sieve analysis (+4)	$25.10 \% \leq +4 \leq 33.40 \%$
Sieve analysis (-200)	$34.90 \% \leq -200 \leq 50.80 \%$
Soil classification (USCS)	CL, SC, GC
Pressuremeter limit pressure (P_{ln})	$5.10 \text{ kgf / cm}^2 \leq P_{ln} \leq 7.73 \text{ kgf / cm}^2$
Pressuremeter modulus (E_p)	$36.45 \text{ kgf / cm}^2 \leq E_p \leq 157.66 \text{ kgf / cm}^2$

5.3.3. Highly to completely weathered Ulus Formation (Ku – W5)

Highly to completely weathered Ulus formation (Ku – W5) was observed in boreholes performed in the study area with a thickness varying from 0.40 to 15.30 meters and represented by sandy lean clay with gravel (CL), silty gravel with sand (GM) and highly to completely weathered claystone – siltstone – sandstone units. Sandy lean clay with gravel consisted of grey – dark grey – light brown – yellowish brown – stiff to very stiff, moist, low to medium plastic, locally high plastic; 20 – 30 % sandy, fine to coarse grained, friable; 10 – 15 % gravelly, fine to coarse grained, angular, hard, locally slightly hard fragments. Partly sandstone originated blocks were observed. Silty gravel with sand consisted of grey, very dense, moist, locally wet, fine to coarse grained, hard, locally friable; 20 – 30 % sandy, fine to medium grained; 15 – 20 % fines with low to medium plasticity clay.

The results of the total core recovery (TCR) and rock quality designation (RQD) values and the laboratory tests performed on samples taken from Standard Penetration Tests (SPT) and pressuremeter tests performed in the highly to completely weathered Ulus formation are given below.

Total core recovery (TCR)	$43 \% \leq \text{TCR} \leq 100 \%$ (Avg. 80 %)
Rock quality designation (RQD)	$0 \% \leq \text{RQD} \leq 26 \%$ (Avg. 2 %)
SPT (N)	$15 \leq \text{SPT (N)} \leq 47$ (Avg. 42)
Water content (W_n)	$6.50 \% \leq W_n \leq 23.20 \%$
Liquid limit (LL)	NP and $32.90 \% \leq \text{LL} \leq 43.50 \%$
Plasticity index (PI)	NP and $12.80 \leq \text{PI} \leq 25.70$
Sieve analysis (+4)	$0.00 \% \leq +4 \leq 74.00 \%$
Sieve analysis (-200)	$12.50 \% \leq -200 \leq 97.70 \%$
Soil classification (USCS)	CL, SC, SM, GC, GM
Pressuremeter limit pressure (P_{ln})	$5.60 \text{ kgf / cm}^2 \leq P_{ln} \leq 43.29 \text{ kgf / cm}^2$
Pressuremeter modulus (E_p)	$62.84 \text{ kgf / cm}^2 \leq E_p \leq 1782.05 \text{ kgf / cm}^2$

5.3.4. Ulus Formation (Ku)

Claystone, siltstone and sandstone units with partly brecciated levels in the investigation area represent the bedrock that form the Ulus formation. Claystones are grey – dark grey, blackish grey, friable to slightly hard, locally soft, weak to very weak, moderately to highly weathered, locally completely weathered. The joints are 20°, 30°, 45°, open, smooth, locally slickensided, locally rough, locally clay – silt filled. The joints could not be observed due to weathering in some sections. Siltstones are grey – dark grey, slightly to moderately hard, locally friable, moderately weak to weak, locally extremely weak, slightly to moderately weathered, locally highly weathered. Open joints are in the range of 0° – 75°, open, shiny, smooth, locally slickensided, locally clay – silt filled. Infilled joints are 10°, 30°, 45°, 60°, calcite filled up to 3 cm thickness. Sandstones are grey – light grey, moderately hard to hard, moderately strong to strong, locally moderately weak, slightly to moderately weathered. Open joints are in the range of 10° – 70°, locally shiny, rough, locally smooth to slickensided. Infilled joints are 30°, 45°, 60°, 75°, calcite filled up to 3 cm thickness. The joints could not be observed due to weathering in some sections. Brecciated levels are grey – dark grey, friable, locally slightly hard, very to extremely weak, locally weak, moderately to highly weathered, locally completely weathered.

The results of the rock mechanics tests conducted on the core samples obtained from the boreholes in the study area with relevant total core recovery (TCR) and rock quality designation (RQD) values and pressuremeter tests performed in Ulus formation (Ku) are summarized below.

Total core recovery (TCR) $40 \% \leq \text{TCR} \leq 100 \%$ (Avg. 94 %)

Rock quality designation (RQD) $0 \% \leq \text{RQD} \leq 100 \%$ (Avg. 54 %)

Uniaxial compressive strength (σ_{ci}) $4.60 \text{ MPa} \leq \sigma_{ci} \leq 33.80 \text{ MPa}$

Unit weight (γ_n) $23.14 \text{ kN} / \text{m}^3 \leq \gamma_n \leq 25.69 \text{ kN} / \text{m}^3$

Elasticity modulus (E_i) $0.70 \text{ GPa} \leq E_i \leq 15.10 \text{ GPa}$

Pressuremeter limit pressure (P_{ln}) $25.08 \text{ kgf / cm}^2 \leq P_{ln} \leq 80.95 \text{ kgf / cm}^2$

Pressuremeter modulus (E_p) $237.55 \text{ kgf / cm}^2 \leq E_p \leq 74\,029.69 \text{ kgf / cm}^2$

In addition, the results of laboratory tests performed on samples taken from Standard Penetration Tests (SPT) performed in weathered upper levels of Ulus formation are given below.

SPT (N)	R (Refusal)
Water content (W_n)	10.70 %
Liquid limit (LL)	32.10 %
Plasticity index (PI)	12.80
Sieve analysis (+4)	18.90 %
Sieve analysis (-200)	45.80 %
Soil classification (USCS)	SC

CHAPTER 6

DETERMINATION OF GEOTECHNICAL PARAMETERS

6.1. Empirical Approach (Effective Parameters)

Geotechnical parameters of the landslide material (Hm), which represented by very stiff sandy lean clay with gravel (CL) units, are determined below:

Unit weight

$\gamma = 18 \text{ kN / m}^3$ (Carter & Bentley, 1991) (Table 6.1)

Table 6.1. *Typical values of natural density (Carter & Bentley, 1991)*

TYPICAL VALUES OF NATURAL DENSITY		Natural density (kg / m ³)	
Material		Bulk density*	Dry density
Sands and gravels:	very loose	1700 – 1800	1300 – 1400
	loose	1800 – 1900	1400 – 1500
	medium dense	1900 – 2100	1500 – 1800
	dense	2000 – 2200	1700 – 2000
	very dense	2200 – 2300	2000 – 2200
Poorly – graded sands		1700 – 1900	1300 – 1500
Well – graded sands		1800 – 2300	1400 – 2200
Well – graded sand / gravel mixtures		1900 – 2300	1500 – 2200
Clays:	unconsolidated muds	1600 – 1700	900 – 1100
	soft, open – structured	1700 – 1900	1100 – 1400
	typical, normally consolidated	1800 – 2200	1300 – 1900
	boulder clays (overconsolidated)	2000 – 2400	1700 – 2200
Red tropical soils		1700 – 2100	1300 – 1800

Effective strength (Long term) parameters

True angle of (effective) internal friction:

$PI_{\text{mean}} = 19.78 \%$ (Mean value) $\rightarrow \phi' = 28^\circ$ (Gibson, 1953) (Figure 6.1)

With the calculated value, angle of internal friction is determined as $\phi' = 28^\circ$.

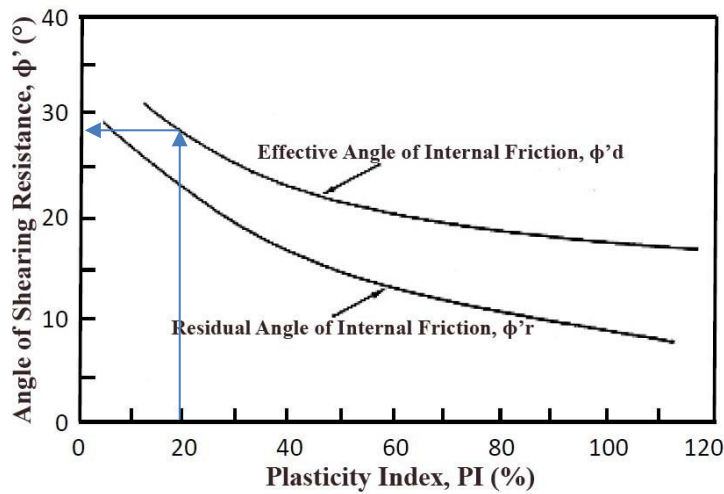


Figure 6.1. Range of shearing resistance angle and plasticity index in clays (Gibson, 1953)

Effective cohesion value:

$$c' = \alpha \times \tan \phi' \quad (\text{Lunne et al., 1997})$$

$$\phi' \text{ (Angle of shearing resistance)} = 28^\circ$$

α = Coefficient according to soil type (= 30) (Lunne et al., 1997) (Table 6.2)

$$c' = 30 \times \tan (28) = 15.95 \text{ kPa}$$

Table 6.2. α coefficient values for different soil types (Lunne et al., 1997)

Soil Type	α^*	$\tan\phi'$
Soft clay	5 – 10	0.35 – 0.45
Medium stiff clay	10 – 20	0.40 – 0.55
Stiff clay	20 – 50	0.50 – 0.60
Soft silt	0 – 5	0.50 – 0.60
Medium stiff silt	5 – 15	0.55 – 0.65
Stiff silt	15 – 30	0.60 – 0.70

With the calculation above, c' is determined as 15 kPa.

Geotechnical parameters for the landslide material are determined as;

$$\gamma = 18 \text{ kN} / \text{m}^3$$

$$c' = 15 \text{ kPa}, \phi' = 28^\circ$$

Analyses regarding residual shear strength parameters that represent a more realistic situation since they present an account for the sliding displacement of the landslide failure surface are presented in Section 7.2.

6.2. Rock Mass Rating (RMR)

The “Rock Mass Rating (RMR)” system was developed by Bieniawski (1989). In this method, five different parameters are considered in order to perform rock mass classification. These parameters are:

- Strength of the Intact Rock Material
- Rock Quality Designation (RQD) value
- Spacing of Discontinuities
- Condition of Discontinuities
- Ground Water Conditions

In this method, each parameter receives a specific numeric value according to the specific properties of the rock mass. Then, the sum of these numerical values is adjusted by discontinuity conditions. The adjusted total value is defined as the RMR value.

The RMR calculation of the rock units of the Ulus formation (Ku) has been performed (Tables 6.3 and 6.4). Then, using the equation $GSI = RMR - 5$ (Hoek and Brown, 1997), Geological Strength Index (GSI) values were obtained for the same units (Table 6.5).

Table 6.3. Rock Mass Rating (Bieniawski, 1989)
for highly to completely weathered Ulu formation (Ku – W5)

A. CLASSIFICATION PARAMETERS AND THEIR RATINGS									
Parameter		Range of values							
1	Strength of intact rock material	Point-load strength index	>10 MPa	4 - 10 MPa	2 - 4 MPa	1 - 2 MPa	For this low range - uniaxial compressive test is preferred		
		Uniaxial comp. strength	>250 MPa	100 - 250 MPa	50 - 100 MPa	25 - 50 MPa	5 - 25 MPa	1 - 5 MPa	< 1 MPa
	Rating		15	12	7	4	2	1	0
2	Drill core Quality RQD		90% - 100%	75% - 90%	50% - 75%	25% - 50%	< 25%		
	Rating		20	17	13	8	3		
3	Spacing of discontinuities		> 2 m	0.6 - 2 . m	200 - 600 mm	60 - 200 mm	< 60 mm		
	Rating		20	15	10	8	5		
4	Condition of discontinuities (See E)		Very rough surfaces Not continuous No separation Unweathered wall rock	Slightly rough surfaces Separation < 1 mm Slightly weathered walls	Slightly rough surfaces Separation < 1 mm Highly weathered walls	Slickensided surfaces or Gouge < 5 mm thick or Separation 1-5 mm Continuous	Soft gouge >5 mm thick or Separation > 5 mm Continuous		
		Rating		30	25	20	10	0	
5	Ground water	Inflow per 10 m tunnel length (l/m)	None	< 10	10 - 25	25 - 125	> 125		
		(Joint water press/ (Major principal)	0	< 0.1	0.1, - 0.2	0.2 - 0.5	> 0.5		
	General conditions	Completely dry	Damp	Wet	Dripping	Flowing			
	Rating		15	10	7	4	0		
B. RATING ADJUSTMENT FOR DISCONTINUITY ORIENTATIONS (See F)									
Strike and dip orientations			Very favourable	Favourable	Fair	Unfavourable	Very Unfavourable		
Ratings	Tunnels & mines		0	-2	-5	-10	-12		
	Foundations		0	-2	-7	-15	-25		
	Slopes		0	-5	-25	-50			
C. ROCK MASS CLASSES DETERMINED FROM TOTAL RATINGS									
Rating		100 81	80 61	60 41	40 21	< 21			
Class number		I	II	III	IV	V			
Description		Very good rock	Good rock	Fair rock	Poor rock	Very poor rock			
D. MEANING OF ROCK CLASSES									
Class number		I	II	III	IV	V			
Average stand-up time		20 yrs for 15 m span	1 year for 10 m span	1 week for 5 m span	10 hrs for 2.5 m span	30 min for 1 m span			
Cohesion of rock mass (kPa)		> 400	300 - 400	200 - 300	100 - 200	< 100			
Friction angle of rock mass (deg)		> 45	35 - 45	25 - 35	15 - 25	< 15			
E. GUIDELINES FOR CLASSIFICATION OF DISCONTINUITY conditions									
Discontinuity length (persistence)		< 1 m	1 - 3 m	3 - 10 m	10 - 20 m	> 20 m			
Rating		6	4	2	1	0			
Separation (aperture)		None	< 0.1 mm	0.1 - 1.0 mm	1 - 5 mm	> 5 mm			
Rating		6	5	4	1	0			
Roughness		Very rough	Rough	Slightly rough	Smooth	Slickensided			
Rating		6	5	3	1	0			
Infilling (gouge)		None	Hard filling < 5 mm	Hard filling > 5 mm	Soft filling < 5 mm	Soft filling > 5 mm			
Rating		6	4	2	2	0			
Weathering Ratings		Unweathered	Slightly weathered	Moderately weathered	Highly weathered	Decomposed			
		6	5	3	1	0			
F. EFFECT OF DISCONTINUITY STRIKE AND DIP ORIENTATION IN TUNNELLING**									
Strike perpendicular to tunnel axis				Strike parallel to tunnel axis					
Drive with dip - Dip 45 - 90°		Drive with dip - Dip 20 - 45°		Dip 45 - 90°		Dip 20 - 45°			
Very favourable		Favourable		Very unfavourable		Fair			
Drive against dip - Dip 45-90°		Drive against dip - Dip 20-45°		Dip 0-20 - Irrespective of strike°					
Fair		Unfavourable		Fair					

Table 6.4. Rock Mass Rating (Bieniawski, 1989) for Ulus formation (Ku)

A. CLASSIFICATION PARAMETERS AND THEIR RATINGS								
Parameter		Range of values						
1	Strength of intact rock material	Point-load strength index	>10 MPa	4 - 10 MPa	2 - 4 MPa	1 - 2 MPa	For this low range - uniaxial compressive test is preferred	
		Uniaxial comp. strength	>250 MPa	100 - 250 MPa	50 - 100 MPa	25 - 50 MPa	5 - 25 MPa	1 - 5 MPa
	Rating	15	12	7	4	2	1	0
2	Drill core Quality RQD	90% - 100%	75% - 90%	50% - 75%	25% - 50%	< 25%		
	Rating	20	17	13	8	3		
3	Spacing of discontinuities	> 2 m	0.6 - 2 . m	200 - 600 mm	60 - 200 mm	< 60 mm		
	Rating	20	15	10	8	5		
4	Condition of discontinuities (See E)	Very rough surfaces Not continuous No separation Unweathered wall rock	Slightly rough surfaces Separation < 1 mm Slightly weathered walls	Slightly rough surfaces Separation < 1 mm Highly weathered walls	Slickensided surfaces or Gouge < 5 mm thick or Separation 1-5 mm Continuous	Soft gouge >5 mm thick or Separation > 5 mm Continuous		
		Rating	30	25	20	10	0	
5	Ground water	Inflow per 10 m tunnel length (l/m)	None	< 10	10 - 25	25 - 125	> 125	
		(Joint water press)/ (Major principal)	0	< 0.1	0.1, - 0.2	0.2 - 0.5	> 0.5	
	General conditions	Completely dry	Damp	Wet	Dripping	Flowing		
	Rating	15	10	7	4	0		
B. RATING ADJUSTMENT FOR DISCONTINUITY ORIENTATIONS (See F)								
Strike and dip orientations		Very favourable	Favourable	Fair	Unfavourable	Very Unfavourable		
Ratings	Tunnels & mines	0	-2	-5	-10	-12		
	Foundations	0	-2	-7	-15	-25		
	Slopes	0	-5	-25	-50			
C. ROCK MASS CLASSES DETERMINED FROM TOTAL RATINGS								
Rating	100 81	80 61	60 41	40 21	< 21			
Class number	I	II	III	IV	V			
Description	Very good rock	Good rock	Fair rock	Poor rock	Very poor rock			
D. MEANING OF ROCK CLASSES								
Class number	I	II	III	IV	V			
Average stand-up time	20 yrs for 15 m span	1 year for 10 m span	1 week for 5 m span	10 hrs for 2.5 m span	30 min for 1 m span			
Cohesion of rock mass (kPa)	> 400	300 - 400	200 - 300	100 - 200	< 100			
Friction angle of rock mass (deg)	> 45	35 - 45	25 - 35	15 - 25	< 15			
E. GUIDELINES FOR CLASSIFICATION OF DISCONTINUITY conditions								
Discontinuity length (persistence)	< 1 m	1 - 3 m	3 - 10 m	10 - 20 m	> 20 m			
Rating	6	4	2	1	0			
Separation (aperture)	None	< 0.1 mm	0.1 - 1.0 mm	1 - 5 mm	> 5 mm			
Rating	6	5	4	1	0			
Roughness	Very rough	Rough	Slightly rough	Smooth	Slickensided			
Rating	6	5	3	1	0			
Infilling (gouge)	None	Hard filling < 5 mm	Hard filling > 5 mm	Soft filling < 5 mm	Soft filling > 5 mm			
Rating	6	4	2	2	0			
Weathering Ratings	Unweathered	Slightly weathered	Moderately weathered	Highly weathered	Decomposed			
Rating	6	5	3	1	0			
F. EFFECT OF DISCONTINUITY STRIKE AND DIP ORIENTATION IN TUNNELLING**								
Strike perpendicular to tunnel axis				Strike parallel to tunnel axis				
Drive with dip - Dip 45 - 90°		Drive with dip - Dip 20 - 45°		Dip 45 - 90°		Dip 20 - 45°		
Very favourable		Favourable		Very unfavourable		Fair		
Drive against dip - Dip 45-90°		Drive against dip - Dip 20-45°		Dip 0-20 - Irrespective of strike°				
Fair		Unfavourable		Fair				

Table 6.5. Summary of RMR values of the rock units

Lithology	Strength of Intact Rock Material		RQD		Spacing of Discontinuities		Condition of Discontinuities		Ground water	RMR	GSI (*)
	Description	Rating	Description	Rating	Description	Rating	Description	Rating	Rating	Rating	Rating
Weathered Ulus formation (Ku – W5)	5 MPa	1	2	3	< 60 mm	5	Smooth, soft filling, highly weathered	6	10	25	20
Ulus formation (Ku)	16 MPa	2	65	13	60 – 200 mm	8	Slightly rough, hard filling, moderately weathered	11	10	44	39

* GSI = RMR – 5 (Hoek and Brown, 1997)

The strength of the intact rock material represents the weighted average values of uniaxial compressive strength (σ_{ci}) tests performed on the rock samples of the related unit. The Rock Quality Designation (RQD) was developed by Deere (1963) and determined as the ratio of the total length of core pieces greater than 10 cm to the total core run. The average length of discontinuities through the core run was calculated as “Spacing of Discontinuities”. Observable properties of joints were defined as “Condition of Discontinuities”.

6.3. Geological Strength Index (GSI)

The Geological Strength Index (GSI) system was also used to estimate rock mass properties of the rock units observed in the study area. The GSI classification was initially introduced by Hoek (1994) and was developed by various researches during the years. In this study, the GSI Chart of Sonmez and Ulusay (2002) was preferred to classify the rock units, where Structure Rating (SR) and Surface Condition Rating (SCR) were evaluated. SCR was evaluated by discontinuity conditions observed at the outcrops and in the core samples. To obtain SR, Volumetric Joint Count (J_v) is needed.

J_v is obtained by the $RQD = 110 - 2.5 \times J_v$ (Palmstrom, 2005) relation where RQD is calculated from the core samples. Accordingly, intersection of SCR and SR gives the individual GSI value for each rock unit (Tables 6.6 and 6.7). A summary of the GSI values are given in Table 6.8.

Table 6.6. Geological Strength Index (Sonmez and Ulusay, 2002) for the highly to completely weathered Ulus formation (Ku – W5)

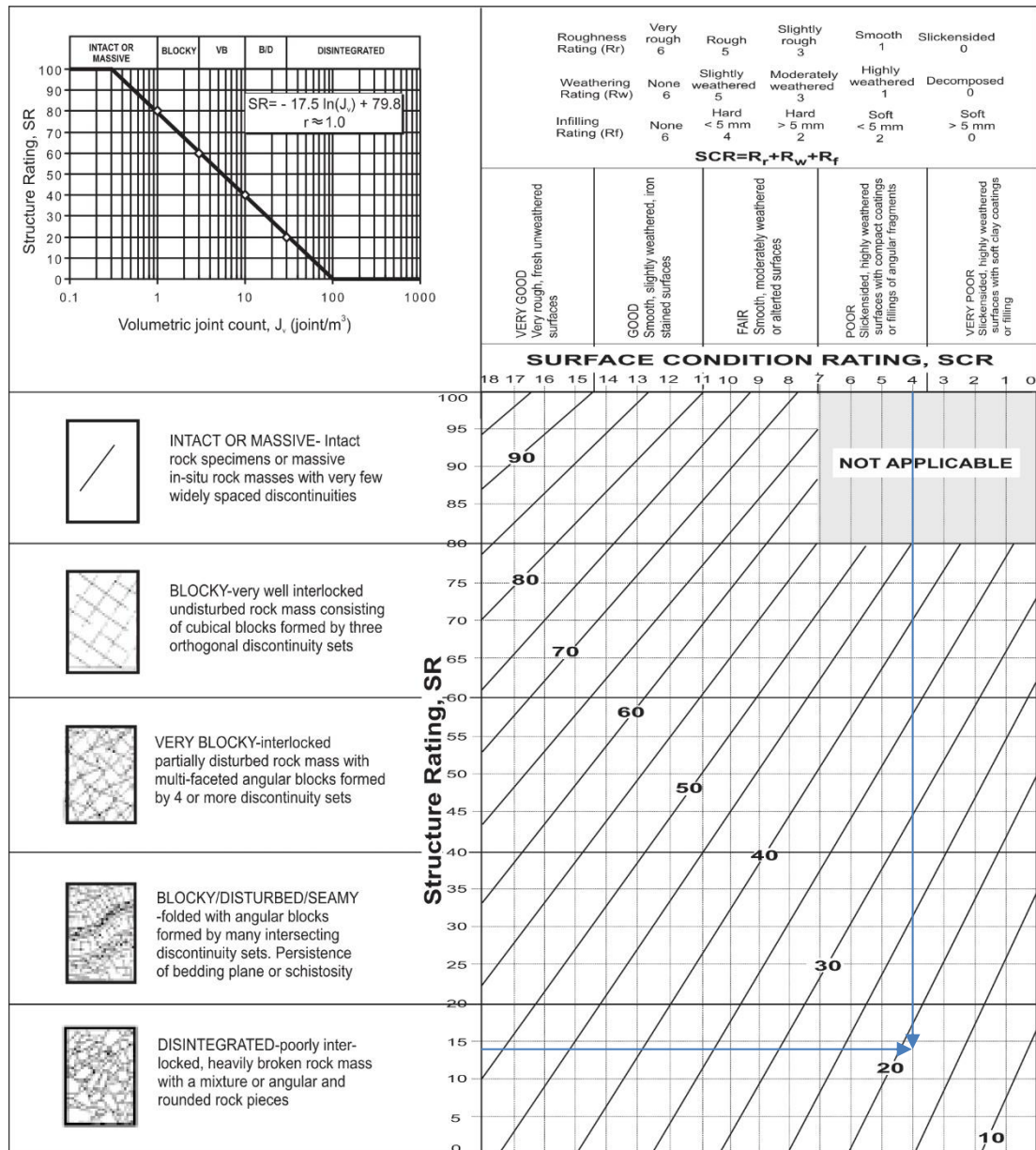


Table 6.7. Geological Strength Index (Sonmez and Ulusay, 2002) for the Ulus formation (Ku)

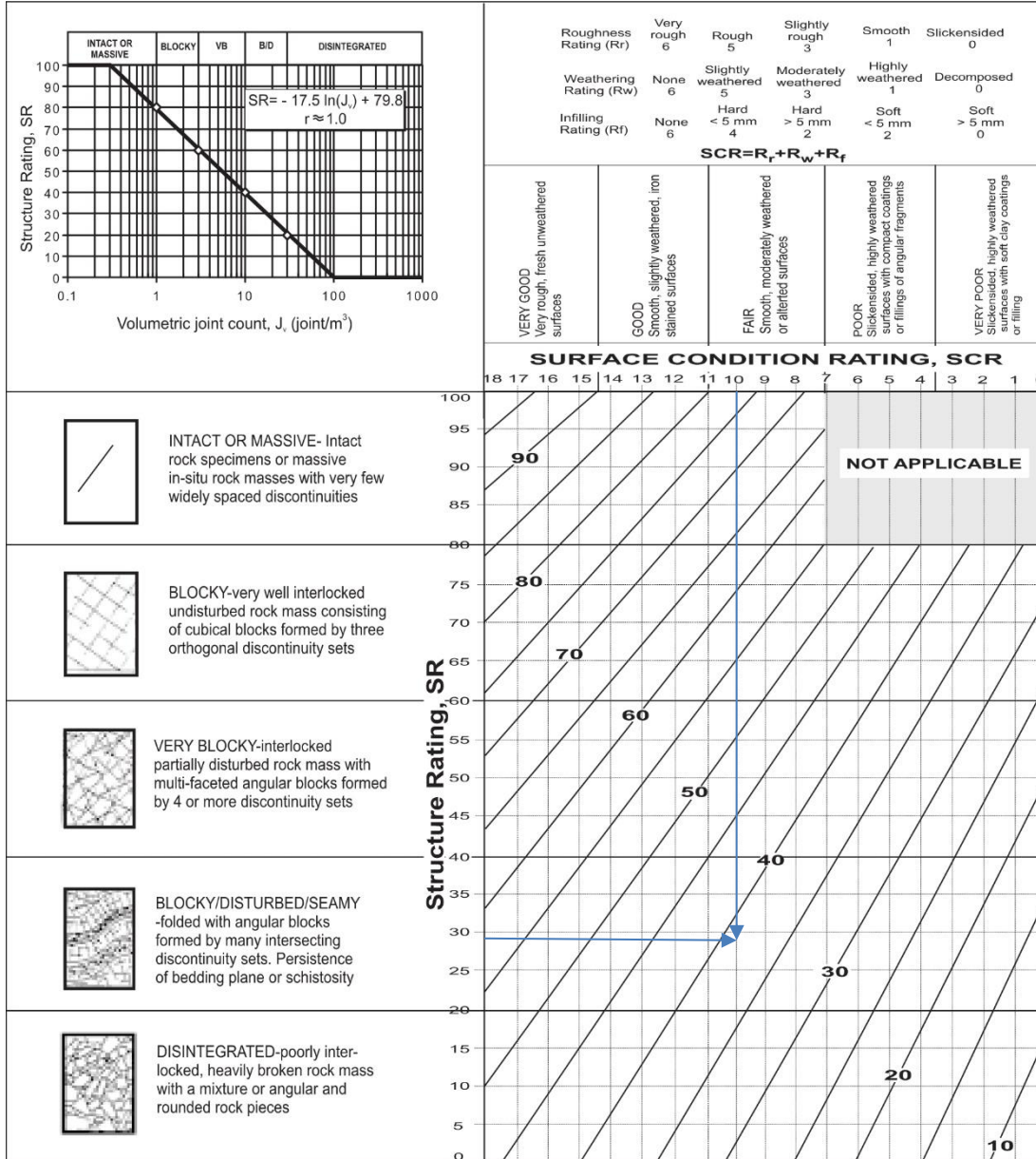


Table 6.8. Calculation of Geological Strength Index (GSI) ratings with Sonmez and Ulusay's (2002) Chart

Lithology	RQD (%)	Jv	SR	Joint ratings			SCR	GSI	GSI (RMR – 5)
				Roughness (Rr)	Weathering (Rw)	Infilling (Rf)			
Weathered Ulus formation (Ku – W5)	2	43	14	1	1	2	4	19	20
Ulus formation (Ku)	65	18	29	4	4	2	10	39	39

Therefore, the geomechanical and structural properties of the rock units observed in the study area were evaluated and the GSI values for each unit were calculated by the RMR and the GSI methods. The obtained results from the two methods give almost the same GSI values. To be on the safe side, GSI of 19 has been chosen for the Ku – W5 unit (i.e., the landslide material).

6.4. Analysis of Rock Strength Using RocData

RocData is a software to determine the rock strength parameters, based on the Generalized Hoek – Brown Failure Criterion (2002). The data obtained from in – situ and laboratory tests are evaluated and used as input parameters (Table 6.9) in RocData software (v 5.006). Accordingly, the output (rock strength) parameters are obtained to be used in landslide stability analysis. The input parameters used in the RocData software are listed below:

- Uniaxial compressive strength (σ_{ci}),
- Geological Strength Index (GSI),
- Intact rock parameter (m_i),
- Disturbance factor (D),
- Intact modulus (E_i),
- Unit weight (γ)

The rock strength parameters and normal vs shear stress graphs for the Ulus formation (Ku) units obtained from the RocData software are also given in Figures 6.2 and 6.3.

Table 6.9. Input rock mass parameters

Lithology	Uniaxial compressive strength (σ_{ci}) (MPa)	GSI	Intact rock parameter (m_i)	Disturbance factor (D)	Intact modulus (E_i) (MPa)	Unit weight (γ) (kN / m ³)
Weathered Ulus formation (Ku – W5)	5	19	10	0.7	1 000	24.00
Ulus formation (Ku)	16	39	10	0	4 500	25.00

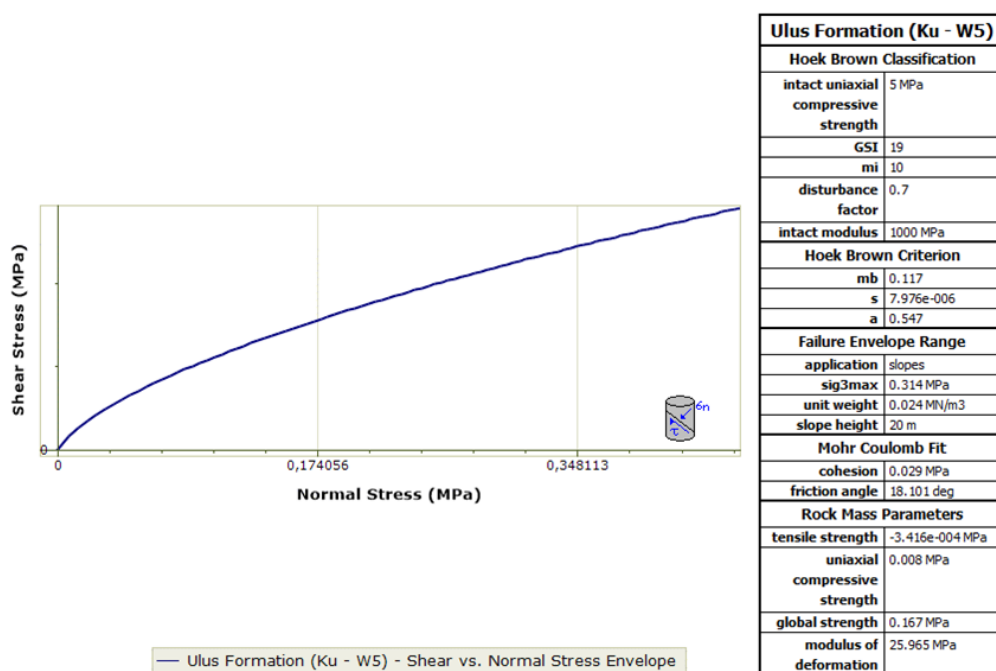


Figure 6.2. Normal vs Shear Stress graph for highly to completely weathered Ulus formation (Ku – W5) unit (h = 20.00 m)

The rock mass strength parameters determined for the 20.00 m high, highly to completely weathered Ulus formation (Ku – W5) are given below.

$$\gamma = 24.0 \text{ kN / m}^3$$

$$c = 29 \text{ kPa}, \phi = 18^\circ$$

$$E = 25 \text{ MPa}$$

It needs to be stated that this result was also compatible with the avg. Pressuremeter Modulus (E_p) value obtained from pressuremeter tests (i.e., 30.63 MPa).

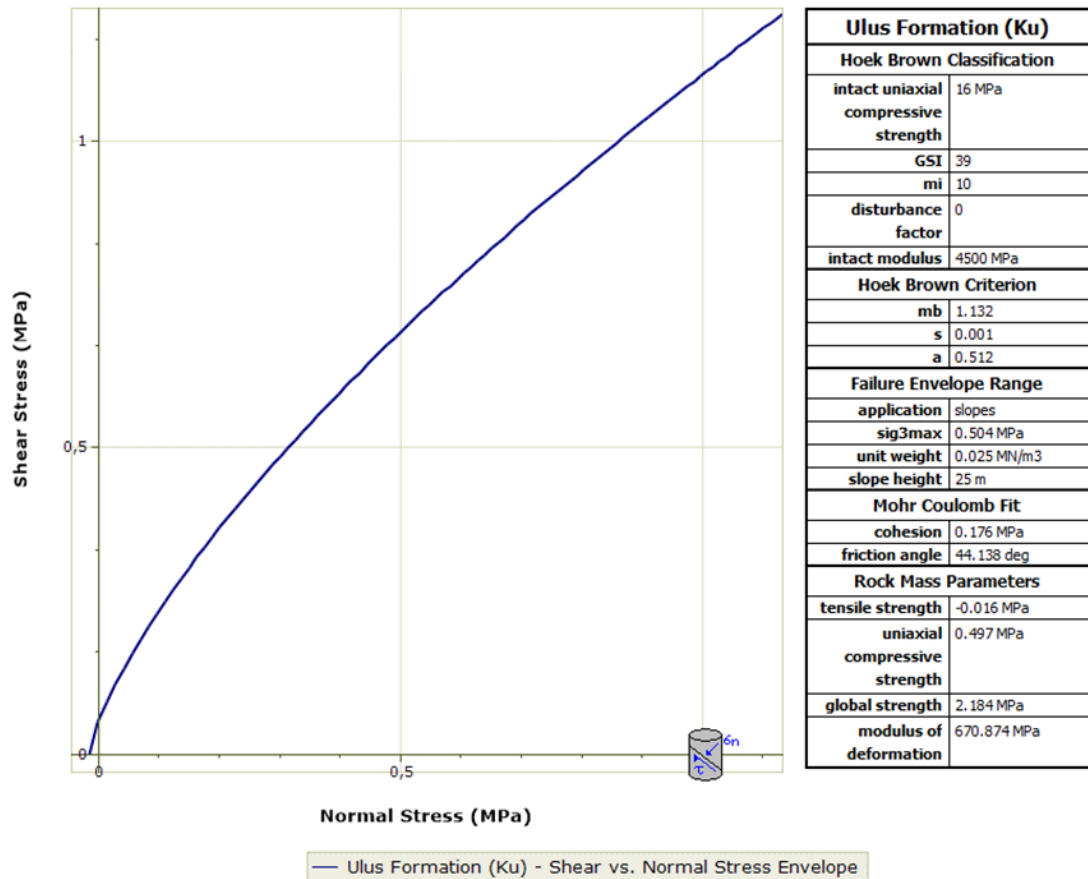


Figure 6.3. Normal vs Shear Stress graph for the Ulus formation (Ku) unit (h = 25.00 m)

The rock mass strength parameters determined for the 25.00 m high Ulus formation (Ku) are given below.

$$\gamma = 25.0 \text{ kN} / \text{m}^3$$

$$c = 176 \text{ kPa}, \phi = 44^\circ$$

$$E = 670 \text{ MPa}$$

It needs to be stated that this result was also compatible with the average Pressuremeter Modulus (E_p) value obtained from pressuremeter tests (i.e., 707.01 MPa).

CHAPTER 7

GEOTECHNICAL ASSESMENT OF SLOPE

7.1. Slope Stability Analysis Methods

7.1.1. Limit Equilibrium Methods

Once appropriate shear strength properties such as pore water pressures, slope geometry, and other soil and slope properties are established, slope stability calculations need to be performed to ensure that the resisting forces are sufficiently greater than the forces tending to cause a slope to fail. Calculations usually consist of computing a factor of safety using one of several limit equilibrium procedures of analysis. All of these procedures of analysis employ the same definition of the factor of safety and compute the factor of safety using the equations of static equilibrium (Duncan, 2014).

This method is based on the definition of a safety factor that is the ratio of shearing strength, as determined by resistive forces, to the shearing or disruptive forces. At a safety factor of 1.00, the forces are exactly in balance. A safety factor less than 1.00 implies slope failure, and a safety factor greater than 1.00 indicates stability. When the mean value of the material properties is used, the safety factor is defined as a deterministic safety factor. When the material properties are entered into the analyses as statistical populations, a probabilistic safety factor and an estimate of the probability of slope failure may be computed (Hustrulid et al., 2001).

The equilibrium shear stress is equal to the available shear strength divided (factored) by the factor of safety. The factor of safety represents the factor by which the shear strength must be divided so that the reduced strength is just in equilibrium with the

shear stress (τ) (i.e., the slope is in a state of just-stable limiting equilibrium). The procedures used to perform such computations are known as limit equilibrium procedures (Duncan, 2014).

The shear strength can be expressed by the Mohr – Coulomb equation. If the shear strength is expressed in terms of total stresses, Eq. (7.1) and (7.2) is written as: (Duncan, 2014)

$$\tau = \frac{c + \sigma \tan \phi}{F} \text{ (Eq. 7.1)}$$

or

$$\tau = \frac{c}{F} + \frac{\sigma \tan \phi}{F} \text{ (Eq. 7.2)}$$

Where c and ϕ are the cohesion and friction angle for the soil, respectively, and σ is the total normal stress on the shear plane. The same values for the factor of safety are applied to cohesion and friction angle in this equation. Equation (7.2) can also be written as

$$\tau = c_d + \sigma \tan \phi_d \text{ (Eq. 7.3)}$$

where

$$c_d = \frac{c}{F} \text{ (Eq. 7.4)}$$

$$\tan \phi_d = \frac{\tan \phi}{F} \text{ (Eq. 7.5)}$$

The quantities c_d and ϕ_d represent the developed (or mobilized) cohesion and friction angle, respectively. If the shear strength is expressed in terms of effective stresses (e.g., drained shear strengths are being used), the only change from the above is that Eq. (7.1) is written in terms of effective stresses as: (Duncan, 2014)

$$\tau = \frac{c' + (\sigma - u) \tan \phi'}{F} \text{ (Eq. 7.6)}$$

Where c' and ϕ' represent the shear strength parameters in terms of effective stresses, and u is the pore water pressure.

7.1.1.1. The Method of Slices

The distribution of the effective normal stresses along the failure surface must be known to calculate the mobilized strength for a soil. This condition is usually analyzed by discretizing the mass of the failure slope into smaller slices and treating each individual slice as a unique sliding block. Most computer programs use the method of slices, as it can readily accommodate complex slope geometries, variable soil conditions, and the influence of external boundary loads (Abramson et al., 2002).

All limit equilibrium methods for slope stability analysis divide a slide – mass into n smaller slices (Figure 7.1). Each slice is affected by a general system of forces (Figure 7.2).

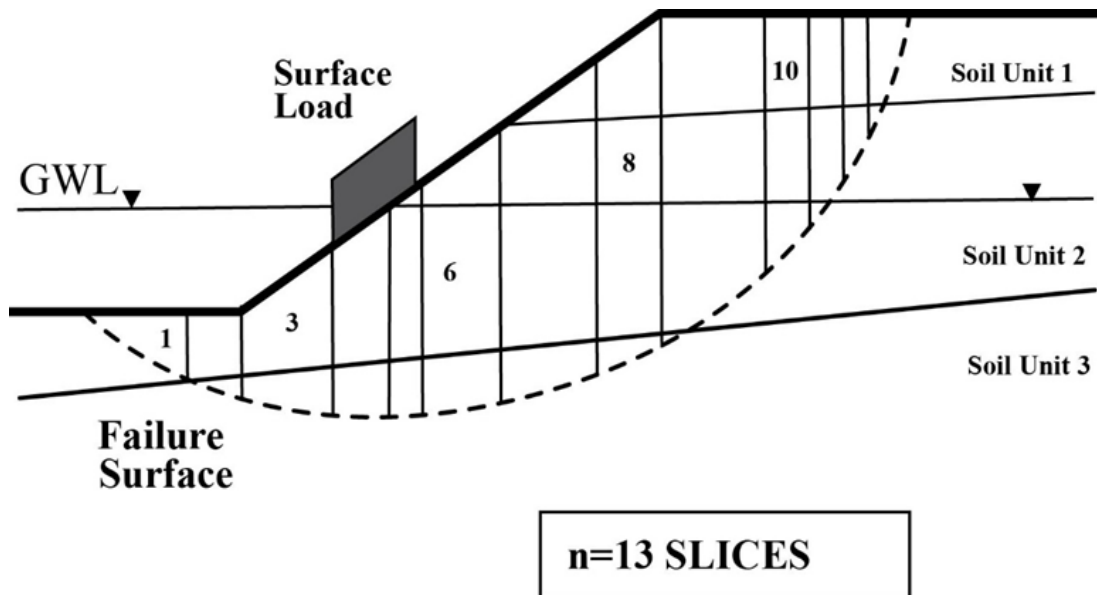


Figure 7.1. Division of a potential sliding mass into slices (Abramson, 2002)

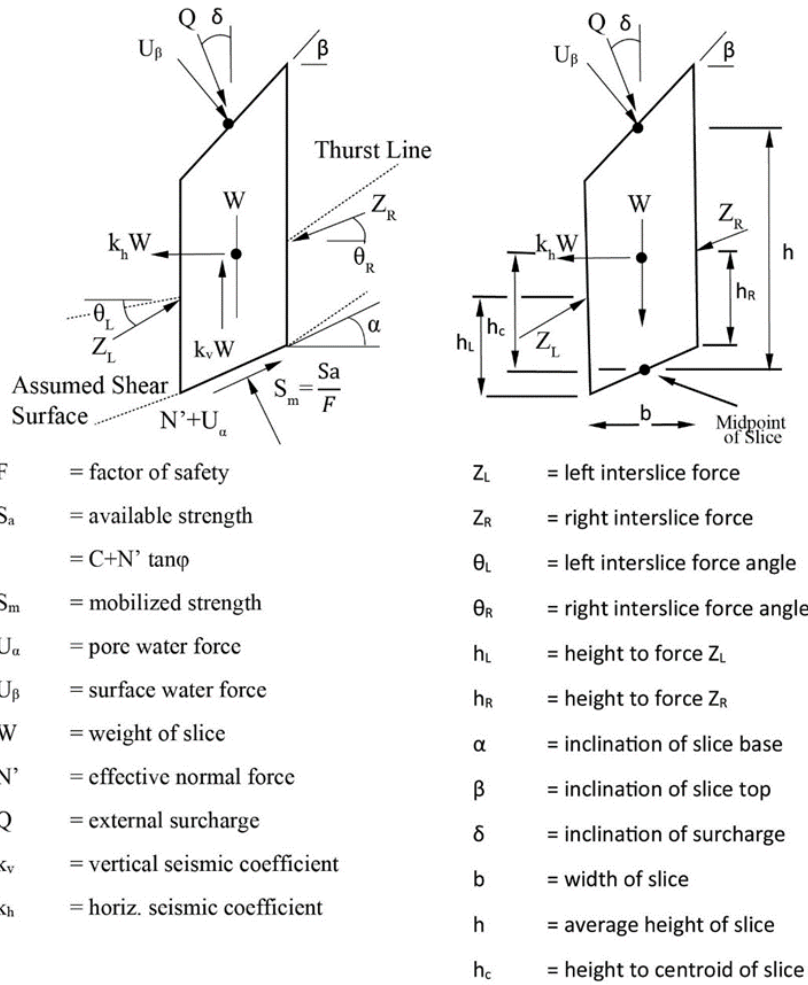


Figure 7.2. Forces acting on a typical slice (Abramson, 2002)

The assumptions made by each of these methods to render the problem statically determinate are summarized below (Aryal, 2006).

Bishop's Simplified Method

In the Simplified Bishop procedure, the forces on the sides of the slice are assumed to be horizontal (i.e., there are no shear stresses between slices). Forces are summed in the vertical direction to satisfy equilibrium in this direction and to obtain an expression for the normal stress on the base of each slice. Referring to the Figure 7.3 and resolving forces in the vertical direction, the following equilibrium equation can be written for forces in the vertical direction (Duncan, 2014):

$$N \cos \alpha + S \sin \alpha - W = 0 \text{ (Eq. 7.7)}$$

The equation for this method is written by the following equation

$$n = \frac{W - (1/F)(c' \Delta l - u \Delta l \tan \phi') \sin \alpha}{\cos \alpha + (\sin \alpha \tan \phi')/F} \text{ (Eq. 7.8)}$$

This equation is modified to compute the safety factor as:

$$F = \frac{\Sigma[(c' \Delta l \cos \alpha + (W - u \Delta l \cos \alpha) \tan \phi') / (\cos \alpha + (\sin \alpha \tan \phi')/F)]}{\Sigma W \sin \alpha} \text{ (Eq. 7.9)}$$

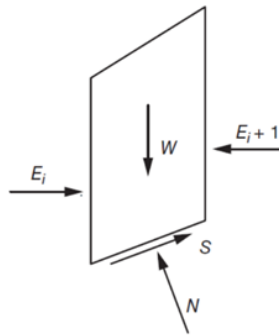


Figure 7.3. Slice with forces for the Simplified Bishop

Janbu's Simplified Method

Janbu's simplified method is based on a composite shear surface (i.e. non-circular) and the Factor of Safety is determined by horizontal force equilibrium. As in Bishop's Simplified Method, the method considers interslice normal forces (E) but neglects the shear forces (T). The method satisfies vertical force equilibrium to determine the effective base normal (N) (Janbu, 1968). Computation of the safety factor is:

$$F = \frac{\Sigma(c' l + (N - ul) \tan \phi') \sec \alpha}{\Sigma W \tan \alpha + \Sigma \Delta E} \text{ (Eq. 7.10)}$$

Janbu Simplified Method;

- Satisfies both force equilibriums,
- Does not satisfy moment equilibrium,
- Considers interslice normal forces,
- Is commonly used for composite shear surface.

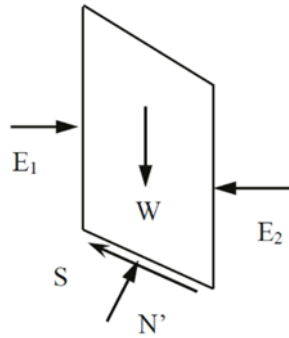


Figure 7.4. Slice with forces for the Simplified Janbu

Morgenstern – Price Method

The Morgenstern – Price method also satisfies both force and moment equilibrium and assumes an interslice force function. The method suggests assuming any type of force function, for example half – sine, trapezoidal or user defined. This method also considers interslice normal forces (E) but neglects the shear forces (T). For a given force function, the interslice forces are computed by an iteration procedure until, F_f equals F_m (Morgenstern and Price, 1955).

$$F_f = \frac{\Sigma[(c'l + (N-ul)\tan\phi')\sec\alpha]}{\Sigma(W - (T_2 - T_1))\tan\alpha + \Sigma(E_2 - E_1)} \text{ (Eq. 7.11)}$$

$$F_m = \frac{\Sigma(c'l + (N-ul)\tan\phi')}{\Sigma W \sin\alpha} \text{ (Eq. 7.12)}$$

Morgenstern – Price Method;

- Considers both interslice forces,
- Assumes an interslice force function,
- Allows selection for interslice force function,
- Computes safety factor for both force and moment equilibrium.

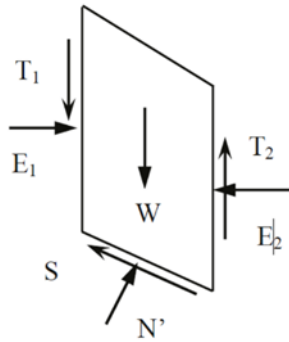


Figure 7.5. Slice with forces for the Morgenstern – Price

Spencer's Method

Spencer's method (SM) is the same as M&PM except the assumption made for interslice forces. A constant inclination is assumed for interslice forces and the FOS is computed for both force and moment equilibrium (Spencer, 1967). According to this method, the interslice shear force is expressed by:

$$T = E \tan \theta \text{ (Eq. 7.13)}$$

Spencer's Method;

- Considers both interslice forces,
- Assumes a constant interslice force function,
- Satisfies both moment and force equilibrium,
- Computes safety factor for force and moment equilibrium.

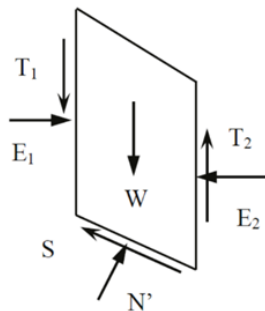


Figure 7.6. Slice with forces for the Spencer's Method

7.1.1.2. Selection of the Appropriate Slice Method

The limit equilibrium methods are based on the principles of equilibrium of the forces and / or moments. Although they are subject to the same principles, their results are different due to different assumptions. A summary of the differences of the most common methods are given in Table 7.1.

Table 7.1. *Limit equilibrium methods*

Limit – Equilibrium Method	Characteristics
Method of Slices (Fellenius, 1927)	The method addresses circular failure surfaces only; satisfies moment equilibrium only; does not satisfy force equilibrium
Bishop's Simplified Method (Bishop, 1955)	The method addresses circular failure surfaces only; satisfies vertical force equilibrium only
Janbu's Simplified Method of Slices (Janbu, 1968)	The method can be applied to any shaped surface; satisfies force equilibrium only
Morgenstern and Price Method (Morgenstern and Price, 1955)	Applies to any shaped surface; satisfies all conditions of equilibrium, but side forces are assumed to be variables
Spencer's Method (Spencer, 1967)	The method can be applied to any shaped surface; satisfies all conditions of equilibrium, but assumes side forces are parallel

Regarding the rock mass conditions on the investigated landslide's non – circular failure surface, Janbu's Simplified Method along with Spencer's and Morgenstern – and Price methods were performed on the stability analysis in Section 7.3. In this regard, the results obtained with all three methods were compared in Section 7.3.7 to reveal which limit equilibrium method is more appropriate for the rock mass conditions of the Bartın Kirazlı Bridge Landslide.

7.1.2. Seismic Slope Stability Method

One of the earliest procedures for seismic slope stability analysis is the load – based procedure, in which earthquake loading is represented by a horizontal static force, equal to the soil weight multiplied by a coefficient, which can be estimated by empirical guidelines or codes (e.g., Seed, 1977). The pseudo – static force is then integrated in a conventional limit equilibrium slope stability analysis and the factor of safety is computed. The computed factor of safety provides an indication of the possible magnitude of the seismically induced displacement (Makdisi and Seed, 1978).

Pseudo – static method is one of the first and simplest methods used in seismic slope stability analysis which was first applied by Terzaghi (1950).

This approach is analyzed by representing the effects of the earthquake with fixed horizontal (a_h) and / or vertical (a_v) accelerations. However, the vertical acceleration is neglected because the effect of the vertical force is small relative to the horizontal force. The earthquake load is defined as a static force equal to the multiplication of the soil unit weight and a seismic coefficient (k):

$$F_h = \frac{a_{max}W}{g} = k_h W \text{ (Eq. 7.14)}$$

where;

W is total weight of the landslide material.

a_{max} is the horizontal peak ground acceleration

k_h is the seismic coefficient.

The most difficult and the most important part of the pseudo – static method is selection of the seismic coefficient. Seed (1979), Hynes – Griffin and Franklin (1984), Bray (1998), Kavazanjian (1997), Bray and Travararou (2009) have performed some pseudo – static analyses. The summary of their studies about; the determination of the seismic coefficient, the determination of an acceptable safety

coefficient, the comparison of the pseudo – static analysis results with the field observations and the deformation analysis results are given in Table – 7.2.

Regarding the seismicity of the region, the Amasra Earthquake, which occurred in 1968 with magnitude of 6.5 is the major earthquake that is in the close vicinity of the study area (Table 2.1). Then, the reference acceleration (a_{ref}) value for an earthquake with a magnitude of 6.5 was taken according to Seed (1979) from Table 7.2. This value is also compatible with the expected peak horizontal ground acceleration (PGA 475) value (0.220 g) in the study area according to The Earthquake Hazard Map of Turkey and the PGA value (0.244 g) estimated from the calculation of NGA models in Section 2.4.1.

Seed (1979) has also suggested that the a_{ref} value for an earthquake with a magnitude of 8.25 is taken as 0.75 g (Table 7.2). Considering Section 2.4.1, to evaluate seismic condition in the stability analysis, a_{ref} value (0.75 g) is multiplied by the acceleration multipliers for an earthquake with a magnitude of 6.5 (0.133) and 8.25 (0.167) to estimate the horizontal seismic load coefficient as 0.1 g and 0.13 g respectively. Considering the seismic activity potential of the area regarding the possibility of the estimated PGA values in between 0.2 to 0.244 (Section 2.4.1), the horizontal seismic load coefficient to evaluate in slope stability analysis was re-scaled and selected as 0.12 g.

Table 7.2. Suggested Methods for Performing Pseudostatic Screening Analysis (Duncan, 2014)

(1) Reference	(2) Reference acceleration, a_{ref}	(3) Acceleration multiplier, a / a_{ref}	(4) Strength reduction factor	(5) Minimum factor of safety	(6) Tolerable displacement
Seed (1979)	0.75g ($M \approx 6\frac{1}{2}$)	0.133	0.85	1.15	Approx. 1 m
Seed (1979)	0.75g ($M \approx 8\frac{1}{4}$)	0.167	0.85	1.15	Approx. 1 m
Hynes – Griffin and Franklin (1984)	PHA _{rock} ($M \leq 8.3$)	0.5	0.8	1.0	1 m
Bray et al. (1998)	PHA _{rock}	0.75	Recommend using conservative, (e.g. residual) strengths.	1.0	0.30 m for landfill covers; 0.15 m for landfill base sliding
Kavazanjian et al. (1997)	PHA _{soil}	0.17 if PGA accounts for amplification	0.8 ^a	1.0	1 m
Kavazanjian et al. (1997)	PHA _{soil}	0.5 for free – field PGA determined	0.8 ^a	1.0	1 m
NCHRP 12 – 70 (2008) FHWA (2011)	PHA _{soil}	0.2 – 0.5 (PGA includes site amplification effects)	0.8	1.0	5 cm or less
Bray and Travasarou (2009)	Spectral accel., S_a (5% damped at specified period)	Depends on slope height and displacement	1.0 Median or “best estimate”	Varies	Varies

^a For fully saturated or sensitive clays.

7.2. Geotechnical Parameters of the Sliding Surface

Geotechnical parameter estimations for the landslide material (Hm) are determined in this section.

7.2.1. Empirical Approach (Residual Parameters)

Utilization of the data obtained from in – situ and laboratory testing, an empirical approach was performed to determine the geotechnical parameters of the landslide material (Hm) in this section. The landslide material (Hm) is represented by very stiff sandy lean clay with gravel (CL). The approach follows from Section 6.1 and is re-emphasized below for the sake of clarity:

Unit weight

$$\gamma = 20 \text{ kN} / \text{m}^3 \text{ (Carter \& Bentley, 1991) (Table 7.3)}$$

Table 7.3. Typical values of natural density (Carter & Bentley, 1991)

TYPICAL VALUES OF NATURAL DENSITY		Natural density (kg / m ³)	
Material		Bulk density*	Dry density
Sands and gravels:	very loose	1700 – 1800	1300 – 1400
	loose	1800 – 1900	1400 – 1500
	medium dense	1900 – 2100	1500 – 1800
	dense	2000 – 2200	1700 – 2000
	very dense	2200 – 2300	2000 – 2200
Poorly – graded sands		1700 – 1900	1300 – 1500
Well – graded sands		1800 – 2300	1400 – 2200
Well – graded sand / gravel mixtures		1900 – 2300	1500 – 2200
Clays:	unconsolidated muds	1600 – 1700	900 – 1100
	soft, open - structured	1700 – 1900	1100 – 1400
	typical, normally consolidated	1800 – 2200	1300 – 1900
	boulder clays (overconsolidated)	2000 – 2400	1700 – 2200
Red tropical soils		1700 – 2100	1300 – 1800

Residual strength (Short term) parameters

True angle of (residual) internal friction:

$$PI_{\text{mean}} = 25.10 \% \text{ (Mean value)} \rightarrow \phi' = 22^\circ \text{ (Gibson, 1953) (Figure – 7.7)}$$

With the calculated value, angle of internal friction is determined as $\phi' = 22^\circ$.

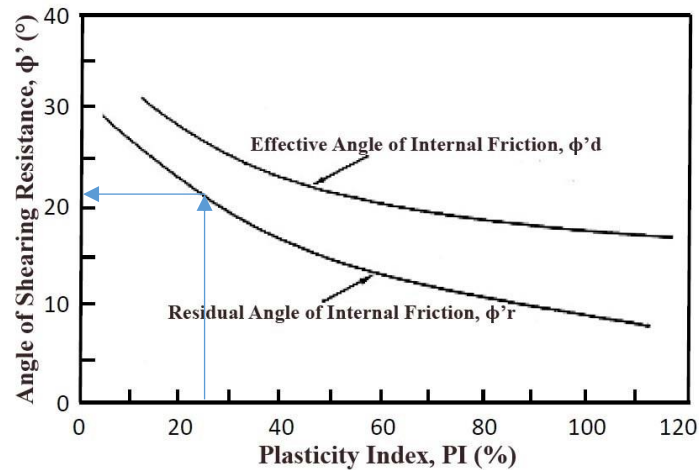


Figure 7.7. Range of shearing resistance angle and plasticity index in clays (Gibson, 1953)

Residual cohesion value:

$$c' = \alpha \times \tan \phi' \quad (\text{Lunne et al., 1997})$$

$$\phi' \text{ (Angle of shearing resistance)} = 22^\circ$$

α = coefficient according to soil type (= 20) (Lunne et al., 1997) (Table 7.4)

$$c' = 20 \times \tan (22) = 8.08 \text{ kPa}$$

Table 7.4. α coefficient values for different soil types (Lunne et al., 1997)

Soil Type	α^*	$\tan \phi'$
Soft clay	5 – 10	0.35 – 0.45
Medium stiff clay	10 – 20	0.40 – 0.55
Stiff clay	20 – 50	0.50 – 0.60
Soft silt	0 – 5	0.50 – 0.60
Medium stiff silt	5 – 15	0.55 – 0.65
Stiff silt	15 – 30	0.60 – 0.70

With the calculation above, c' is determined as 8 kPa.

With this approach, geotechnical parameters for sliding surface are determined as;

$$\gamma = 20 \text{ kN} / \text{m}^3, c' = 8 \text{ kPa}, \phi' = 22^\circ$$

7.2.2. RocData Analysis

RocData analysis that was used to estimate the geotechnical parameters of the landslide material (Hm) are explained in this chapter. The GSI value of the landslide material (Hm) which was used as an input parameter in the RocData software was determined with the same procedure as that explained in Chapter 6.3 (Table – 7.5 and 7.6) by using the GSI Chart of Sonmez and Ulusay (2002).

Table 7.5. Geological Strength Index (Sonmez and Ulusay, 2002) for the landslide material (Hm)

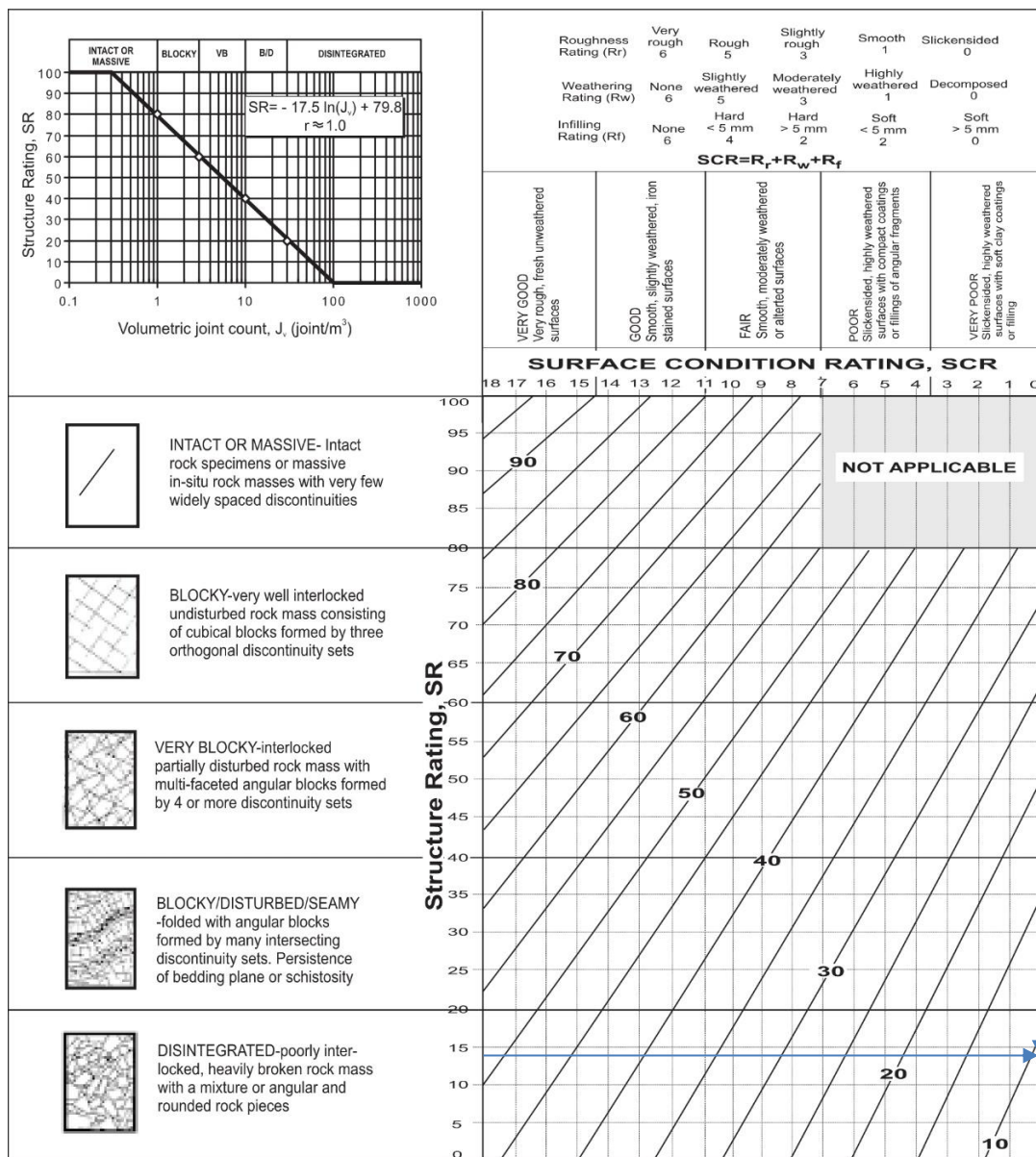


Table 7.6. Calculation of Geological Strength Index (GSI) rating
with Sonmez and Ulusay's (2002) Chart

Lithology	RQD (%)	Jv	SR	Joint ratings			SCR	GSI
				Roughness (Rr)	Weathering (Rw)	Infilling (Rf)		
Landslide material (Hm)	0	44	14	0	0	0	0	9

After obtaining the GSI value, the other input parameters of the RocData software for the landslide material (Hm) such as uniaxial compressive strength (σ_{ci}), intact rock parameter (m_i), disturbance factor (D), intact modulus (E_i) and unit weight (γ) were determined and evaluated with the same procedure that was explained in Chapter 6.4.

The material parameters determined for a slope height of 15.00 meters for the landslide material (Hm) unit are given below (Table 7.7, Figure 7.8).

Table 7.7. Rock mass parameters (For slope, height = 15.00 m)

Lithology	Uniaxial compressive strength (σ_{ci}) (MPa)	GSI	Intact rock parameter (m_i)	Disturbance factor (D)	Intact modulus (E_i) (MPa)	Unit weight (γ) (kN / m^3)
Landslide material (Hm)	1	9	7	0	1000	20.00

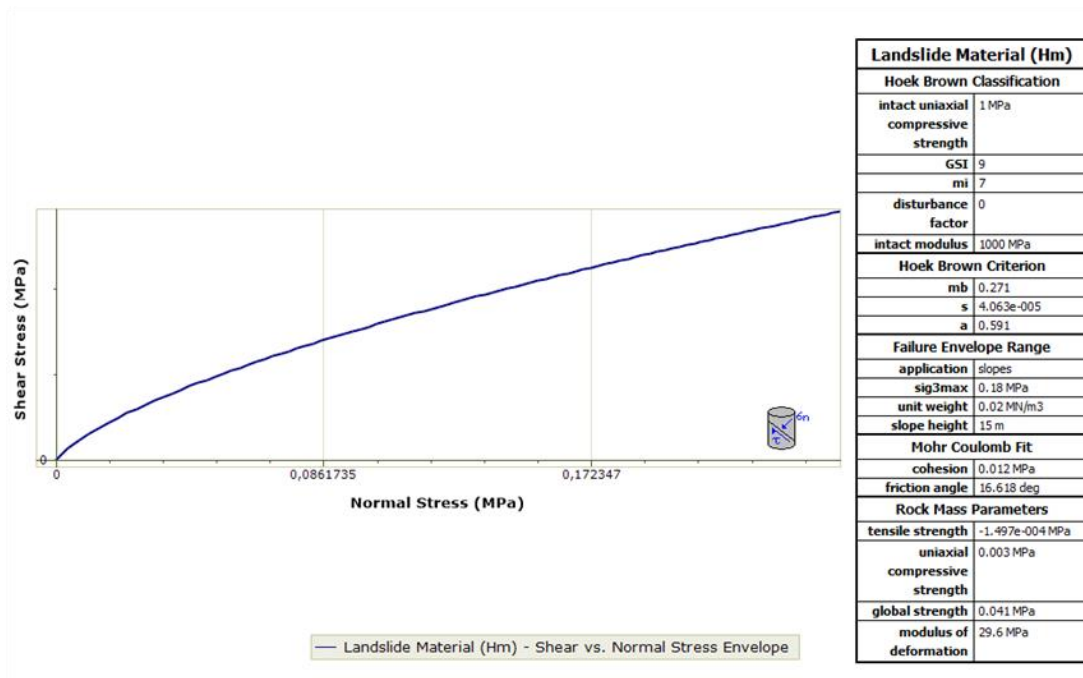


Figure 7.8. Normal vs shear stress graph for the landslide material (Hm) unit (h = 15.00 m)

Accordingly, rock strength parameters determined for a slope height of 15.00 meters for the landslide material (Hm) are given below.

$$\gamma = 20.0 \text{ kN} / \text{m}^3$$

$$c = 12 \text{ kPa}, \phi = 17^\circ$$

$$E = 30 \text{ MPa}$$

It needs to be noted that this result was also compatible with the average Pressuremeter Modulus (E_p) value obtained from the pressuremeter tests (i.e., 26.70 MPa).

7.2.3. Back Analysis

Estimating the shear strength parameters of a landslide material for limit equilibrium condition (i.e., from a Factor of Safety value accepted as 1.0) is known as back analysis. This method is performed after the determination of the relevant geometric and geotechnical parameters of the soil / rock units of a landslide area to determine the residual strength parameters of the landslide material that has just failed or is at the verge of failure (i.e., under imminent failure conditions).

In this regard, it is accepted that the landslide material is formed by highly to completely weathered Ulus formation and the common parameters have been selected for the landslide mass. RocScience Slide 6.0 Software has been used for back analysis through the collection of the following five geometric and geotechnical parameters:

1. The geometry of the landslide with surface topography, profile of the slip surface, and determination of the material boundaries,
2. The pressure of the void (pore) water at the time instability occurred, which is required for effective stress analysis,
3. The external loads and its effects on the slope at the time of instability,
4. The unit weight of the landslide material,
5. The strength of the landslide material along the slip surface.

The first, third and fourth components can be evaluated with reasonable accuracy from in – situ and laboratory tests. The second component, pore water pressure represents the groundwater conditions in the stability analysis. The level of the groundwater can be determined by the measurements within the boreholes. The fifth parameter can be obtained by assuming limiting equilibrium conditions (i.e., a factor of safety of 1.00) at the time of landsliding.

By back analysis, shear strength data pairs (i.e., c , ϕ) that satisfied a safety factor value of 1.00 along three different cross sections of the landslide slip surface were computed. These critical cross sections were located along sections at Km: 18 + 353, Km: 18 + 368 and Km: 18 + 407, respectively (Figures 7.10 to 7.15).

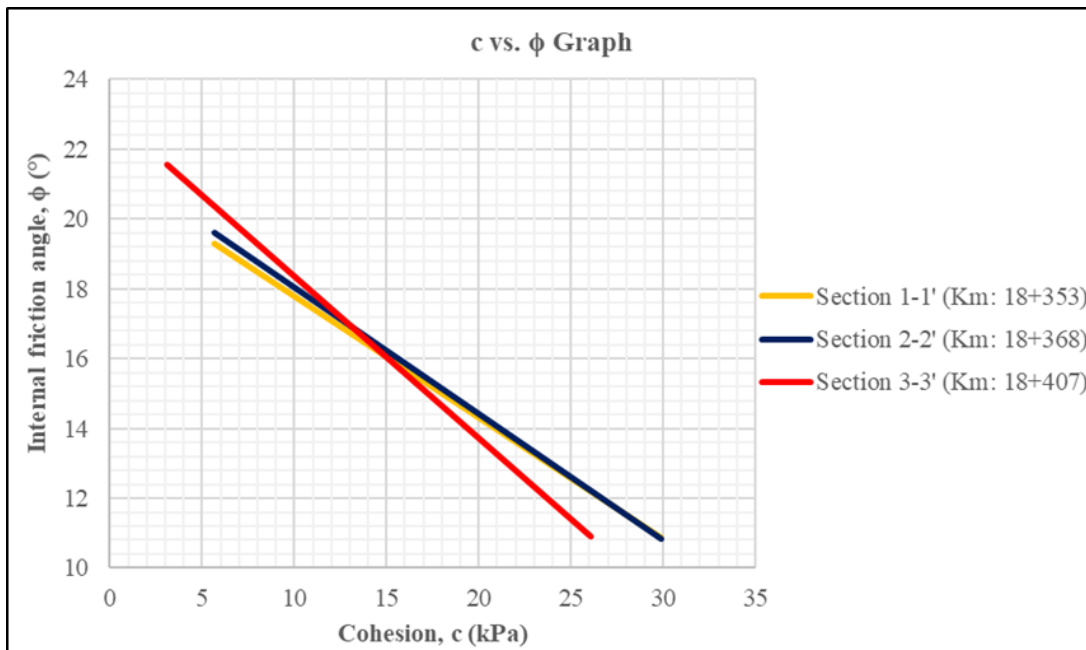


Figure 7.9. Best fit lines of $c - \phi$ pairs obtained from back analysis

Table 7.8. $c - \phi$ pair values satisfying $F.S. = 1.0$ condition for each section

Section 1-1' (Km: 18 + 353)		Section 2-2' (Km: 18 + 368)		Section 3-3' (Km: 18 + 407)	
c (kPa)	ϕ (°)	c (kPa)	ϕ (°)	c (kPa)	ϕ (°)
6.00	19.18	6.00	19.50	3.00	21.60
10.00	17.78	10.00	18.05	10.00	18.86
15.00	16.04	15.00	16.24	15.00	16.04
20.00	14.30	20.00	14.42	20.00	13.72
25.00	12.56	25.00	12.61	26.00	10.94
30.00	10.82	30.00	10.80		

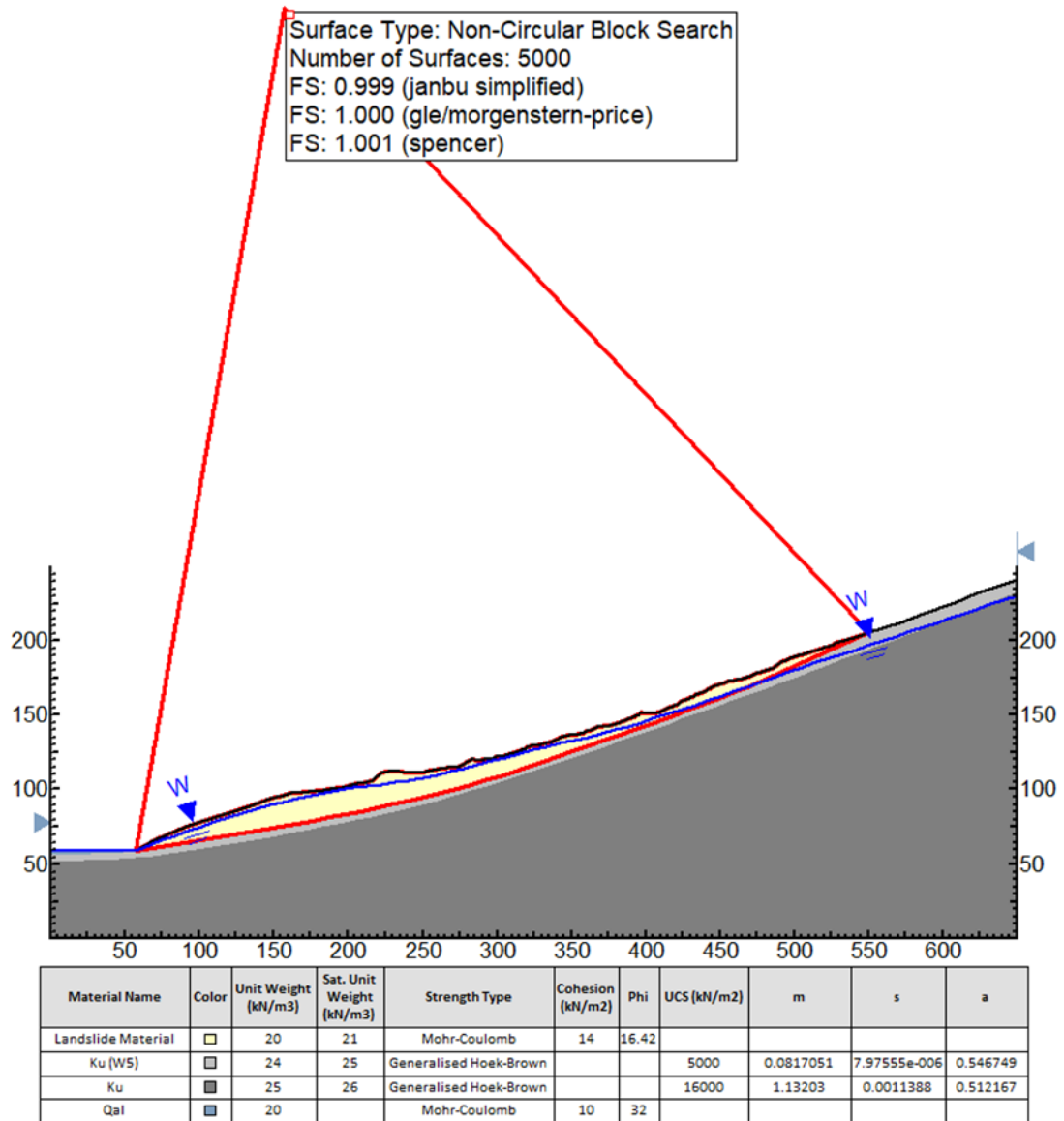


Figure 7.10. Back Analysis of Section 1-1' (Km: 18 + 353) (Exported from Slide 6.0)

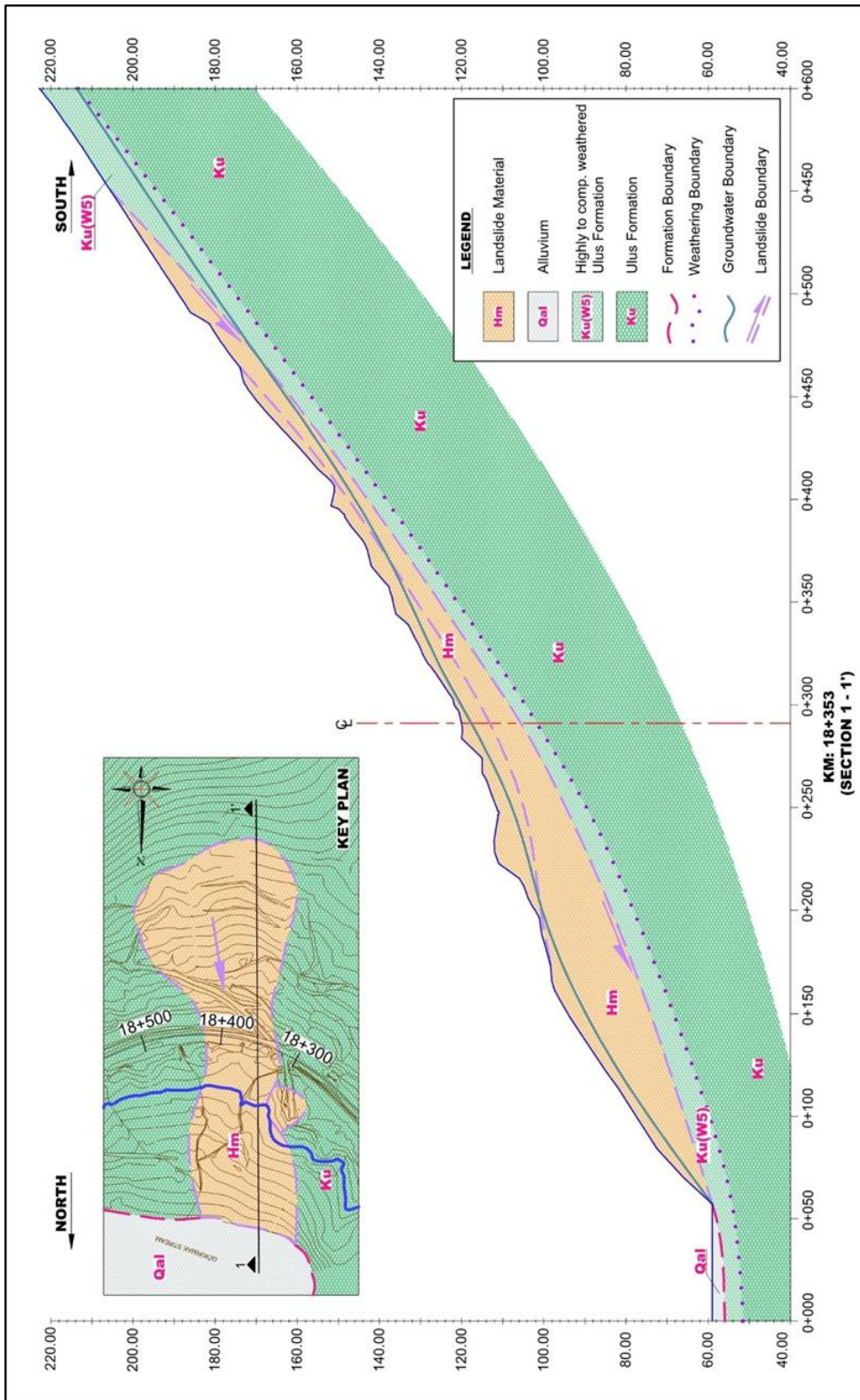


Figure 7.11. Back Analysis of Section 1-1' (Km: 18 + 353) (Detailed view)

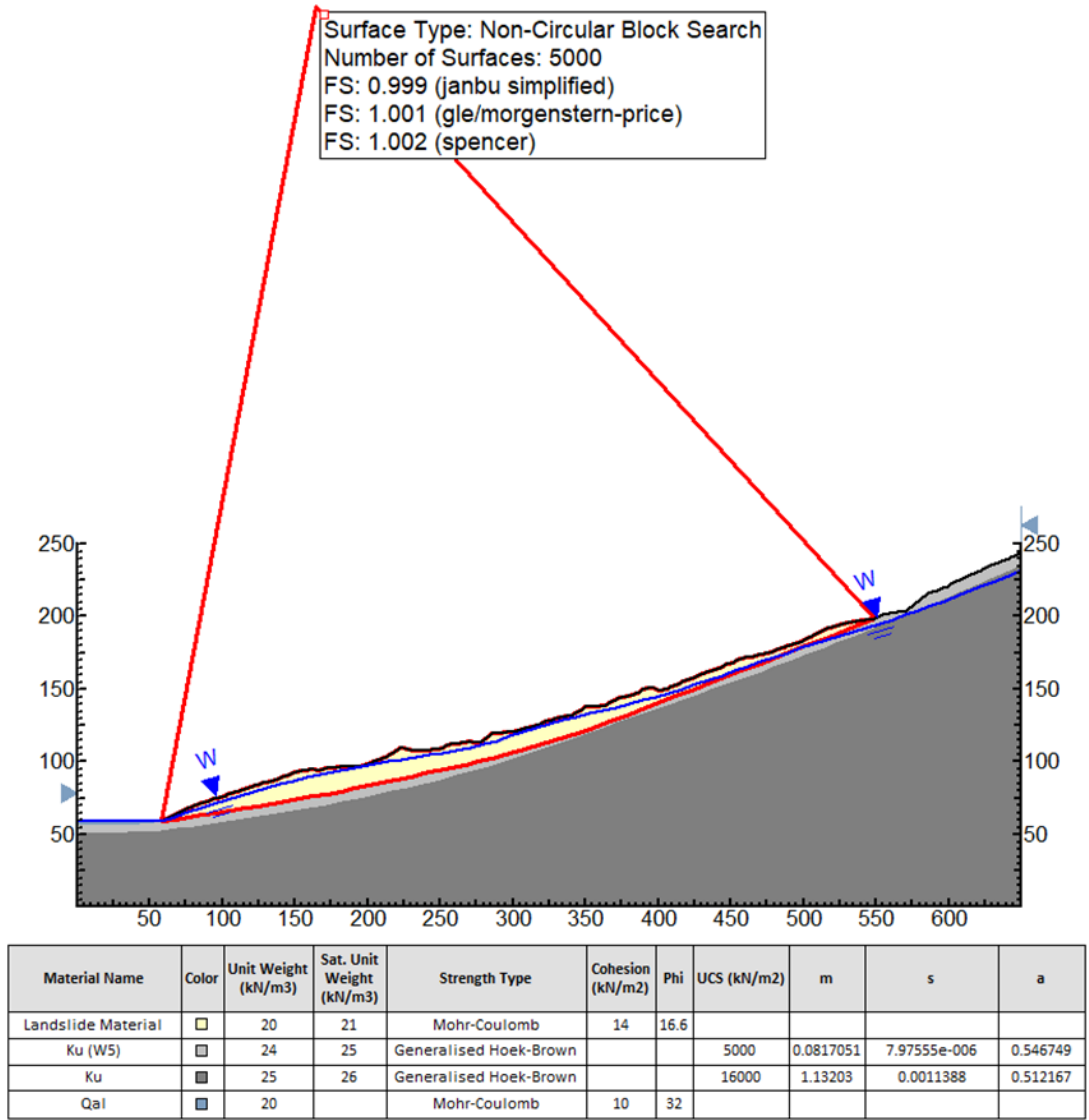


Figure 7.12. Back Analysis of Section 2-2' (Km: 18 + 368) (Exported from Slide 6.0)

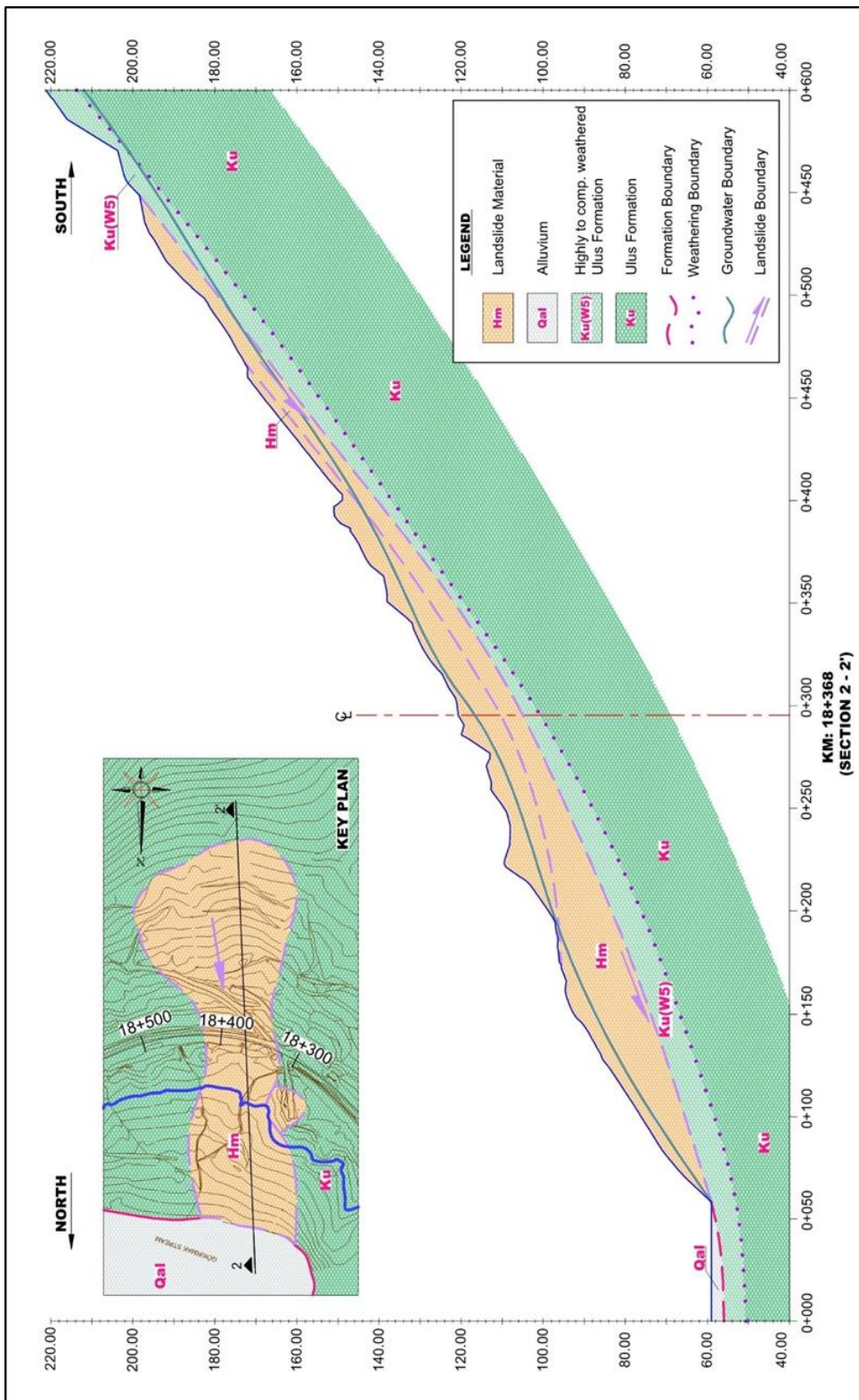


Figure 7.13. Back Analysis of Section 2-2' (Km: 18 + 368) (Detailed view)

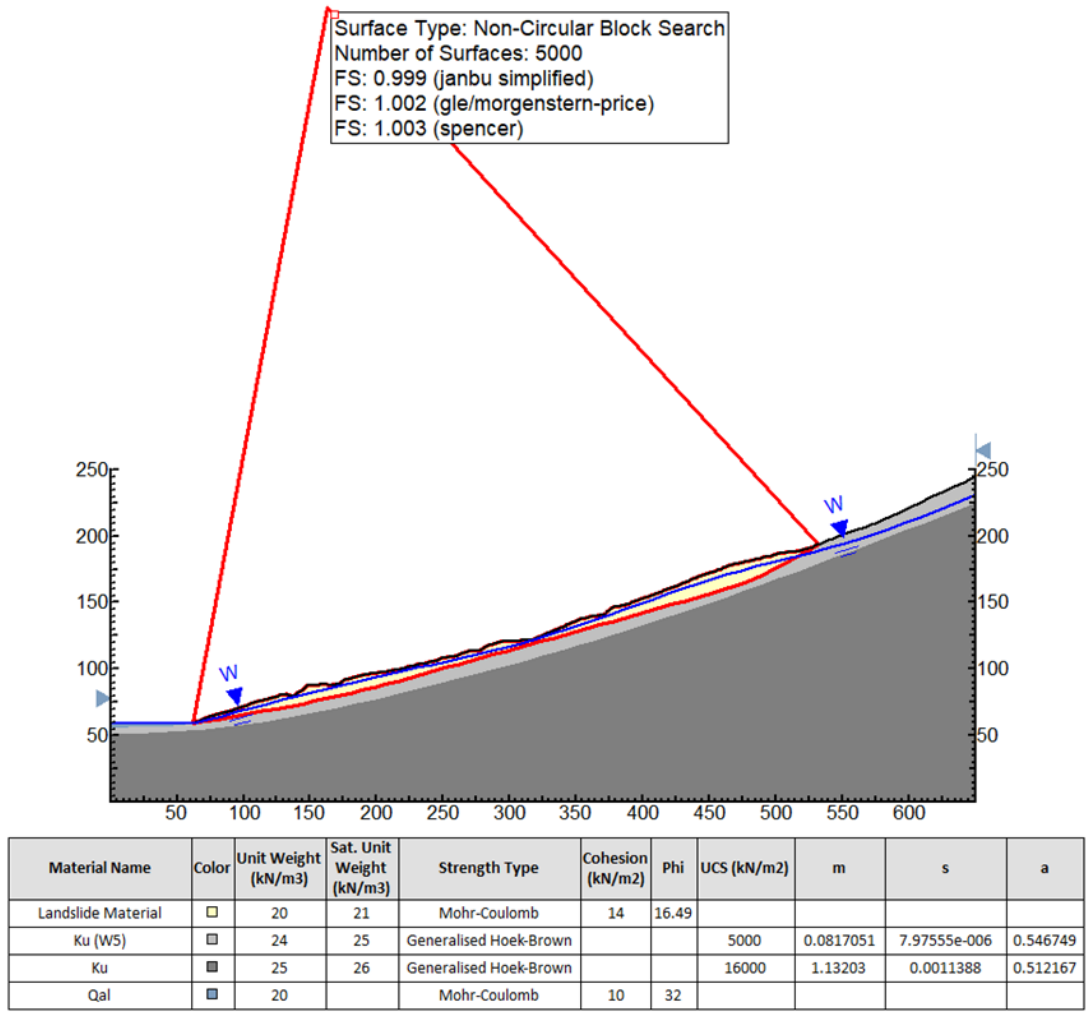


Figure 7.14. Back Analysis of Section 3-3' (Km: 18 + 407) (Exported from Slide 6.0)

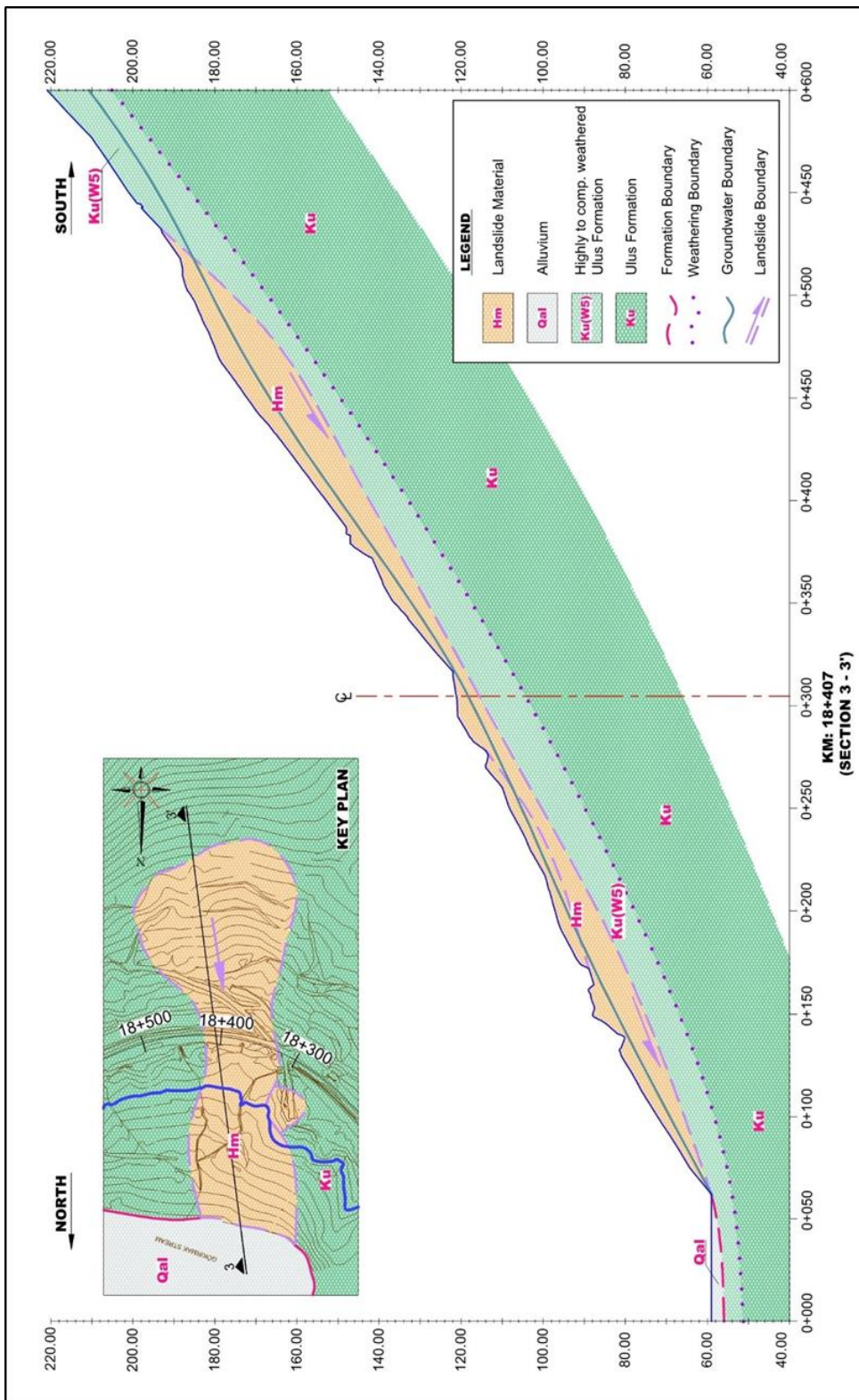


Figure 7.15. Back Analysis of Section 3-3' (Km: 18 + 407) (Detailed view)

The three curves intersect at a single point (Figure 7.9 and Table 7.8) which is represented by a cohesion of 14 kPa and an internal friction angle of 16.6° for the landslide material based on the back analysis.

The geotechnical parameters that are determined to be used in the limit equilibrium analysis are given in Table 7.9.

Table 7.9. A summary of the estimated geotechnical parameters of the landslide material

Parameter	Empirical Estimation	RocData	Back Analysis
Unit weight, γ (kN / m ³)	20.00 (*)	20.00	–
Cohesion, c (kPa)	8.00 (**)	12.00	14.00
Internal friction angle, ϕ (°)	22.00 (***)	17.00	16.60

(*) Carter and Bentley (1991), (**) Gibson (1953), (***) Lunne et al. (1997)

The shear strength parameters obtained from the back analysis were selected to be used in the stability analysis since back analysis represents the most precise estimation in this regard.

7.3. Slope Stability Assessment

The geotechnical remediation methods for the Bartın Kirazlı Bridge Landslide are discussed in this section. Considering the velocity, width, depth and length of the landslide along with the regional topography; rock buttress implementation after toe excavation was found to be acceptable for long term stability.

The stability analysis was performed on Section 2-2' (Km 18 + 368), which was also used in the back analysis. The limit equilibrium analysis was performed by the RocScience Slide 6.0 Software with multi – staged approach for stability analysis. Janbu's Simplified Method of Slices along with Spencer's and Morgenstern and Price methods were used in the limit equilibrium analysis.

Factor of Safety values considered minimum 1.50 for static condition and minimum 1.10 for pseudo – static case regarding Republic of Turkey General Directorate of Highways (KGM) Research Engineering Services Technical Specification (2014) in the stability analysis. It needs be noted that Seed (1979) have suggested a 1.15 value for the Factor of Safety under pseudo – static conditions.

Input material parameters used in the stability analysis are given in Table 7.10. Each application phase and sequence for landslide stability are summarized below.

Table 7.10. Summary of material parameters used in stability analysis

Property	Landslide Material	Ku (W5)	Ku	Qal	Rock Buttress
Color					
Strength Type	Mohr-Coulomb	Generalised Hoek-Brown	Generalised Hoek-Brown	Mohr-Coulomb	Mohr-Coulomb
Unsaturated Unit Weight [kN/m ³]	20	24	25		
Saturated Unit Weight [kN/m ³]	21	25	26		
Cohesion [kPa]	14			10	5
Friction Angle [deg]	16.6			32	35
Unconfined Compressive Strength (intact) [kPa]		5000	16000		
m		0.0817051	1.13203		
s		7.97555e-006	0.0011388		
a		0.546749	0.512167		

It needs to be noted that the back analysis case, which includes the failure surface of Section 2-2' that was obtained from the inclinometer measurements, was used in the initial phase of the stability analysis prior to the remediation phases (Figures 7.16 and 7.17).

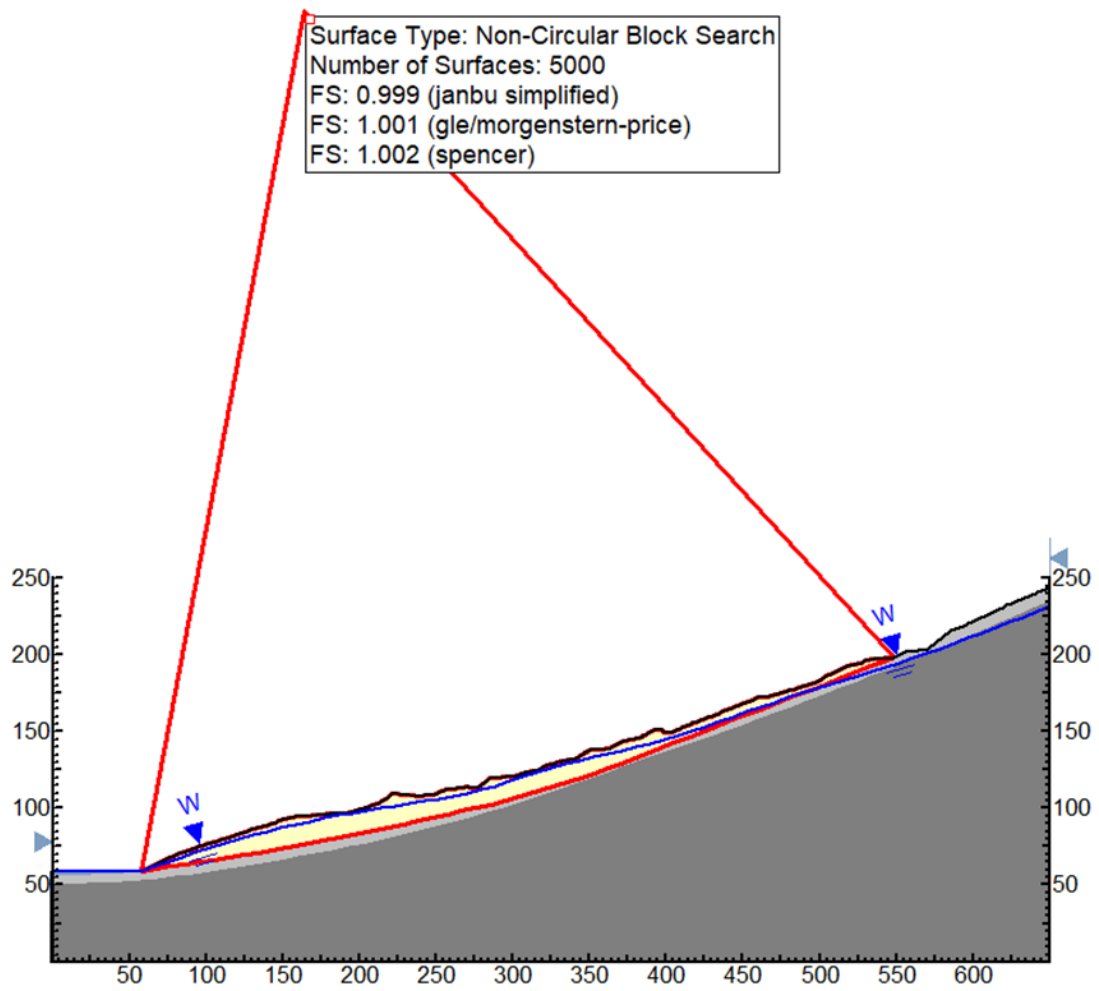


Figure 7.16. Initial Phase of Section 2-2' (Exported from Slide 6.0)

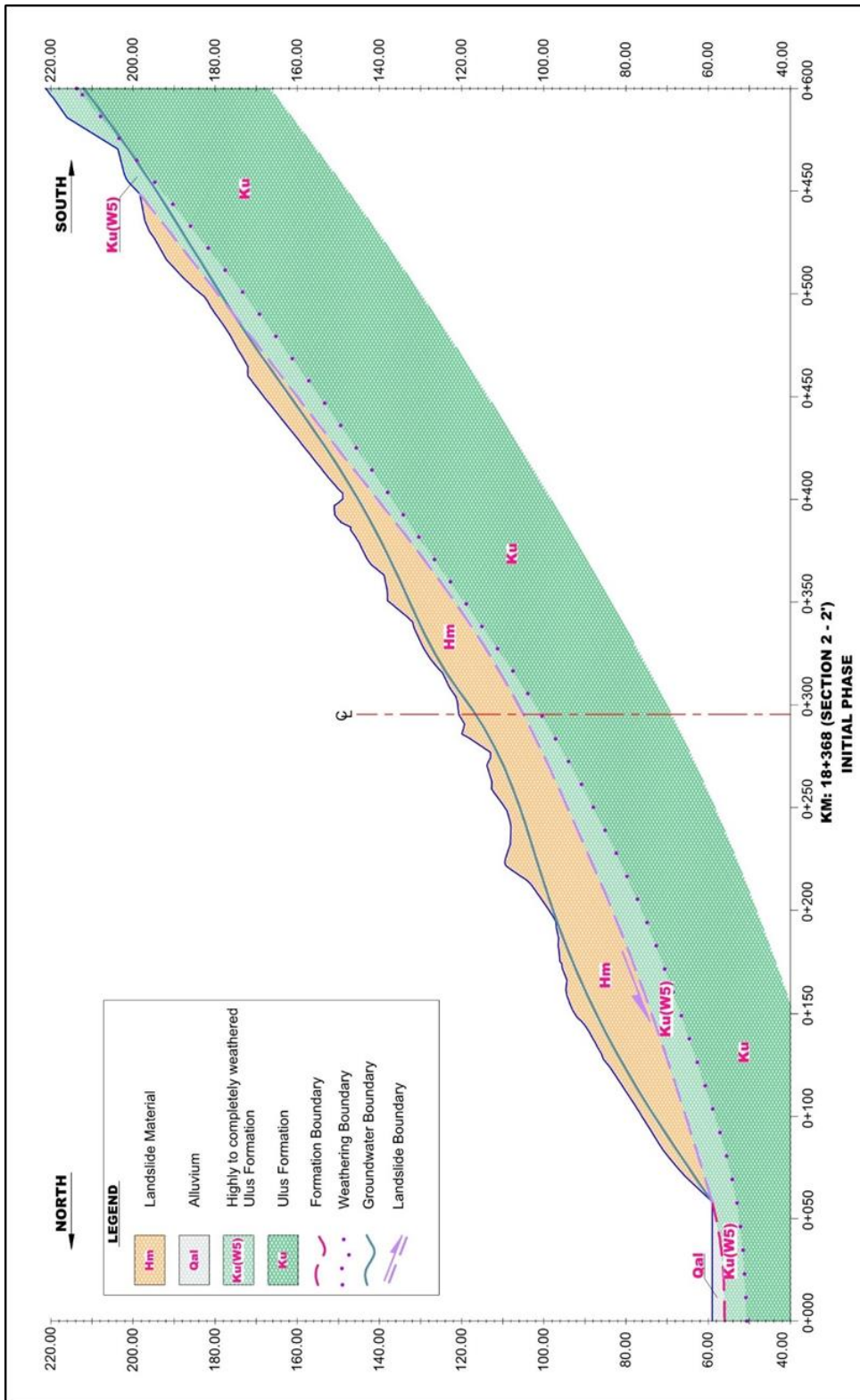


Figure 7.17. Initial Phase of Section 2-2' (Detailed view)

7.3.1. Subsurface Drainage by Pumping

Subsurface drainage by pumping was considered in order to reduce the groundwater level in order to increase the factor of safety and to allow dry excavation conditions for temporary toe excavation prior to rock buttress application. In this phase, the groundwater level is reduced by approximately 10 meters from the landslide material (Hm) levels to the highly to completely weathered Ulus formation (Ku – W5) levels which are less permeable. After the decrease of the groundwater level to by the pumping drainage application, the factor of safety values increased to 1.252 (Janbu Simplified), 1.255 (Morgenstern – Price) and 1.255 (Spencer) (Figures 7.18 and 7.19).

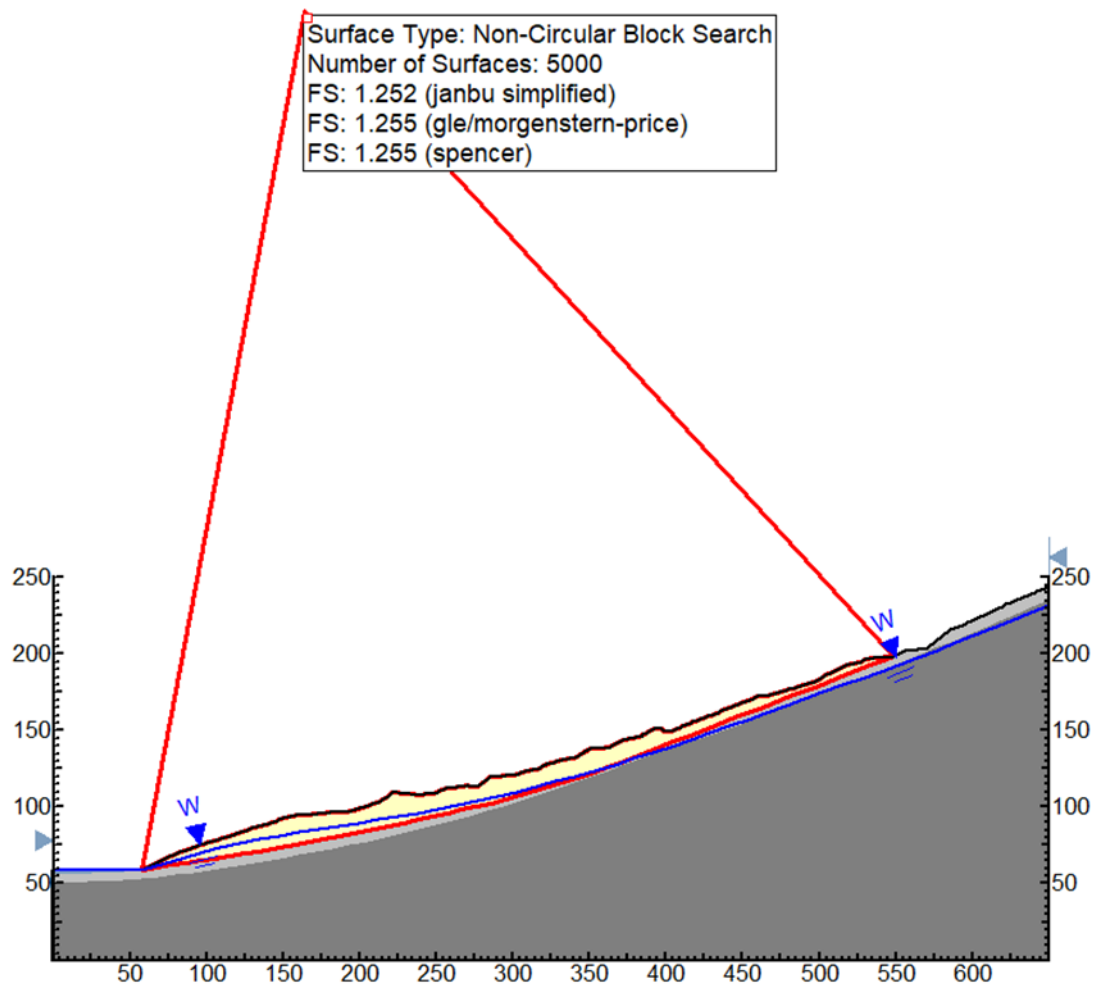
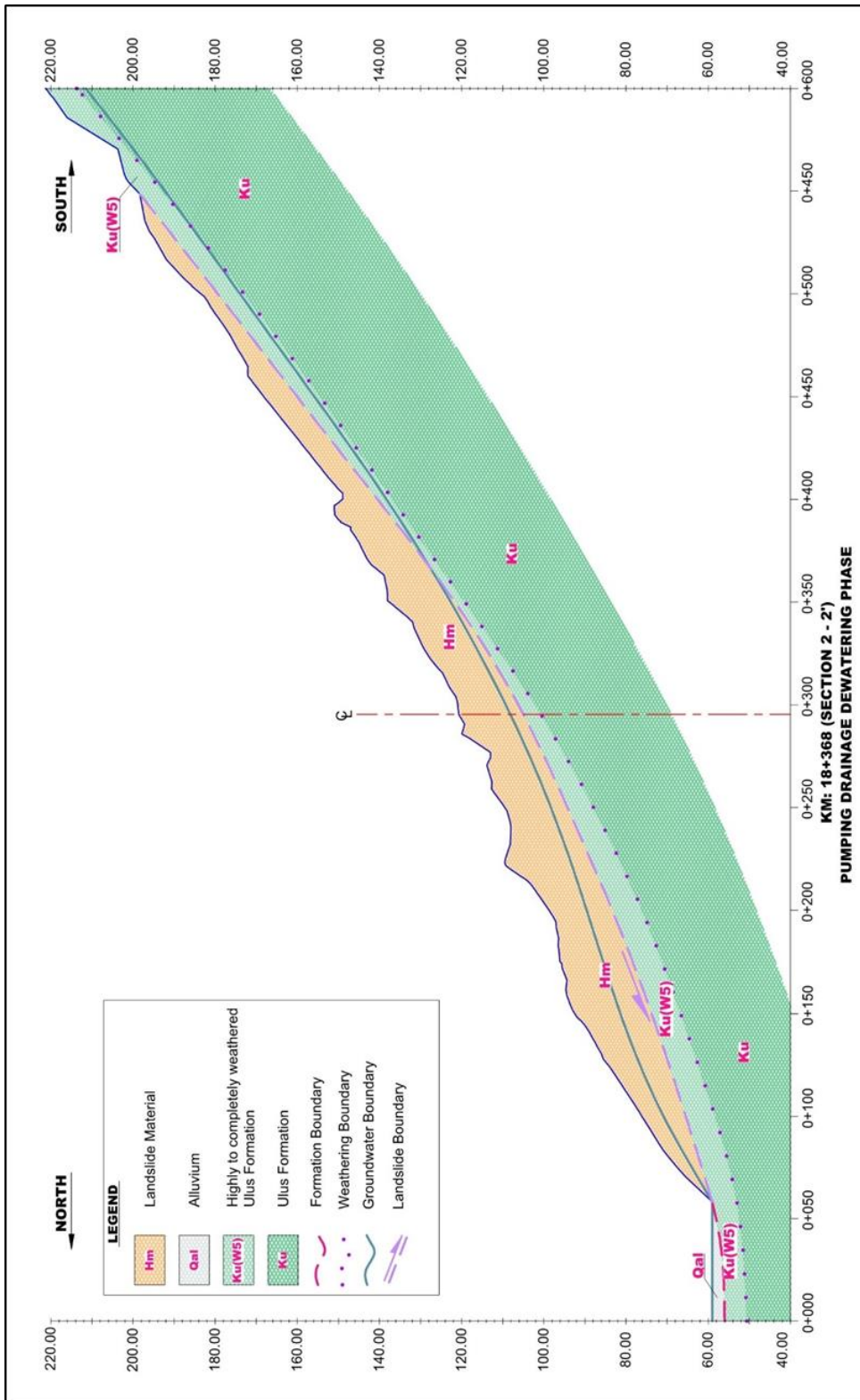


Figure 7.18. Pumping Drainage Dewatering Phase for Section 2-2' (Exported from Slide 6.0)



7.3.2. Toe Excavation

After reducing of groundwater level by pumping drainage, the toe excavation phase needs to be performed before the application of the rock buttress. By the analysis performed on the temporary excavation of landslide material (Hm) with 2 H / 1 V slope ratio, the factor of safety values decreases to 1.183 (Janbu Simplified), 1.185 (Morgenstern – Price) and 1.185 (Spencer) (Figures 7.20 and 7.21). In this phase, approximately 100 000 m³ of landslide material will need to be excavated.

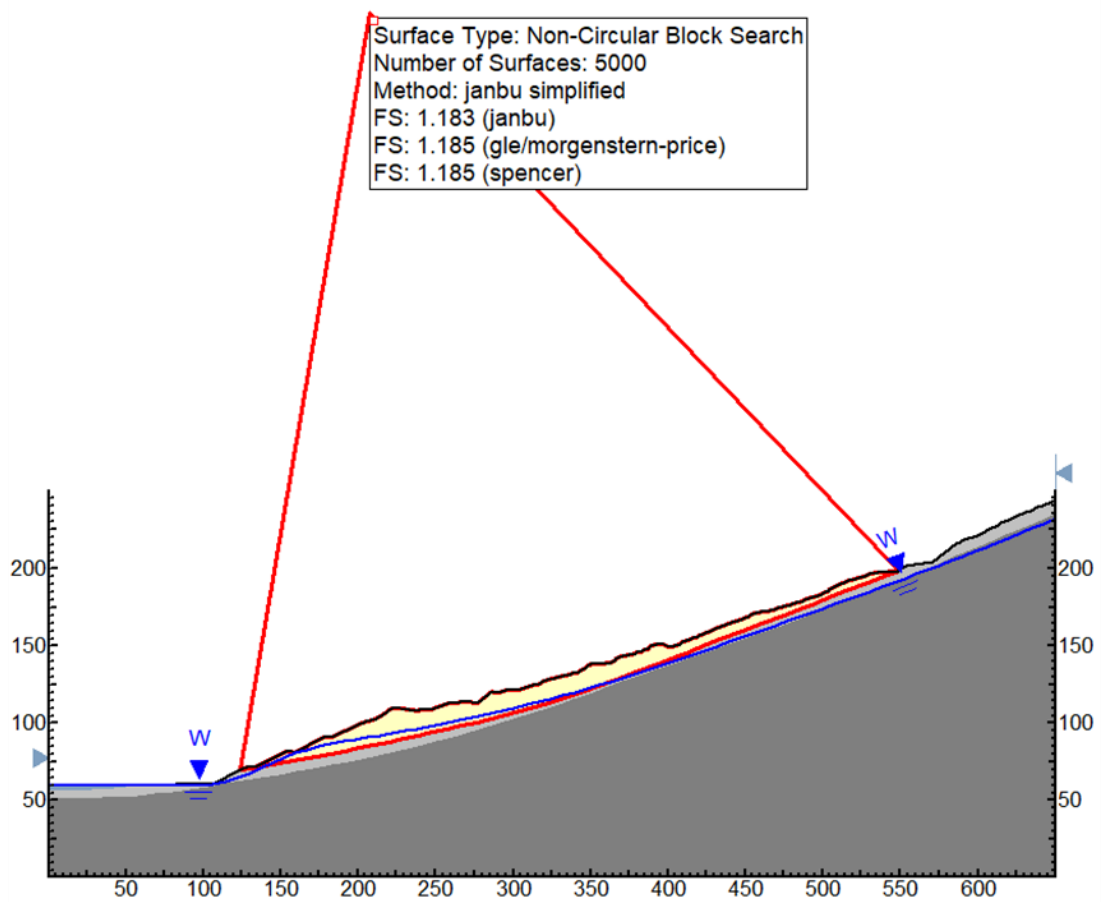
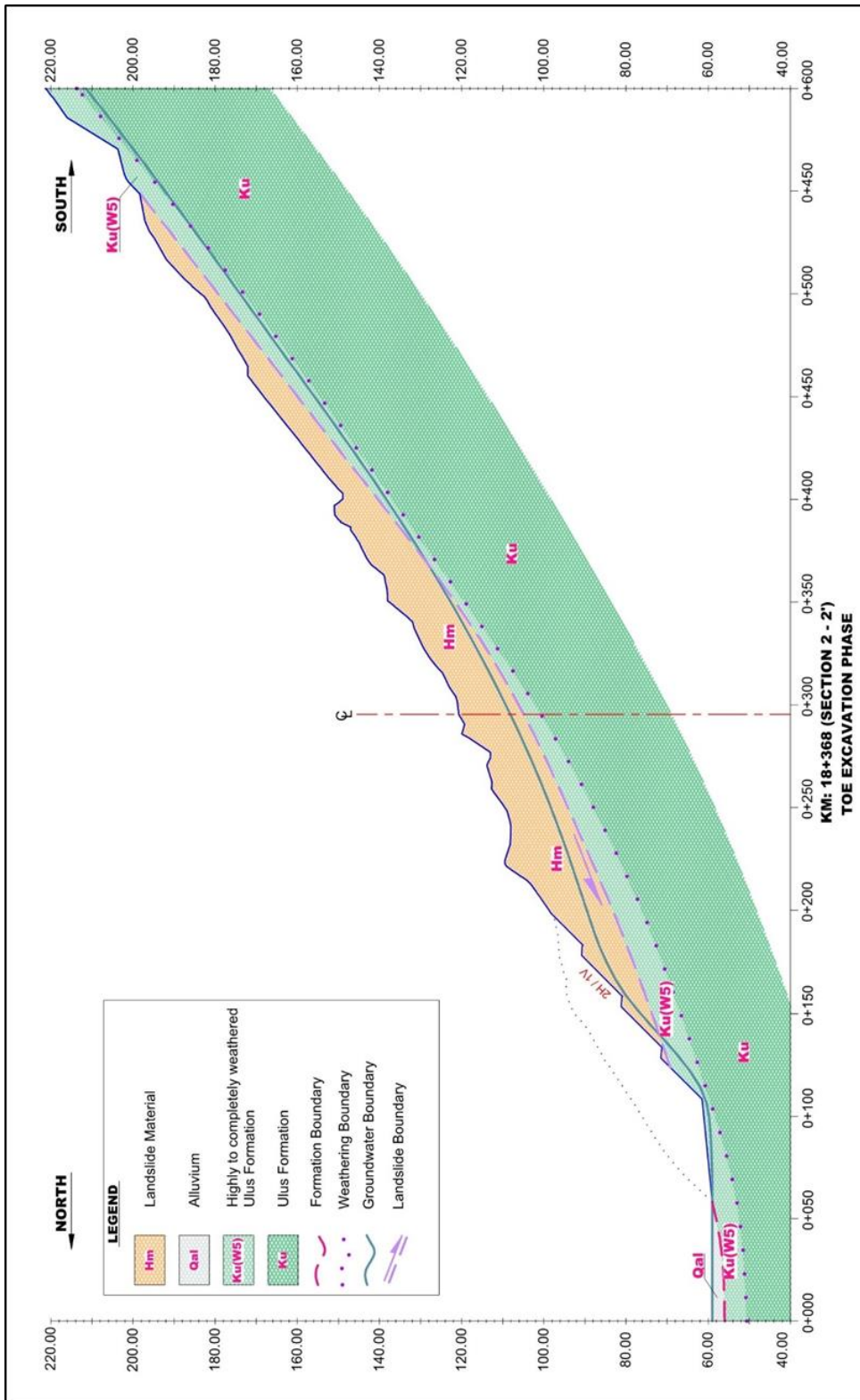


Figure 7.20. Toe Excavation Phase of Section 2-2' (Exported from Slide 6.0)



7.3.3. Rock Buttress

The rock buttress fill application needs to be applied with a 1 H / 1 V slope ratio after the temporary toe excavation phase for the long term stability of the landslide area. The material properties of the rock buttress fill were determined as $c = 5 \text{ kPa}$ and $\phi = 35^\circ$ (Table 7.10). The factor of safety values increases to 1.731 (Janbu Simplified), 1.756 (Morgenstern – Price) and 1.765 (Spencer) after the rock buttress application (Figures 7.22 and 7.23). In this phase, approximately $300\,000 \text{ m}^3$ of granular material will be required for the fill.

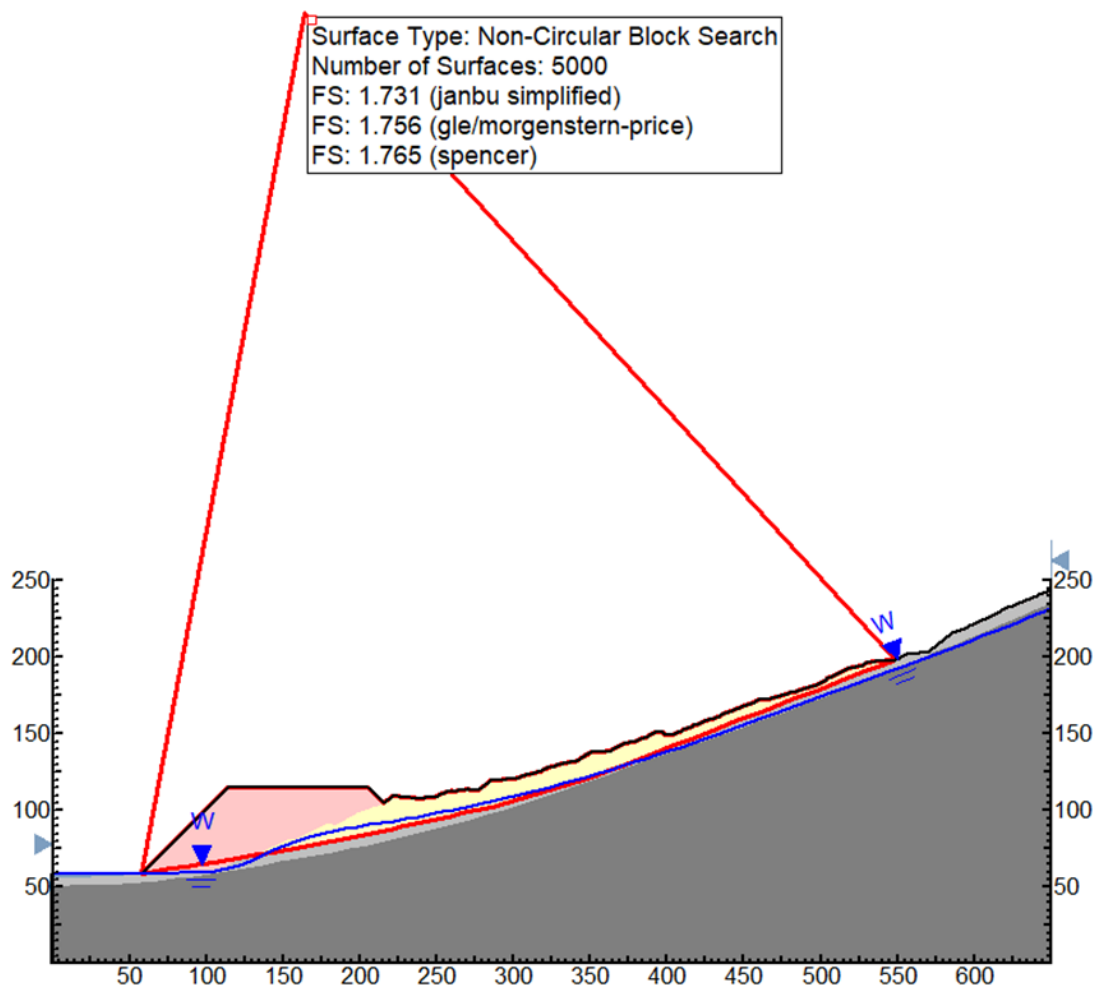


Figure 7.22. Rock Buttress Application Phase of Section 2-2' (Exported from Slide 6.0)

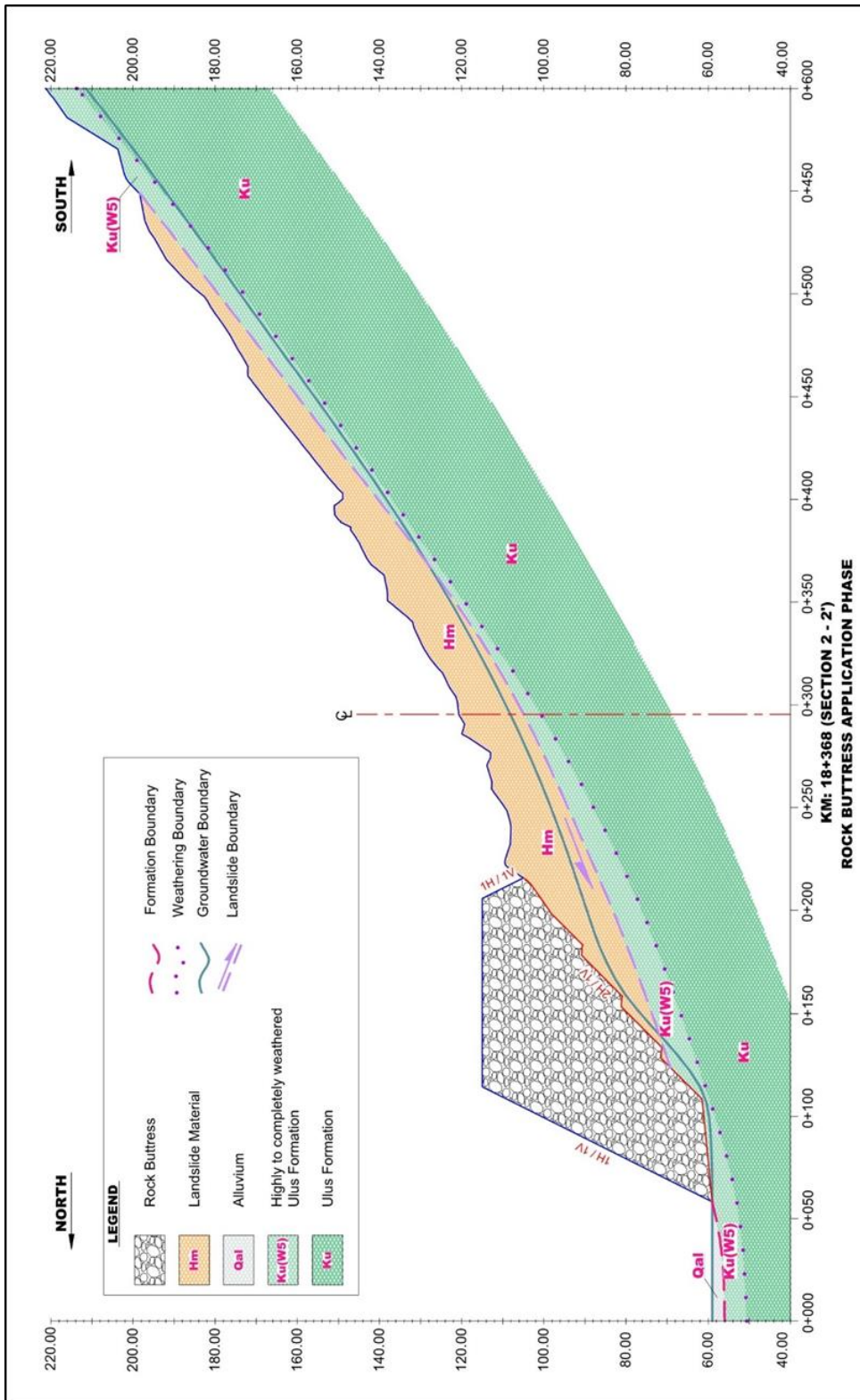


Figure 7.23. Rock Butress Application Phase of Section 2-2' (Detailed view)

7.3.4. Increase of Water Level after Dam Construction

In this phase, the increase of the groundwater level after dam construction is considered. The elevation of the Gökırmak stream level will increase to + 105 m after the construction of the Kirazlı Bridge Dam, which will lead to the increase of the groundwater level in parallel and hence to a decrease of the factor of safety values to 1.510 (Janbu Simplified), 1.535 (Morgenstern – Price) and 1.542 (Spencer) (Figures 7.24 and 7.25).

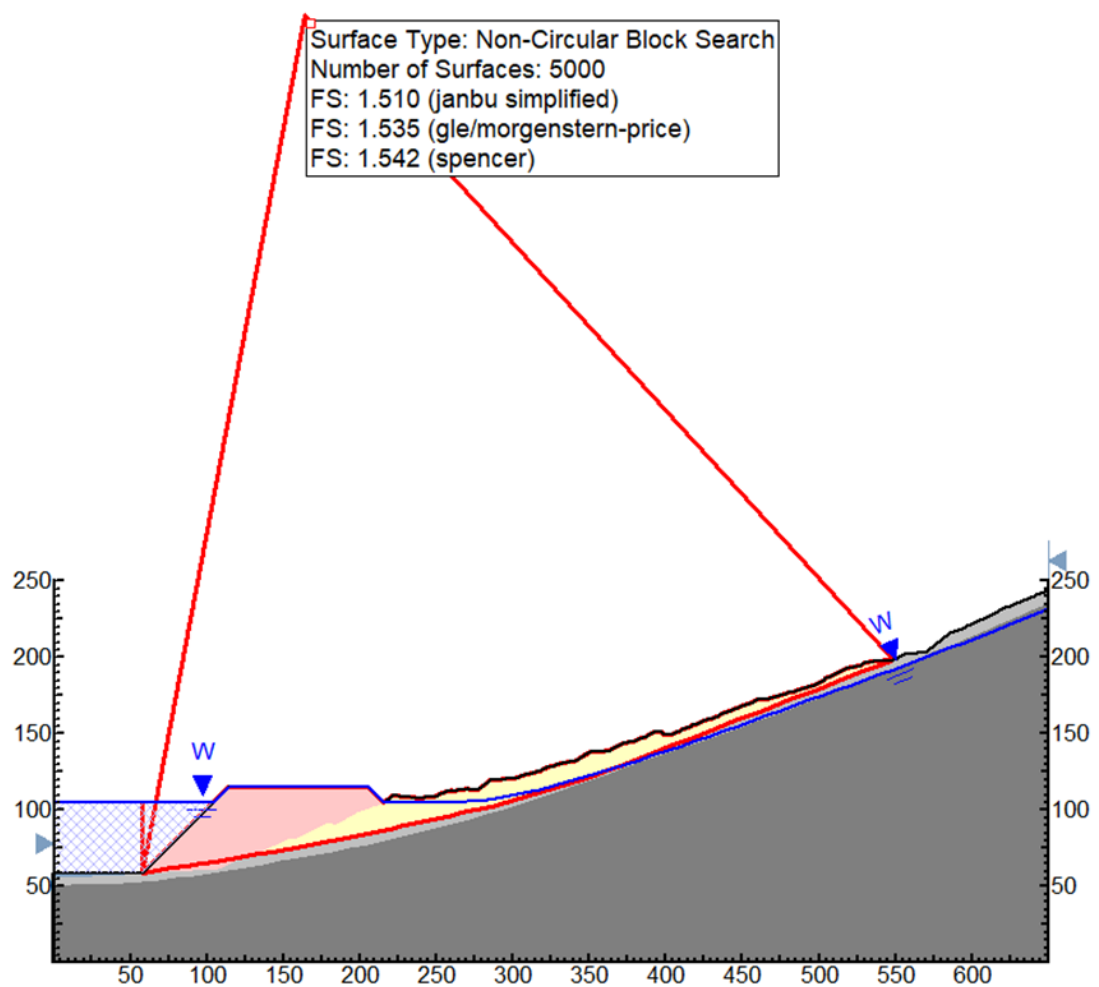


Figure 7.24. Increase of Water Level after Dam Construction for Section 2-2'
(Exported from Slide 6.0)

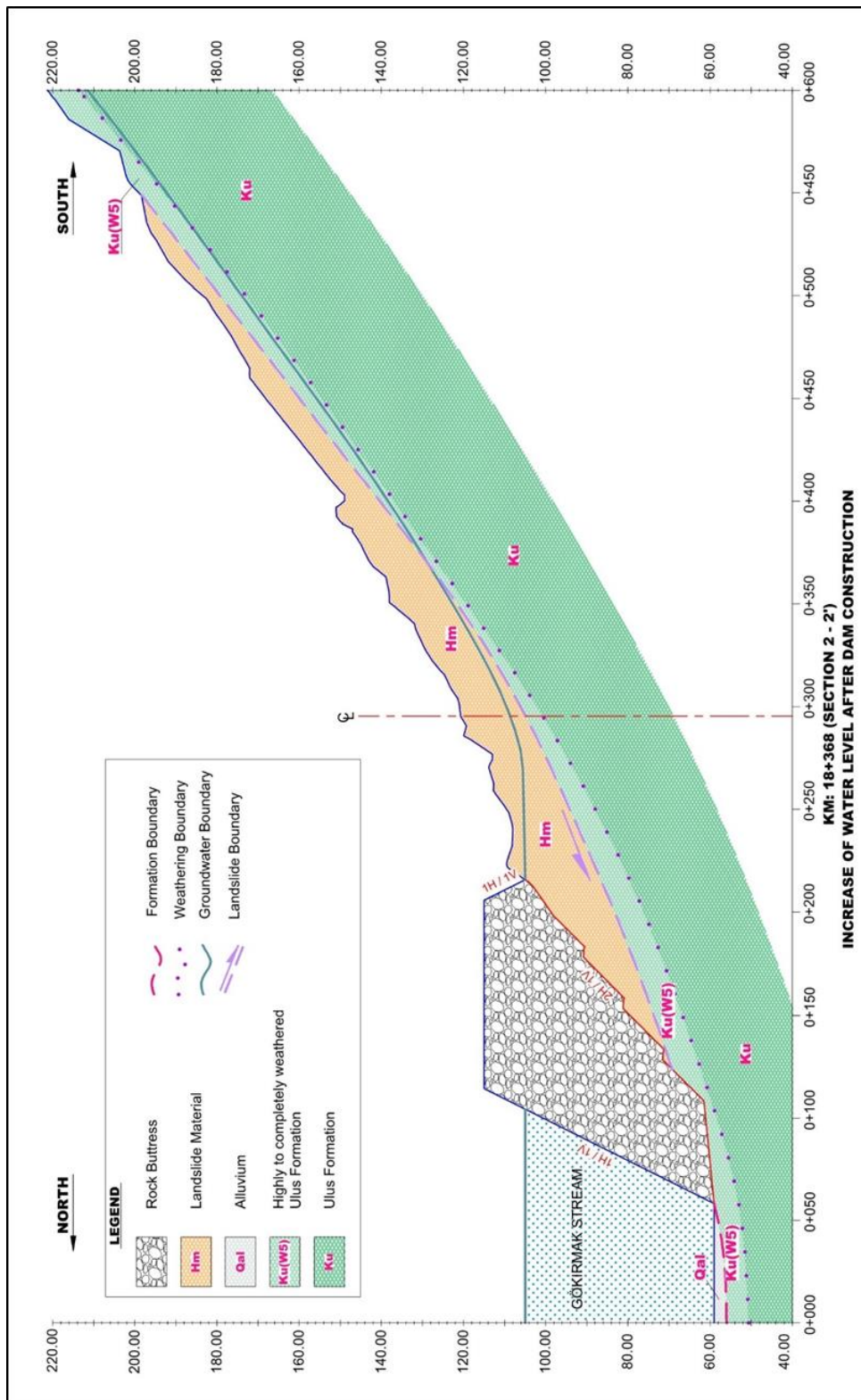


Figure 7.25. Increase of Water Level after Dam Construction for Section 2-2' (Detailed view)

7.3.5. Surface and Subsurface Drainage

The influence of drainage applications in addition to the rock buttress application in the landslide area on long term stability are investigated in this section. The active surface water potential of the area also affects the ground water movement and an increase of the water level especially in fluvial periods (Figure 3.2) causes stability problems in the area. Accordingly, dewatering by surface and subsurface drainage applications (such as watercourse and trench) will increase long term stability and the safety of the area where supported by the rock buttress.

Based on this study, typical cross sections for the application of the surface and subsurface drainage details are given in Figure 7.26.

In accordance with drainage and rock buttress applications for a long term stability measure of the landslide area, the factor of safety values are determined to increase to 2.103 (Janbu Simplified), 2.144 (Morgensten – Price) and 2.153 (Spencer) (Figures 7.27 and 7.28).

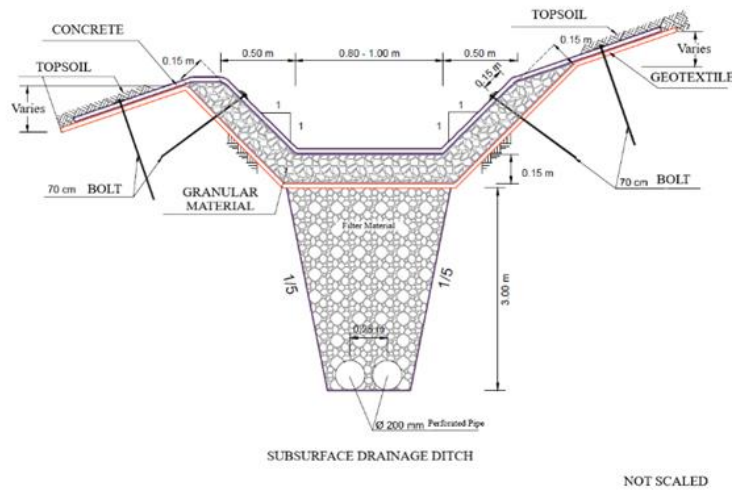
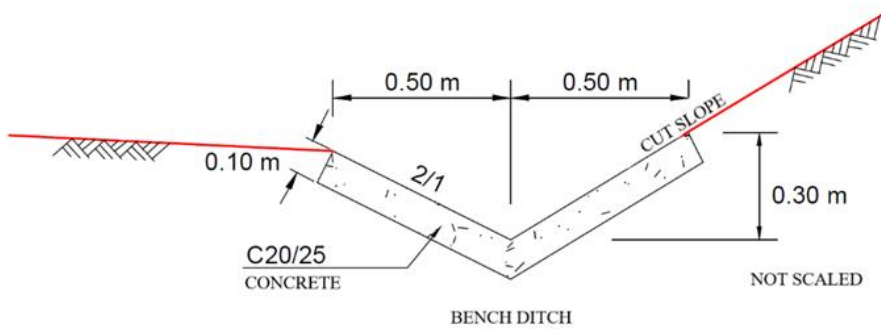
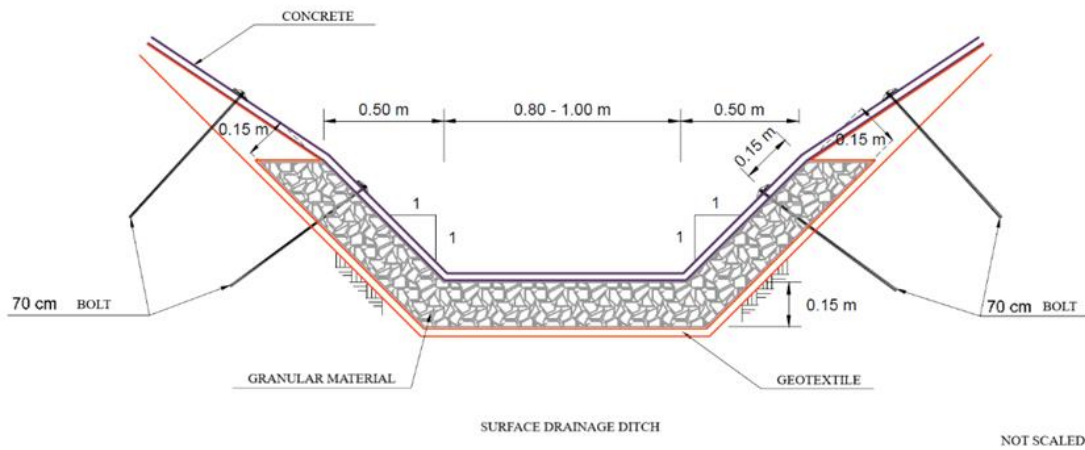


Figure 7.26. Details of the surface and subsurface drainage

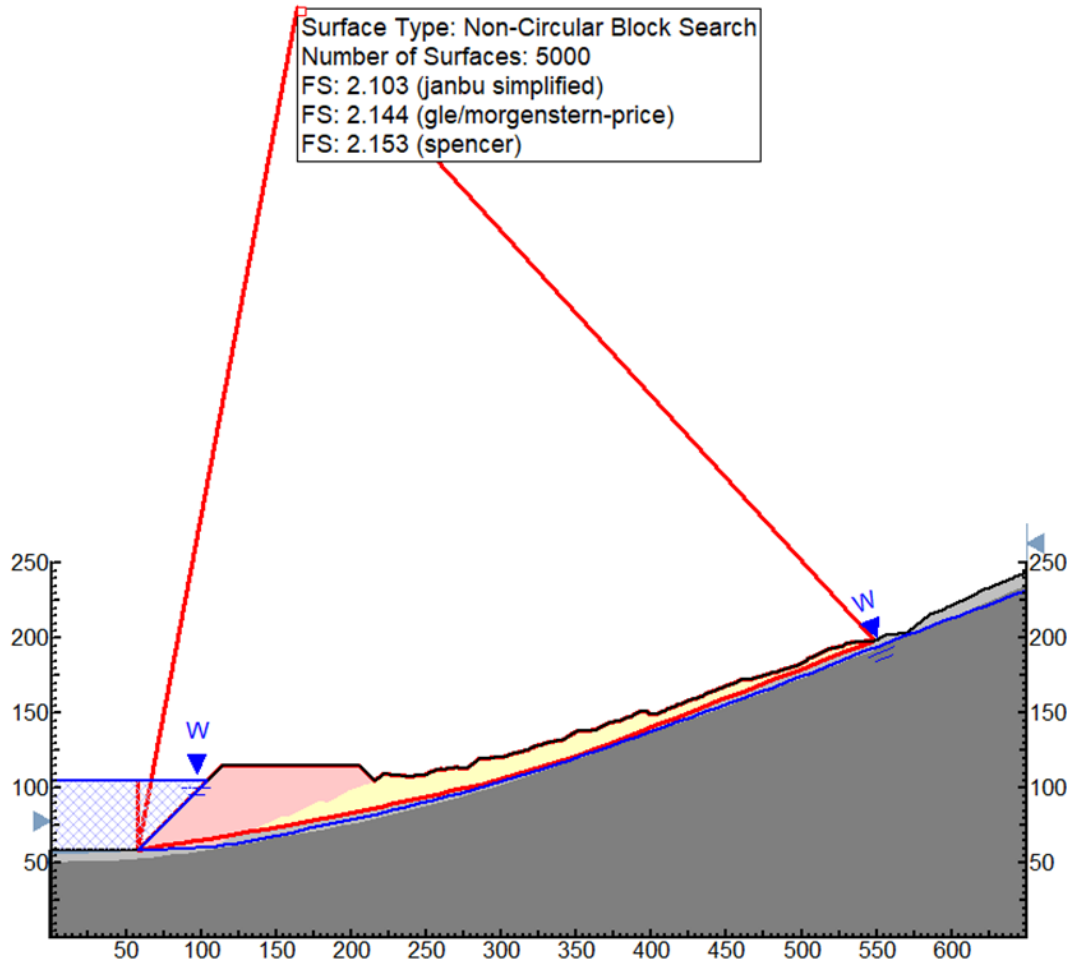


Figure 7.27. Surface and Subsurface Dewatering Phase of Section 2-2' (Static Condition)
 (Exported from Slide 6.0)

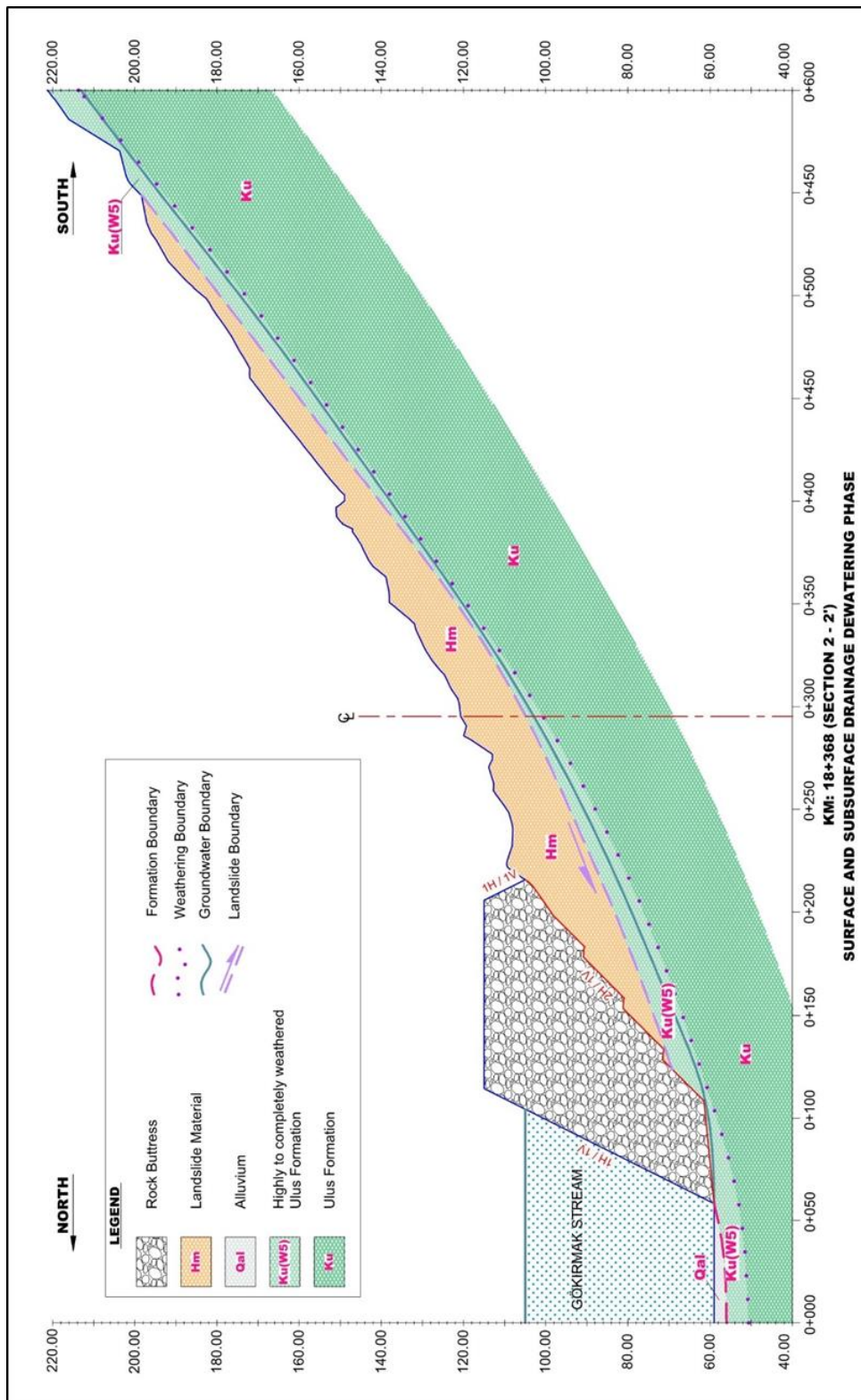


Figure 7.28. Surface and Subsurface Dewatering Phase of Section 2-2' (Detailed view)

7.3.6. Seismic Load

For the final situation, stability analysis under dynamic (seismic) condition was evaluated along with a combination of all of remediation phases that were presented previously. In seismic slope stability analysis, the effect of the horizontal seismic coefficient (k_h) was considered as a percentage of the gravitational acceleration value.

The peak horizontal ground acceleration (PGA) was rescaled as 0.12 g previously in Chapter 7.1.2 considering the seismicity potential of the area. In this regard, by the analysis performed through considering the PGA value, the factor of safety values were determined as 1.235 (Janbu Simplified), 1.265 (Morgenstern – Price) and 1.276 (Spencer) which are slightly greater than 1.15 and hence, represent stable conditions (Figure 7.29). In other words, these results were deemed satisfactory regarding the factor of safety values that are required by KGM Research Engineering Services Technical Specification (2014) as well as Seed (1979).

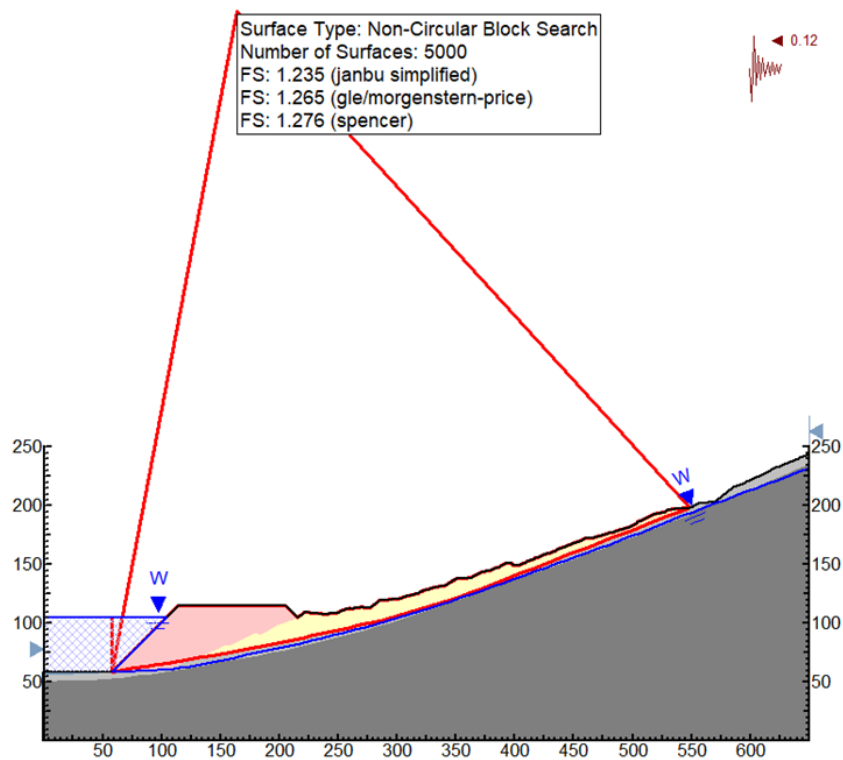


Figure 7.29. Surface and Subsurface Dewatering Phase of Section 2-2' (Seismic Condition)
(Exported from Slide 6.0)

7.3.7. Assessment of the Stability Analysis

Regarding the rock mass conditions and the determined factor of safety values on the investigated landslide's non – circular failure surface, Janbu's Simplified Method along with Spencer's and Morgenstern – Price methods were utilized. It seems as if all three methods led to similar factor of safety values. However, Janbu's Simplified Method that satisfies only force equilibrium led to the lowest factor of safety value for assessing the stability of the Bartın Kirazlı Bridge Landslide. The results obtained with all three methods are presented in Table 7.11.

Table 7.11. *Summary of factor of safety values*

Slope Stabilization Steps	Factor of Safety (FS) Value		
	Janbu Simplified	Morgenstern – Price	Spencer
Slope Instability (Back Analysis)	0.999	1.001	1.002
Pumping Drainage	1.252	1.255	1.255
Toe Excavation	1.183	1.185	1.185
Rock Buttress	1.731	1.756	1.765
Dam Construction	1.510	1.535	1.542
Surface and Subsurface Drainage	2.103	2.144	2.153
Seismic Load Condition	1.235	1.265	1.276

CHAPTER 8

DISCUSSION, CONCLUSIONS AND RECOMMENDATIONS

The construction of the Bartın Kirazlı Bridge Dam on the Gökırmak stream has started in 1999. After completion of the dam, the Gökırmak stream elevation will increase to + 105 m and the existing Bartın – Safranbolu Highway (D755) will be submerged. For relocation of the submerged road, a new alignment is determined but some paleo – landslides are present throughout the area. During the construction works of the new highway, a large landslide occurred at Km: 18 + 325 – 18 + 421 of the alignment.

In order to identify the characteristics of this landslide, a geological – geotechnical site investigation consisting of in – situ site investigation studies (geotechnical borings at 11 locations with a total number 83 SPT's and with a total number of 120 pressuremeter tests, inclinometer monitoring at 10 boreholes, etc.) and laboratory tests (on a total number of 81 soil samples and a total number of 12 rock samples) were performed. According to site investigation and laboratory data, the study area is represented by landslide material (Hm), artificial fill (Yd), Ulus formation (Ku) and its highly to completely weathered levels (Ku – W5). By the help of the site investigation works, the sliding surface was determined in order to perform landslide modelling. After modelling of the landslide, investigation studies for a suitable remediation technique have been performed. For this purpose, determination of the strength parameters of the rock units observed at the study area was performed at first by using the RocData software. Then, a back analysis was conducted in order to obtain the shear strength parameters of the landslide material. Back analysis was performed on three critical sections of the landslide and the shear strength parameters of the landslide material were determined as $c = 14$ kPa and $\phi = 16.6^\circ$, respectively.

After determination of the shear strength parameters of the units, stability analyses were performed by using the Slide software in regards to determine a suitable remediation of the landslide mass. Stability analysis performed by limit equilibrium methods of Janbu's Simplified, Morgenstern – Price and Spencer's considering the rock mass conditions of the investigated landslide's non – circular failure surface. Accordingly, application of pumping drainage was considered in the initial phase to decrease the ground water level in short term. By the help of drainage, a dry area with a 2H / 1V slope was created for rock buttress application. Then, the rock buttress with a slope ratio of 1H / 1V was applied. Moreover, the dewatering of the area by surface and subsurface drainages in the final phase led to long term stability and safety. As a consequence of these remediation applications, the necessary factor of safety value (1.50) for static condition was satisfied for all three limit – equilibrium methods (2.103 for Janbu Simplified, 2.144 for Morgenstern – Price and 2.153 for Spencer) in the stability analyses.

In addition to the stability analysis for a static condition, seismic slope stability analysis that considered the regional earthquake conditions of the study area was also performed. In this case, the peak ground acceleration (PGA) value was estimated by using the evaluations of the regional earthquake hazard map, a deterministic method and the Seed (1979) relation. The horizontal seismic load coefficient to evaluate in slope stability analysis was re-scaled and calculated as 0.12 g regarding these evaluations and considering the seismicity potential of the study area. As a result, the required safety factor value (1.15) under seismic conditions was also satisfied for all three limit – equilibrium methods (1.235 for Janbu Simplified, 1.265 for Morgenstern – Price and 1.276 for Spencer) in the slope stability analysis. These results were deemed satisfactory regarding the factor of safety values that are required by KGM Specification (2005) as well as Seed (1979).

As a conclusion, stability assessments consisting of investigation, monitoring and slope stability analyses studies were completed in order to assess the long term stability of the Bartın Kirazlı Bridge Landslide.

REFERENCES

- Abrahamson, N. A., Silva, W. J., 2008, "Summary of the Abrahamson & Silva NGA ground – motion relations", *Earthquake Spectra*, vol. 24, no. 1, p. 67 – 97.
- Abramson, L. W., Lee, T. S., Sharma, S., Boyce, G. M., 2002, "Slope Stability and Stabilization Methods", John Wiley & Sons, Inc., New York, pp. 712.
- AFAD, 2018, "Türkiye Deprem Bölgeleri Haritası", Deprem Dairesi Başkanlığı, Ankara.
- Akman, U., 1993, "Amasra – Arıt arasının jeolojisi", Ankara Üniversitesi Fen Bilimleri Enstitüsü, Doktora tezi (yayımlanmamıştır).
- Aksay, A., Akbaş B., Altun, İ., Bilginer, E., Duru, M., Gedik, İ., Pehlivan, Ş., Sevin, M., Timur, E., 2001, "1 / 500 000 ölçekli Türkiye Jeoloji Haritaları, Zonguldak Paftası", MTA.
- Akyol, Z., Arpat, E., Erdoğan, B., Göğer, E., Güner, Y., Şaroğlu, F., Şentürk, İ., Tütüncü, K., Uysal, Ş., 1974, "1 / 50 000 Ölçekli Türkiye Jeoloji Haritası Serisi", MTA yayınları.
- Al Atik, L., 2009, "Calculation of Weighted Average 2008 NGA Models".
- Aryal, K. P., 2006, "Slope Stability Evaluations by Limit Equilibrium and Finite Element Methods", Norwegian University of Science and Technology.
- ASTM, 2007, D4719 – 07, "Standard Test Methods for Prebored Pressuremeter Testing in Soils (Withdrawn 2016)", ASTM International, West Conshohocken, PA.

- ASTM, 2011, D1586 – 11, “Standard Test Method for Standard Penetration Test (SPT) and Split – Barrel Sampling of Soils”, ASTM International, West Conshohocken, PA.
- ASTM, 2013, D6230 – 13, “Standard Test Method for Monitoring Ground Movement Using Probe – Type Inclinerometers”, ASTM International, West Conshohocken, PA.
- Barka, A., Reilinger, R., 1997, “Active tectonics of the eastern Mediterranean region: deduced from GPS, neotectonic, and seismicity data”, *Annali Geofisica*, 40, pp. 587 – 610.
- Bartın İl Planlama ve Koordinasyon Müdürlüğü, 2015, “Bartın İl Brifingi”, T. C. Bartın Valiliği.
- Bengü, 2017, “Post – Paleogene Stress Distribution in the Bartın – Ulus Safranbolu Basins, Western Pontides, Turkey”, Middle East Technical University, pp. 63.
- Bieniawski, Z. T., 1989, “Engineering rock mass classifications: a complete manual for engineers and geologists in mining, civil, and petroleum engineering”, New York, Wiley, xii, pp. 251.
- Boore, D. M., Atkinson, G. M., 2008, “Ground – motion prediction equations for the average horizontal component of PGA, PGV, and 5%-damped PSA at spectral periods between 0.01 s and 10.0 s”, *Earthquake Spectra*, vol. 24, no. 1, p. 99 – 138.
- Bozkurt, E., 2001, “Neotectonics of Turkey – a synthesis”, *Geodinamica Acta*, 14, pp. 3 – 30.
- Bray, J., Travasarou, T., 2009, “Pseudostatic coefficient for use in simplified seismic slope stability evaluation”, *Journal of Geotechnical and Geoenvironmental Engineering*, 135 (9), 1336 – 1340.

- Campbell, K. W., Bozorgnia, Y., 2008, “NGA ground motion model for the geometric mean horizontal component of PGA, PGV, PGD and 5% damped linear elastic response spectra for periods ranging from 0.01 to 10 s”, *Earthquake Spectra*, vol. 24, no. 1, p. 139 – 171.
- Carter, M., Bentley, S. P., 1991, “Correlations of Soil Properties”, Pentech Press, 1st Edition, London.
- Chiou, B. S. J., Youngs, R. R., 2008, “An NGA model for the average horizontal component of peak ground motion and response spectra”, *Earthquake Spectra*, vol. 24, no. 1, p. 173 – 215.
- Climate Data, 2018, “Climate: Derbent, Bartın, Turkey”.
- Cruden, D. M., Varnes, D. J., 1996, “Landslide Types and Processes”, Transportation Research Board, U. S. National Academy of Sciences, Special Report, 247: pp. 36 – 75.
- Deere, D. U., 1963, “Technical Description of Rock Cores for Engineering Purposes”, *Rock Mechanics and Engineering Geology* Vol. 1, No. 1, Vienna, pp. 16 – 22.
- Duncan, J. M., Wright, S. G., 2005, “Soil Strength and Slope Stability”, John Wiley & Sons, Inc., New York.
- Duncan, J. M., Wright, S. G., Brandon, T. L., 2014, “Soil Strength and Slope Stability”, John Wiley & Sons, Inc., New Jersey.
- Emre, Ö., Duman, T. Y., 2012, “1 / 250 000 Ölçekli Türkiye Diri Fay Haritası Serisi, Zonguldak (NK 36 – 10) Paftası, Seri No: 18, Maden Tetkik ve Arama Genel Müdürlüğü, Ankara, Türkiye.
- Erol, O., 1993, “Ayrıntılı Jeomorfoloji Haritaları Çizim Yöntemi”, İstanbul Üniversitesi, Deniz Bilimleri ve Coğrafya Enstitüsü Bülteni, 10, s. 19 – 37.

Esri, 2018, Topographic Map.

Gibson, R. E., 1953, “Experimental determination of the true cohesion and true angle of internal friction in clays”, Proceedings of 3rd International Conference on Soil Mechanics and Foundation Engineering, Zurich, pp. 126 – 130.

Hasancebi, N, Ulusay, R., 2007, “Empirical correlations between shear wave velocity and penetration resistance for ground shaking assessments”, Bull. Eng. Geology and the Environment, 66: 203 – 213.

Hoek, E., 1994, “Strength of Rock and Rock Masses”, ISRM News Journal, 2 (2), pp. 4 – 16.

Hoek, E., Brown, E. T., 1997, “Practical estimates of rock mass strength”, International Journal of Rock Mechanics & Mining Sciences, v. 34, pp. 1165 – 1186.

Hoek, E., Carranza – Torres, C., Corkum, B., 2002, “Hoek – Brown failure criterion”, Proc. NARMS – TAC Conference, Toronto, 1, pp. 267 – 273.

Hunt, R. E., 2005, “Geotechnical Engineering Investigation Handbook, Second Edition”, CRC Press, Taylor & Francis Group, 6000 Broken Sound Parkway NW, Suite 300 Boca Raton, FL 33487-2742, pp. 707.

Hustrulid, W. A., McCarter, M. K., Van Zyl, D. J. A., 2001, “Slope Stability in Surface Mining”, Society for Mining, Metallurgy, and Exploration, Inc. (SME) 8307 Shaffer Parkway Littleton, Colorado, USA, pp. 358.

Idriss, I. M., 2008, “An NGA empirical model for estimating the horizontal spectral values generated by shallow crustal earthquakes”, Earthquake Spectra, vol. 24, no. 1, p. 217 – 242.

International Soil and Rock Mechanics (ISRM), 1981, Rock Characterization, Testing and Monitoring, ISRM Suggested Methods, Brown ET (editor), Pergamon Press, Oxford, p 211.

Kaklamanos, J., Boore, D. M., Thompson, E. M., Campbell, K. W., 2010, "Implementation of the Next Generation Attenuation (NGA) Ground – Motion Prediction Equations in Fortran and R", U. S. Geological Survey Open – File Report 1296.

Karabük Çevre ve Şehircilik İl Müdürlüğü, 2012, "Karabük Zonguldak Bartın İlleri Çevresel Durum Değerlendirmesi", T. C. Karabük Valiliği.

Karayolları Genel Müdürlüğü, 2005, Teknik Araştırma Dairesi Başkanlığı, "Araştırma Mühendislik Hizmetleri Teknik Şartnamesi", Ankara.

Kaya, O., Wiedmanm, J., Kozur, H., 1986, "Preliminary report on the stratigraphy, age and structure of the so-called Late – Paleozoic and / or Triassic Melange or Suture Zone Complex of northwestern and western Turkey", Hacettepe Üniversitesi Yerbilimleri, 13, 1 – 16.

Ketin, İ., Gümüş, A., 1963, "Sinop – Ayancık civarında 3. Bölgeye dahil sahaların jeolojisi", TPAO Rap. No: 213 (yayımlanmamış), Ankara.

Lunne T., Robertson K. P., Powell M. J. J., 1997, "Cone Penetration Testing in Geotechnical Practice" Blackie Academic & Professional, London.

Maden Tetkik ve Arama Genel Müdürlüğü, 2002, "1 / 100 000 Ölçekli Türkiye Jeoloji Haritaları Zonguldak – E28 Paftası", Jeoloji Etütleri Dairesi, Ankara.

Maden Tetkik ve Arama Genel Müdürlüğü, 2012, "1 / 250 000 Ölçekli Türkiye Diri Fay Haritası Serisi – Zonguldak (NK 36 – 10) Paftası", Seri No: 18, Ankara.

- Makdisi, F. I., Seed H. B., 1978, "Simplified Procedure for Estimating Dam and Embankment Earthquake-Induced Deformations", Journal of the Geotechnical Engineering Division, ASCE, Vol. 104, No GT7, pp. 849 – 867.
- Palmström, A., 2005, "Measurements of and correlations between block size and rock quality designation (RQD)", Tunnels and Underground Space Technology, 20, pp. 362 – 377.
- Ralli, G., 1933, "Zonguldak – Ereğli Havzası kömür durumu", MTA Rap. No: 12 (Fransızca).
- Saner, S., 1979, "Batı pontidlerin ve komşu havzaların oluşumlarının levha tektoniği kavramı ile açıklanması", Kuzeypatı Türkiye: MTA Dergisi sayı. 93 / 94, s. 1 – 19.
- Saner, S., Siyako, M., Aksoy, Z., Bürkan, K., Demir, O., 1981, "Zonguldak dolayının jeolojisi", TPAO Rap. No: 1322 (yayımlanmamış).
- Seed, H. B., 1979, "Considerations in the earthquake – resistant design of earth and rockfill dams", Nineteenth Rankine Lecture, Géotechnique, 29 (3), Sept., 215 – 263.
- Serdar, H. S., Demir, O., 1983, "Bolu, Mengen, Devrek dolayının jeolojisi ve petrol olanakları", TPAO Rap. No: 1322 (yayımlanmamış).
- SME, 2001, "Slope Stability in Surface Mining", Littleton, Colorado, US.
- Sonmez, H., Ulusay, R., 1999, "Modification to the Geological Strength Index (GSI) and Their Applicability to Stability of Slopes", International Journal of Rock Mechanics and Mining Sciences (36), pp. 743 – 760.
- Sonmez, H., Ulusay, R., 2002, "A discussion on the Hoek – Brown failure criterion and suggested modification to the criterion verified by slope stability case studies", Yerbilimleri (Earthsciences) 26, pp. 77 – 99.

- Spencer, E., 1967, "A Method of Analysis of the Stability of Embankments Assuming Parallel Inter – Slice Forces", *Geotechnique*, v. 17, pp. 11 – 26.
- Şengör A. M. C., 1979, "The North Anatolian transform fault: Its age, offset and tectonic significance", *Journal of Geological Society of London*, C. 136, 269 – 282.
- Şengör, A. M. C., Görür, N., Şaroğlu, F., 1985, "Strike – slip faulting and related basin formation in zones of tectonic escape: Turkey a case study. Strike-slip Deformation, basin Formation, and Sedimentation (Eds: Biddle, K.T. and Christie-Blick, N.)", *Soc. Econ. Paleont. Min. Spec. Pub. 37* (in honor of J.C. Crowell), pp. 227 – 264.
- Terzaghi K., 1950, "Mechanisms of Landslides. In: Paige S (ed) Application of geology to engineering practice", *Geological Society of America*, Berkley, pp 83 – 123.
- Tokay, M., 1954, "Filyos Çayı Ağızı – Amasra – Bartın – Kozcağız – Çaycuma bölgesinin jeolojisi", *MTA Dergisi* sayı 46 – 47 ve MTA Rap. No: 2099.
- Varnes, D. J., 1978, "Slope Movement Types and Processes", *Landslides: Analysis and Control*, Transportation Research Board Special Report 176, Schuster, R. L., Krizek, R. J. (editors), National Academy of Sciences, Washington, D.C., pp. 11 – 33.
- Waltham, T., 2009, "Foundations of Engineering Geology, Third Edition", Spon Press, London, pp. 70.
- Wells, D. L., Coppersmith, K. J., 1994, "New Empirical Relationships among Magnitude, Rupture Length, Rupture Width, Rupture Area, and Surface Displacement", *Bulletin of the Seismological Society of America*, Vol. 84, No. 4, pp. 974 – 1002.

APPENDICES

A. Borehole Logs

YUKSEL PROJE										YP-9112-FRM-0104										
YUKSEL PROJE ULUSLARARASI A.Ş. Birlik Mahallesi 400. Cadde No:23 09810 ÇAMKIRIYA - ANKARA Tel: (312) 495 70 90 FAX: (312) 495 70 24 yproje@yukselproje.com.tr www.yukselproje.com.tr										Borehole Log										
BORING LOG										BOREHOLE No: BKH-03i										
										PAGE No: 1 / 4										
PROJECT NAME					START - FINISH DATE					: 07.06.2016 - 10.06.2016										
BORING LOCATION					Kirazlı Bridge, Bartın / Landslide					CASING DEPTH		: 4.50 m (HW) 19.50 m (NW)								
CHAINAGE					GROUNDWATER LEVEL & DATE					: 4.00 m - 10.6.2016										
BORING DEPTH					: 30.00 m					COORDINATE SYSTEM		: TM33 ED50								
HOLE DIAMETER					: 76.00 mm (NQWL)					COORDINATE (N-S) X		: 4 599 601.07								
DRILLING RIG & METHOD					: YPSM-05 / ROTARY					COORDINATE (E-W) Y		: 456 359.26								
DRILLER					: Ali DÖNMEZ					ELEVATION (m)		: 139.43								
BORING DEPTH (m)	SAMPLE TYPE	RUN	IN - SITU TEST	PRESS. TEST (kg / cm ²)		STANDARD PENETRATION TEST						GEOTECHNICAL DESCRIPTION	PROFILE	STRENGTH	WEATHERING	FRACTURE (30 cm)	TCR %	RQD %	POINT LOAD / IS ₅₀ (MPa)	
				NET LIMIT PRESSURE	MODULUS OF ELASTICITY	NUM OF BLOWS			GRAPH											
						0 - 15 cm	15 - 30 cm	30 - 45 cm	N	10	20									30
0		0.00																		
1	K-1																			
2	SPT-1	1.50	SPT-1			2	3	6	9											100
3	K-2	1.95																		76
4	SPT-2	3.00	SPT-2			3	5	6	11											
5	K-3	3.45																		57
6	SPT-3	3.90	SPT-3	P-1	3.90	65														
7	K-4	4.50				2	5	8	13											48
8		4.95																		
9		6.00																		
STRENGTH (ISRM)					WEATHERING					FINE GRAINED					COARSE GRAINED					
I STRONG (R5/R6) > 100 MPa					I FRESH					N : 0-2 VERY SOFT					N : 0-4 VERY LOOSE					
II M.STRONG (R4) 50 - 100 MPa					II SLIGHTLY WEATHERED					N : 3-4 SOFT					N : 5-10 LOOSE					
III M.WEAK (R3) 25 - 50 MPa					III MODERATELY WEATHERED					N : 5-8 MEDIUM STIFF					N : 11-30 MEDIUM DENSE					
IV WEAK (R2) 5 - 25 MPa					IV HIGHLY WEATHERED					N : 9-15 STIFF					N : 31-50 DENSE					
V VERY to EXT.WEAK (R1/R0) 0.25 - 5 MPa					V COMPLETELY WEATHERED					N : 16-30 VERY STIFF					N : >50 VERY DENSE					
RQD					FRACTURES - 30 cm					PROPORTIONS										
%0-25 V.POOR					1 WIDE(W)					% 5 SLIGHTLY					%5 SLIGHTLY					
%25-50 POOR					1-2 MODERATE(M)					% 5-15 LITTLE					%5-20 LITTLE					
%50-75 FAIR					2-10 CLOSE(CI)					% 15-35 VERY					%20-50 VERY					
%75-90 GOOD					10-20 INTENSE(I)					% 35 AND										
%90-100 EXCELLENT					>20 CRUSHED(Cr)															
SPT Standard Penetration Test					K Core Sample					LOGGED BY					CHECKED					
UD Undisturbed Sample					P Pressuremeter Test					NAME Onur İLGAR										
NW Hole Dia.=76 mm / Core Dia.=54.7 mm					v Vane Test					Jeofizik Mühendisi										
HW Hole Dia.=114 mm / Core Dia.=100 mm					BST Water Pressure Test					SIGNATURE										
NQWL Hole Dia.=76 mm / Core Dia.=47.6 mm					k Permeability Test															
HQWL Hole Dia.=96 mm / Core Dia.=63.5 mm					S Sediment Sample															

The borehole log is prepared as per ASTM-D 2488-93 and edited by Barış GÖRBİL. It may be revised considering the geological model and laboratory tests.

Rev. No: 00

This document has been drawn by using a program developed by YP IT group.

Rev. Date: 13.07.2011

YÜKSEL PROJE

YP-9112-FRM-0104

YÜKSEL PROJE ULUSLARARASI A.Ş.
 Birlik Etiler Mahallesi 450. Cadde No:23
 06810 ÇAYKAYA - ANKARA
 Tel: (312) 495 70 00 FAX: (312) 495 70 24
 yproje@yukselproje.com.tr
 www.yukselproje.com.tr



Borehole Log

BORING LOG

BOREHOLE No BKH-031

PAGE No 2 / 4

BORING DEPTH (m)	SAMPLE TYPE	RUN	IN - SITU TEST	PRESS. TEST (kg / cm ²)		STANDARD PENETRATION TEST				GEOLOGICAL DESCRIPTION	PROFILE	STRENGTH	WEATHERING	FRACTURE (30cm)	TCR %	RCD %	POINT LOAD / IS (MPa)									
				NET LIMIT PRESSURE	MODULUS OF ELASTICITY	NUM OF BLOWS			GRAPH																	
						0 - 15 cm	15 - 30 cm	30 - 45 cm										N								
6	SPT-4	6.86	SPT-4			6	10	25	35	<p>Sandy lean clay with gravel (CL), grey - greenish grey - partly light brown, very stiff - hard. Moist, medium to high plasticity; 10 - 30%, fine to coarse grained, sandy; 5-15%, angular to subangular, slightly hard, contains claystone and siltstone originated.</p>																
6.45																										
7	K-5	6.90	P-2	9.80	94																					
7.50																										
8	SPT-5	7.80	SPT-5			6	13	50	R																	
7.95																										
8	K-6																									
9	SPT-6	9.00	SPT-6			4	11	15	26																	
9.45																										
10	K-7	9.90	P-3	7.21	91																					
10.50																										
11	SPT-7	10.95	SPT-7			10	18	27	45																	
10.95																										
12	K-8																									
12	SPT-8	12.00	SPT-8			8	19	23	42																	
12.45																										
13	K-9																									
13	SPT-9	13.40	P-4	18.99	441																					
13.50																										
14	SPT-10	13.95	SPT-10			9	14	17	31																	
14.00																										
14.45	K-10					6	11	13	24																	
15	SPT-11	14.90	P-5	3.66	90																					
15.00																										
15.45	K-11					7	15	13	28																	
16																										

LOGGED BY
 NAME Onur ILGAR
 Jeofizik Mühendisi
 SIGNATURE *[Signature]*

CHECKED

The borehole log is prepared as per ASTM-D 2488-93 and edited by Banış GÖRBL. It may be revised considering the geological model and laboratory tests.
 Rev. No: 00 This document has been drawn by using a program developed by YP IT group. Rev. Date: 13.07.2011

YÜKSEL PROJE

YP-9112-FRM-0104

YÜKSEL PROJE ULUSLARARASI A.Ş.
Büyükdere 650, Kat:16/23
06610 ÇANKAYA - ANKARA
Tel: (312) 499 70 00 FAX: (312) 499 70 24
yp@yukselproje.com.tr
www.yukselproje.com.tr



Borehole Log

BORING LOG

BOREHOLE No BKH-031

PAGE No 3 / 4

BORING DEPTH (m)	SAMPLE TYPE	RUN	IN - SITU TEST	PRESS. TEST (kg / cm ²)		STANDARD PENETRATION TEST				GEOTECHNICAL DESCRIPTION	PROFILE	STRENGTH	WEATHERING	FRACTURE (30cm)	TCR %	RQD %	POINT LOAD / IS (MPa)
				NET LIMIT PRESSURE	MODULUS OF ELASTICITY	NUM OF BLOWS			N								
						0 - 15 cm	15 - 30 cm	30 - 45 cm									
16	K-11	16.50	SPT-12			26	36	50	11	R							
		16.91															
17	K-12	17.40	P-6	78.51	1332												62 -
18		18.00															
19	K-13	19.50															97 87
20	K-14	20.40	P-7	43.13	1365												100 73
21		21.00															
22	K-15	23.40	P-8	46.25	5688												100 80
23		24.00															
24																	
25	K-16																100 43
26																	

The borehole log is prepared as per ASTM-D 2488-93 and edited by Barış GÖRBİL. It may be revised considering the geological model and laboratory tests.

Rev. No: 00

This document has been drawn by using a program developed by YP IT group.

Rev. Date: 13.07.2011

YÜKSEL PROJE

YP-9112-FRM-0104

YÜKSEL PROJE ULUSLARARASI A.Ş.
Büyükdere Caddesi No:23
06810 ÇANKAYA - ANKARA
Tel: (312) 495 70 00 FAX: (312) 495 70 24
yproje@yukselproje.com.tr
www.yukselproje.com.tr



Borehole Log

BORING LOG

BOREHOLE No BKH-031

PAGE No 4 / 4

BORING DEPTH (m)	SAMPLE TYPE	RUN	IN - SITU TEST	PRESS. TEST (kg / cm ²)		STANDARD PENETRATION TEST					GEOTECHNICAL DESCRIPTION	PROFILE	STRENGTH	WEATHERING	FRACTURE (30cm)	TCR %	RQD %	POINT LOAD / IS (MPa)			
				NET LIMIT PRESSURE	MODULUS OF ELASTICITY	NUM OF BLOWS			GRAPH												
						0 - 15 cm	15 - 30 cm	30 - 45 cm	N	10									20	30	40
26	K-16	26.40	P-9	43.48	7079										1-2	100	43				
27		27.00											III/IV	III	>20						
28																					
29	K-17	29.40	P-10	45.03	4553								IV/V	IV	1-2	100	93				
30		30.00																			
31																					
32																					
33																					
34																					
35																					
36																					
<p>Note 30.00 meter Inclinator has been installed, 40x40x15 cm protective metal box placed.</p>											LOGGED BY		CHECKED								
											NAME		Onur ILGAR								
											SIGNATURE		Jeofizik Mühendisi								

The borehole log is prepared as per ASTM-D 2488-93 and edited by Banış GÖRBİL. It may be revised considering the geological model and laboratory tests.

Rev. No: 00

This document has been drawn by using a program developed by YP IT group.

Rev. Date: 13.07.2011

B. Core Box Photographs

BOREHOLE NO: BKH – 03i

DEPTH: 30.00 m



CORE BOX NO: 1 / 6 DEPTH: 0.00 – 6.45 m



CORE BOX NO: 2 / 6 DEPTH: 6.45 – 14.45 m

BOREHOLE NO: BKH – 03i

DEPTH: 30.00 m



CORE BOX NO: 3 / 6 DEPTH: 14.45 – 19.50 m



CORE BOX NO: 4 / 6 DEPTH: 19.50 – 24.50 m

BOREHOLE NO: BKH – 03i

DEPTH: 30.00 m

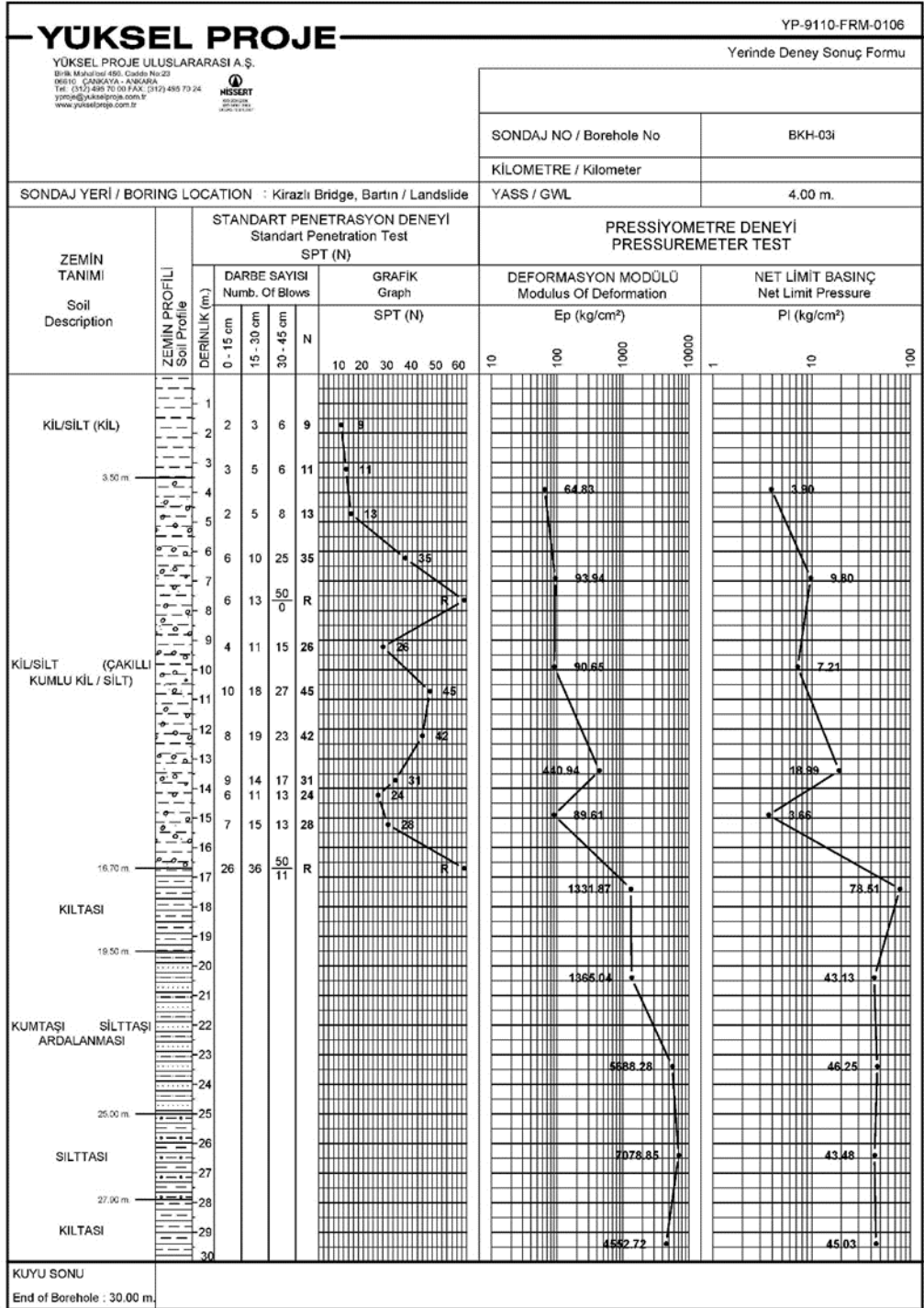


CORE BOX NO: 5 / 6 DEPTH: 24.50 – 29.50 m



CORE BOX NO: 6 / 6 DEPTH: 29.50 – 30.00 m

C. Pressuremeter Test Results

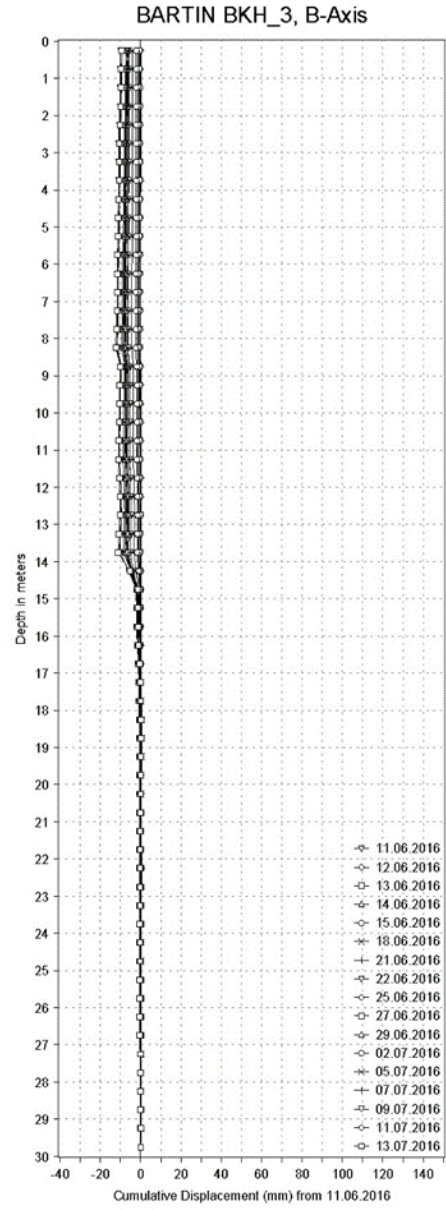
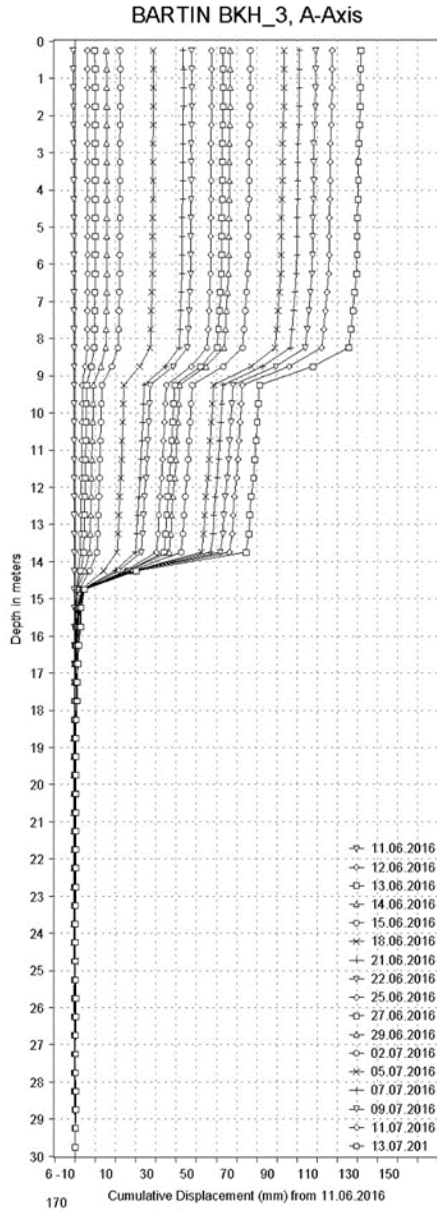


Rev. No: 01

Bu doküman YP IT grubunun programları kullanılarak otomatik olarak çizilmiştir.

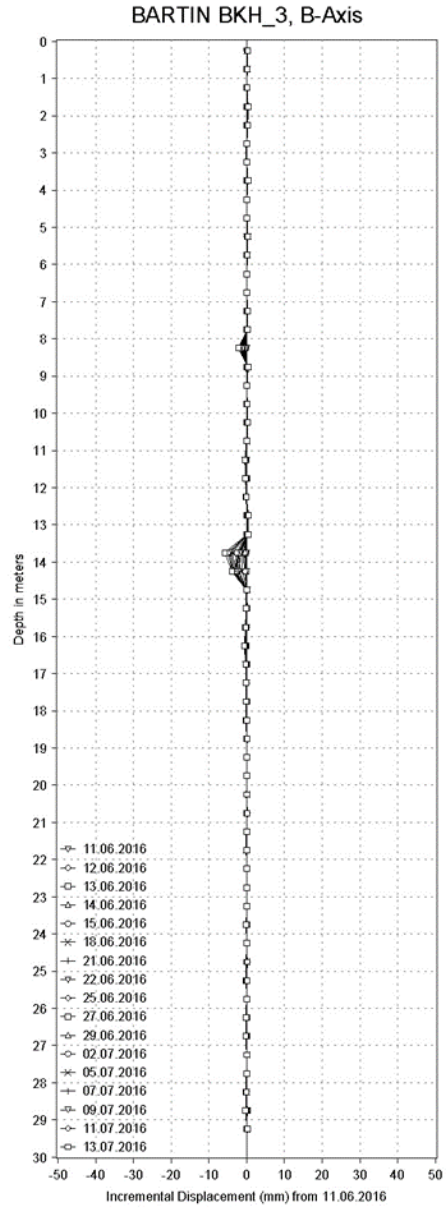
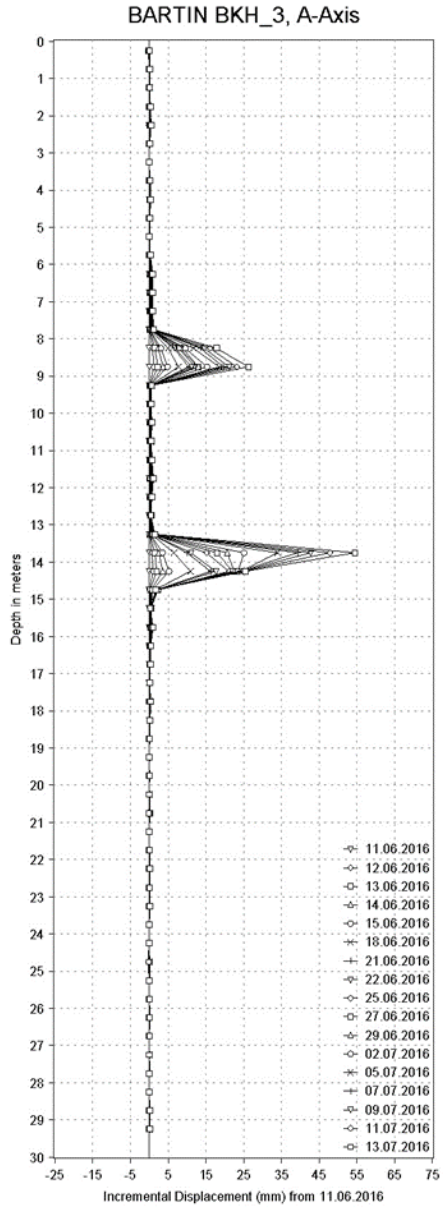
Rev. Tar: 09.01.2012

D. Inclinometer Readings



YÜKSEL PROJE

**BARTIN - KIRAZLI KÖPRÜSÜ
KM:18+300 - 18+780 HEYELANI**



YÜKSEL PROJE

**BARTIN - KIRAZLI KÖPRÜSÜ
KM:18+300 - 18+780 HEYELANI**

